AD-A099 637 AERONAUTICAL RESEARCH LABS MELBOURNE (AUSTRALIA) F/G 20/4
TURBULENT BOUNDARY LAYERS IN STRONG ADVERSE PRESSURE GRADIENTS,(U)
JUL 80 W H SCHOFIELD
UNCLASSIFIED ARL/MECH-ENG-157 NL

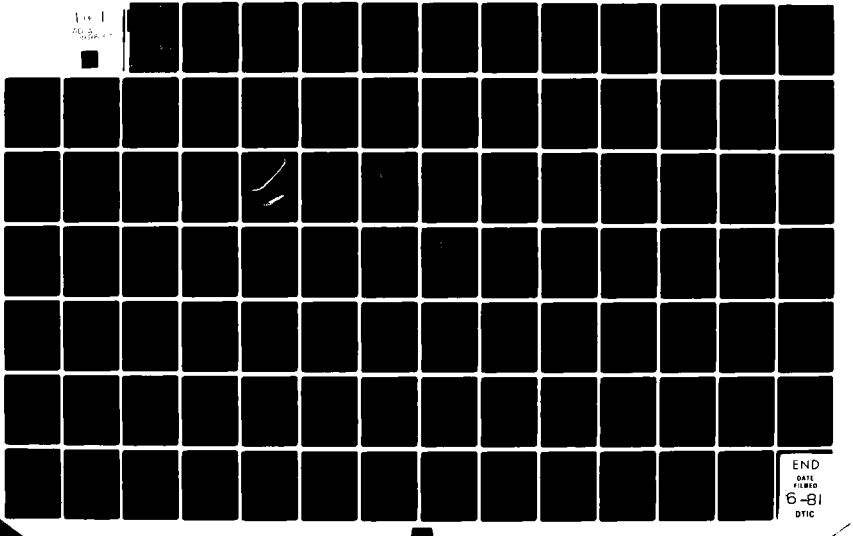

END
DATE FILMED
6-81
DTIC

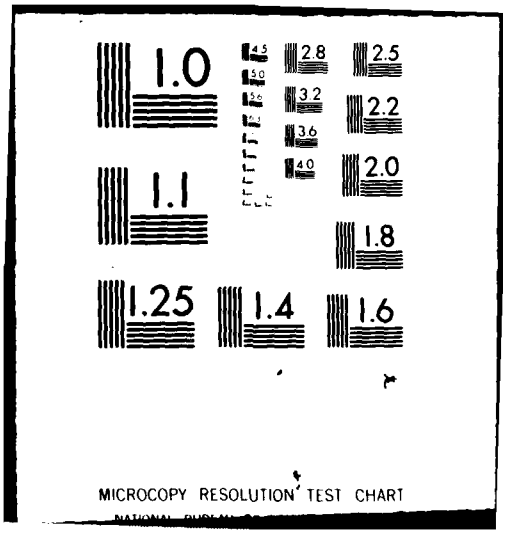
1.0
1.1
1.25
1.4
1.6
1.8
2.0
2.2
2.5
2.8
3.2
3.6
4.0
4.5
5.0
5.6
MICROCOPY RESOLUTION TEST CHART

ARL-MECH-ENG-REPORT-157

(12) LEVEL II

AR-002-218

DEPARTMENT OF DEFENCE

DEFENCE SCIENCE AND TECHNOLOGY ORGANISATION

AERONAUTICAL RESEARCH LABORATORIES

MELBOURNE, VICTORIA

MECHANICAL ENGINEERING REPORT 157

TURBULENT BOUNDARY LAYERS IN STRONG ADVERSE PRESSURE GRADIENTS

by
W. H. SCHOFIELD

Approved for Public Release.

COPY No 15

JULY 1980

AR-002-218

AERONAUTICAL RESEARCH LABORATORIES
DEFENCE SCIENCE AND TECHNOLOGY ORGANISATION
DEPARTMENT OF DEFENCE

MECHANICAL ENGINEERING REPORT 157

TURBULENT BOUNDARY LAYERS IN STRONG ADVERSE PRESSURE GRADIENTS

by
W. H. SCHOFIELD

SUMMARY

A new analysis of equilibrium boundary layers based on the Schofield and Perry defect law for flow in moderate to strong adverse pressure gradient, is presented. The conditions derived for self-preserving or precise equilibrium boundary layers differ from those given by previous analyses based on the usual velocity defect law. It is shown that nine observed boundary layers on smooth walls conform to these new conditions for equilibrium flow. As the analytical expression for the Schofield and Perry defect law does not vary with pressure gradient, an explicit expression for the shear stress profile in any equilibrium layer can be derived. Predicted shear stress profiles show good agreement with experimental data. Limits for the flow parameters within which equilibrium boundary layers can exist are derived and it is shown that observed boundary layers fall within these limits. Results by previous workers are shown to be consistent with these limits.

POSTAL ADDRESS: Chief Superintendent, Aeronautical Research Laboratories,
Box 4331, P.O., Melbourne, Victoria, 3001, Australia.

DOCUMENT CONTROL DATA SHEET

Security classification of this page: Unclassified

1. Document Numbers
   (a) AR Number: AR-002-218
   (b) Document Series and Number: Mechanical Engineering Report 157
   (c) Report Number: ARL-Mech-Eng-Report-157

2. Security Classification
   (a) Complete document: Unclassified
   (b) Title in isolation: Unclassified
   (c) Summary in isolation: Unclassified

3. Title: TURBULENT BOUNDARY LAYERS IN STRONG ADVERSE PRESSURE GRADIENTS

4. Personal Author(s): Schofield, W. H.

5. Document Date: July, 1980

6. Type of Report and Period Covered:

7. Corporate Author(s): Aeronautical Research Laboratories

8. Reference Numbers
   (a) Task: RD 73
   (b) Sponsoring Agency: RD 73

9. Cost Code: 42 7401

10. Imprint: Aeronautical Research Laboratories, Melbourne

11. Computer Program(s) (Titles and Language(s)): Nil

12. Release Limitations (of the document): Approved for public release

12.0 Overseas:	N.O.		P.R.	1	A		B		C		D		E	

13. Announcement Limitations (of the information on this page): No limitation

14. Descriptors:
Turbulent flow
Turbulent boundary layer
Equilibrium layers
Two-dimensional flow
Models
Turbulence

15. Cosati Codes: 2004

16.

ABSTRACT

A new analysis of equilibrium boundary layers based on the Schofield and Perry defect law for flow in moderate to strong adverse pressure gradient is presented. The conditions derived for self-preserving or precise equilibrium boundary layers differ from those given by previous analyses based on the usual velocity defect law. It is shown that nine observed boundary layers on smooth walls conform to these new conditions for equilibrium flow. As the analytical expression for the Schofield and Perry defect law does not vary with pressure gradient, an explicit expression for the shear stress profile in any equilibrium layer can be derived. Predicted shear stress profiles show good agreement with experimental data. Limits for the flow parameters within which equilibrium boundary layers can exist are derived and it is shown that observed boundary layers fall within these limits. Results by previous workers are shown to be consistent with these limits.

CONTENTS

NOTATION

a	Constant in expression for free stream velocity variation with distance
A	Universal constant in the logarithmic law of the wall
B	Schofield and Perry's Integral Layer Thickness
b	Constant in expression for velocity scale variation with distance
C	Fresnel's cosine integral
c	Boundary layer growth rate
c_f'	Skin friction coefficient ($= \tau_0/\frac{1}{2}\rho U_1^2$)
f	Schofield and Perry's defect law function
g	Turbulent shear stress function
G	Clauser's mean velocity shape parameter
I_1, I_2	Non-dimensional functions of η
I_μ	Constant whose value is dependent on μ ($= 0{\cdot}01925$ for $\mu = 0{\cdot}02$)
L	Distance from wall of maximum shear stress
l_0	General length scale for self-preserving flow
m	Exponent of free stream velocity variation
p	Pressure
U_m	Velocity scale based on maximum shear stress
U_s	Velocity scale in Schofield and Perry's defect law
U_1	Free stream velocity
u	Mean velocity in x direction
u_0	General velocity scale for self-preserving flow
u'	Fluctuating velocity component in x direction
$-\overline{u'v'}$	Kinematic Reynolds stress
u_p	Mellor and Gibson's pressure gradient velocity scale
u_τ	Wall friction velocity ($= \sqrt{\tau_0/\rho}$)
v	Mean velocity in y direction
v'	Fluctuating velocity component in y direction
X	$x-x_0$
x	Distance in direction of main flow
x_0	Distance of effective origin of equilibrium flow
y	Distance normal to the wall
y_c	Distance from wall of the junction between the logarithmic and half-power laws
α	Kinematic pressure gradient $[(1/\rho)(dp/dx)]$

β_C	Clauser's pressure gradient parameter $(-\delta^*/u_\tau^2)(U_1 dU_1/dx)$
β^*	Adverse pressure gradient parameter $(-\delta^*/U_s^2)(U_1 dU_1/dx)$
γ	Entrainment parameter
δ	Total boundary layer thickness
δ^*	Displacement boundary layer thickness
Δ	Clauser's integral thickness $(= 0{\cdot}3\delta^* U_1/u_\tau)$
ϵ	Distance from wall at which the Schofield and Perry defect law describes the mean velocity data points within an accuracy band of 3%
η	y/B, y/l_0
η_m	Value of η at τ_m
κ	Universal constant in the logarithmic law of the wall
μ	ϵ/B: value of η at which the Schofield and Perry defect law describes the mean velocity data points within an accuracy band of 3% (taken as constant in this report at 0·02)
ν	Kinematic viscosity of the fluid
ρ	Density of the fluid
τ	Shear stress
τ_m	Maximum shear stress
τ_0	Wall shear stress
ϕ	Function in the zero pressure gradient defect law

1. INTRODUCTION

The numerous papers that have been published on turbulent boundary layers developing in adverse pressure gradients attest to both the engineering significance of the problem and its intractability. A review of this literature does not inspire hope that a general analysis of the flows will be available in the near future. A central reason making analysis difficult is that the outer region of a turbulent boundary layer possesses a complex non-linear memory of events upstream and hence velocity distributions at any position depend on both upstream conditions as well as local conditions. To reduce the complexity of the problem Clauser (1954) set out to study a sub-set of adverse pressure gradient boundary layers that had a constant force history and could thus be described by local parameters alone. As the external forces acting on a boundary layer arise from the pressure gradient dp/dx and the wall shear τ_0, a layer with a constant force history was conceived by Clauser as a layer in which the non-dimensional force ratio,

$$\beta_C = (\delta^* dp/dx)\,(1/\tau_0),$$

was held constant along the layer's development. Clauser called these layers equilibrium layers and expected them to be dynamically similar at all stations in both the mean and fluctuating velocity field.† Clauser did not, however, use this force ratio to set up his experimental flows. He worked instead by analogy from the only equilibrium layer that was then known, the zero pressure gradient case (where $\beta_C = 0$ as $dp/dx = 0$) where it was well established that the velocity defect law

$$(U_1 - u)/u_\tau = \phi(y/\delta) \tag{1}$$

accurately described the mean velocity through the layer from the free stream down almost to the wall. Clauser reasoned that defect laws of the same general form should apply to equilibrium layers in pressure gradient flows. Therefore to set up an equilibrium boundary layer Clauser adjusted the adverse pressure gradients acting on a two-dimensional boundary layer until mean flow profiles along the layer agreed with an equation in the form of Equation (1). Two such layers were produced in which the functional form, $\phi(y/\delta)$, was different for the two flows and in turn different from the zero pressure gradient form. By defining equilibrium layers in terms of equation (1) Clauser tacitly assumed that the length and velocity scales for zero pressure gradient flow (u_τ, δ) were the relevant scales for equilibrium layers in adverse pressure gradient flow. Later work shows that this assumption causes analytical and conceptual difficulties for equilibrium layers near separation where $u_\tau \to 0$.

The values of β_C for Clauser's two experimental layers did vary somewhat along the flow. Clauser's data have also been criticized on the grounds that the layers were slightly three-dimensional (Coles and Hirst 1969) and that no turbulence measurements were taken to test the similarity of the fluctuating components. Nevertheless over 25 years Clauser's paper has remained relevant and the starting point for many useful studies of adverse pressure gradient boundary layers.

Townsend analysed Clauser's flows in the first of a series of theoretically important papers (Townsend 1956, 1960, 1961*a*,*b*, 1965*a*,*b*) through which his self-preserving‡ flow analysis emerged. Self-preserving flow is defined as a flow in which "the conditions at the initiation of flow are

† The small eddy end of the turbulence spectrum was to be excluded from this dynamic similarity.

‡ Townsend reserves the term "equilibrium" to describe a different property of turbulent flow. In Townsend's papers an equilibrium layer is one in which the turbulent energy production and dissipation are equal and considerably greater than the other turbulent energy processes, advection and diffusion.

largely irrelevant, and so the flow depends on one or two simple parameters and is geometrically similar in all stations". Townsend has developed the following procedure to determine whether a self-preserving flow is possible and if it is, what form the variation of velocity and length scales must take (*see* Townsend 1976). Firstly, self-preserving forms for the mean and fluctuating components are assumed,

$$u = U_1 + u_0 f(y/l_0) \tag{2a}$$

$$-\overline{u'v'} = u_0^2 g(y/l_0) \tag{2b}$$

$$u'^2 = u_0^2 h(y/l_0) \tag{2c}$$

$$\ldots\ldots\ldots\ldots \tag{..}$$

etc. for all flow variables

where u_0 and l_0 are (as yet) undefined velocity and length scales of the flow. These relations are substituted into the equation of motion† and for self-preserving flow to be possible, the resulting equation must be identical in meaning for all x and η. For this condition to be fulfilled coefficients in the equation must be either zero or proportional to each other. This stipulation‡ produces relationships between u_0, l_0 and x, U_1 which are the conditions for self-preserving flow. This analytical procedure has been applied to boundary layer flow in adverse pressure gradient by Townsend (1956*a*,*b*, 1961) and also by Rotta (1962). The length and velocity scales were taken as $\delta^* U_1/u_\tau$ and u_τ and the conditions for self-preserving flow were found to be

$$u_\tau/U_1 = \text{constant} \tag{3a}$$

$$(d/dx)[\delta^*(U_1/u_\tau)] = \text{constant} \tag{3b}$$

with the corollary

$$\beta_C = \text{constant} \tag{3c}.$$

Equation (3c) implies that these self-preserving layers are the equilibrium layers originally conceived by Clauser. Rotta (1962) lists six combinations of pressure gradient and wall roughness distribution that will satisfy Equation (3) and these are often termed "precise equilibrium layers" in the literature. It is certain that Clauser's layers were not precise equilibrium layers because Clauser's layers developed on smooth walls in adverse pressure gradients and Rotta's listing shows that precise equilibrium layers in zero or adverse pressure gradients require a wall roughened with a roughness geometry whose effective height increases linearly from the effective origin of the flow. Clauser's layers are therefore sometimes termed approximate equilibrium layers. The analysis shows that equilibrium layers in adverse pressure gradients require a free stream velocity variation of the form

$$U_1 = a(x - x_0)^m \qquad \text{where } m < 0 \tag{4}.$$

Subsequent workers (e.g. Bradshaw 1966, 1967; Bradshaw and Ferriss 1965) set up adverse pressure gradient equilibrium layers by producing a flow with a free stream variation given by equation (4). As these later flows were on smooth walls they also were approximate equilibrium boundary layers. To the author's knowledge only one case of a precise self-preserving layer has been observed. Perry, Schofield and Joubert (1969) reported measurements of a boundary layer in zero pressure gradient developing over a "d-type" rough wall. This unusual roughness geometry produced an effective roughness length scale that was proportional to flow development distance and thus conditions for precise equilibrium flow were fulfilled. The mean flow field showed good agreement with several predicted consequences of the layer's self-preservation.

An important piece of work was reported by Stratford (1959) who took measurements in near separating layers. Stratford aimed to produce layers in which the wall shear stress was held

† It is usually assumed that viscous and normal stress terms may be omitted. This makes the analysis easier (or possible) but restricts the analysis to flow outside the viscous sublayer and to flows not very near to separation.

‡ Which is the condition for the equations of motion to reduce to an ordinary differential equation.

at zero over an extended length. Unfortunately the data are not of high quality and the wall shear stress was probably not zero throughout. However, the flows are of enormous theoretical interest because if $u_\tau = 0$ then $\beta_C = \infty$ which is the limiting case for equilibrium boundary layers. Stratford claimed that these near separating layers did not display the usual logarithmic distributions of mean velocity near the wall† but correlated instead with a half-power law of the form

$$u \propto (\alpha y)^{1/2} + \text{constant}(\alpha\nu)^{1/3} \tag{5}.$$

Stratford presented both a mixing length and a dimensional analysis to support equation (5).

Townsend (1960, 1961*b*) and Mellor and Gibson (1966) have both theoretically analysed the limiting case of $\beta_C = \infty$. Mellor and Gibson calculated the family of defect profiles for the complete range of equilibrium layers which they gave as $-0{\cdot}5 \leqslant \beta_C \leqslant \infty$. This was done by solving the equations of motion (using Equation (1)) and closing the equations with a plausible eddy viscosity assumption. They presented theoretical curves showing good agreement with both Clauser's data ($\beta_C \simeq 1{\cdot}8$ and $8{\cdot}0$) and Stratford's data ($\beta_C \simeq \infty$). By basing their analysis on equation (1) Mellor and Gibson assumed that the velocity scale for the layers was u_τ. This assumption presented them (and subsequent authors) with conceptual problems for the case $\beta_C \to \infty$. Firstly as $\beta_C \to \infty$ the logarithmic law of the wall, which gives the inner boundary condition of the flow, disappears. Secondly the question of what a defect law based on u_τ means for the case $u_\tau \to 0$ arises. This difficulty was overcome by Mellor and Gibson by abandoning u_τ as the velocity scale for flow near separation and adopting instead a scale based on α. The choice of α as the relevant variable was prompted by the experimental evidence of Stratford that for $\beta_C \to \infty$ the inner boundary condition of the flow appears to change from a logarithmic law based on u_τ to a half-power law based on α. Thus using a velocity scale

$$u_p = (\alpha\delta^*)^{1/2} \tag{6}$$

and suitably transforming the equations of motion, Mellor and Gibson were able to calculate Stratford's profiles.

Mellor and Gibson's (1966) work includes a unique relation between Clauser's mean profile shape parameter, G, and the exponent m which defines the pressure gradient (equation (4)).‡ That is they propose a relation implying a unique equilibrium layer for a given free stream velocity variation with a limit at $m = -0{\cdot}23$ (after which no equilibrium layer can exist). This conclusion is at variance with Townsend's (1961) approximate calculations that show for large negative m two alternative equilibrium layers can exist. Head (1976) applying the integral calculation method of Head and Patel (1970) to the flows of Bradshaw (1966) presents results supporting:

(i) the existence of a wide range of possible equilibrium boundary layers for $m = -0{\cdot}255$. These different equilibrium layers are generated by different initial momentum thicknesses;

(ii) only one equilibrium boundary layer for $m > -0{\cdot}255$;

(iii) no equilibrium layers possible for $m = -0{\cdot}35$. Bradshaw (1966), however, concluded that probably only one equilibrium layer is possible at any value of m. The resolution of these differences is an important aim of the work presented here.

Another consequence of Stratford's work was that his reported half-power law, Equation (5), inspired a series of papers (Townsend 1961; Perry, Bell and Joubert 1966; Perry 1966; McDonald 1969; Schofield and Perry 1972; Perry and Schofield 1973; Kader and Yaglom 1978) devoted to half-power distributions of mean velocity in non-equilibrium adverse pressure gradient boundary layers not necessarily near separation. There is disagreement in this literature but a conservative summary of conclusions would include—

† Coles and Hirst's (1968) detailed analysis shows that most of the profiles have in fact very small logarithmic regions.

‡ The relationship does involve a weak dependence on Reynolds number, but the relationship between G and m is effectively single valued.

(i) Half-power distributions exist in all turbulent boundary layers developing in moderate to strong adverse pressure gradients.

(ii) The half-power distribution lies outside the logarithmic region and joins it tangentially or with a very small blending region.

(iii) Half-power laws based on α, cannot give accurate descriptions of a large proportion of the half-power distributions observed (*see* for instance, Schofield and Perry 1972; Perry and Schofield 1973; Kader and Yaglom 1978; Yaglom 1979). As Stratford's half-power law based on α does not appear to be universal it is instructive to examine the type of arguments presented in support of α as the dominant variable within the half-power regime. Kader and Yaglom (1978) have recently presented the argument in detail. They start by noting that near the wall where inertia forces are small the equation of motion can be approximated by

$$\tau(y) \simeq \tau_0 + \rho\alpha y \tag{7}$$

(*see* Townsend 1976, Section 5.2) where the accuracy of the approximation depends on the relative magnitude of the mean flow inertia forces. If α is large and τ_0 small then $\tau(y)$ outside the logarithmic region is largely determined by α and thus α is seen as more important than τ_0 in determining mean flow distribution. This is, however, unsatisfying, as α and τ_0 are different types of boundary layer parameters; α is an externally set input variable to the flow while τ_0 is a flow response variable. If τ_0 determines the flow near the wall (in the logarithmic region) it seems plausible that in an adjacent region where its relative magnitude is reduced it should be replaced by a variable of the same type, i.e. another shear stress. The Schofield and Perry (1972) (*see also* Perry and Schofield 1973) half-power law was therefore based on the maximum shear stress in the layer (τ_m) and uses the velocity scale U_m defined as

$$U_m = \sqrt{\tau_m/\rho} \tag{8}$$

This half-power law, discussed in detail in the next section, was found to accurately describe 145 half-power distributions analysed by Schofield and Perry (1972). They showed that this half-power law was the analytical expression of the inner part of a mean velocity defect law based on U_m that applied from the free stream almost to the wall for *all* adverse pressure gradient layers provided only that $\tau_m \geqslant 3\tau_0/2$. The validity of this defect law has been extensively demonstrated in Schofield and Perry (1972), Perry and Schofield (1973) and Perry and Fairlie (1975) and is further demonstrated in this report. Unlike previous defect laws based on u_τ that have been used to describe (equilibrium) adverse pressure gradient boundary layers the Schofield and Perry defect law has an invariant analytical form for all pressure gradients. It is applied here to the analysis of equilibrium boundary layers in adverse pressure gradient flows resulting in:

(i) a particularly economical description of the mean profile;

(ii) prediction of the shear stress profile of any equilibrium boundary layer;

(iii) a set of conditions for the existence of equilibrium boundary layers in adverse pressure gradients.

The results represent a significant improvement on recent work by Kader and Yaglom (1978) who retain α as a variable in their defect law. By retaining α, their analytical description of the mean profile requires a set of complicated equations separated by complex blending functions. Also the Kader and Yaglom defect law does not describe the data as accurately as the Schofield and Perry defect law. This is shown in Figure 1. In addition Kader and Yaglom's half-power relation is complex and conceptually unsatisfying in that they initially argue that u_τ is not important in the half-power region but later are forced to reintroduce u_τ into their half power relation in order to describe all the half-power distributions reported in the literature. It is noted that if in the dimensional analysis, on which the Kader and Yaglom work is based, $\alpha\delta$ had been replaced by U_m^2, the Schofield and Perry relations could have been derived.

2. SIMILARITY LAWS IN ZERO AND ADVERSE PRESSURE GRADIENT BOUNDARY LAYERS

The accepted model for zero pressure gradient boundary layers is a laminar sublayer

immediately adjacent to the wall blending into the logarithmic law of the wall

$$u/u_\tau = (1/\kappa)\log_e(yu_\tau/\nu) + A \tag{9}$$

This logarithmic law forms the innermost part of a velocity defect law which describes the mean profile from the sublayer to the free stream. This defect law is accurately described by

$$(U_1-u)/u_\tau = 9{\cdot}6(1-y/\Delta)^2 \tag{10}$$

where Δ is Clauser's integral thickness ($= 0{\cdot}3\delta^* U_1/u_\tau$).

The model proposed by Schofield and Perry (1972) is similar in form but applies to attached boundary layers in moderate to strong adverse pressure gradients (specifically layers in which $\tau_m \geqslant 3\tau_0/2$). The model consists of the same laminar sublayer and (a smaller) logarithmic law that tangentially joins a half-power law of the form

$$u/U_1 = 0{\cdot}80(yU_m^2/LU_1^2)^{1/2} + 1 - (U_s/U_1) \tag{11a}$$

$$= 0{\cdot}47(U_s/U_1)^{3/2}(y/\delta^*)^{1/2} + 1 - (U_s/U_1) \tag{11b}$$

This half-power law forms the innermost part of the defect law which describes the mean profile from the sublayer to the free stream. This defect law is accurately described by

$$\left.\begin{aligned}(U_1-u)/U_s &= 1-0{\cdot}4(y/B)^{1/2}-0{\cdot}6\sin[(\pi/2)(y/B)]\\ &= f(y/B)\end{aligned}\right\} \tag{12}$$

where B is an integral layer thickness [$= 2{\cdot}86\delta^*(U_1/U_s)$].

The velocity scale U_s is a slip velocity determined by extrapolating the half-power relations, equation (11), to $y = 0$. It has been shown by Schofield and Perry (1972) that it is related to U_m by

$$U_s = 8{\cdot}0(B/L)^{1/2}U_m \tag{13}$$

which is a notable equation in as much as it relates mean flow parameters to a turbulent flow parameter. It is discussed further in the following section.

Perry and Schofield (1973) have also shown that the height (y_c) of the tangential junction between the logarithmic layer and the half-power layer is given by

$$y_c/B = 37{\cdot}1(u_\tau^2/U_s^2) \tag{14}$$

from which it easily follows that

$$y_c = 18{\cdot}6c_f'(U_1/U_s)^2 B \tag{15}$$

For a boundary layer held at incipient separation where $c_f' = 0$, Equation (15) shows that $y_c = 0$ which implies that in this case the half-power law extends to the wall and there is no logarithmic layer.† This disappearance of the logarithmic region as separation is approached is consistent with Stratford's results and with the well known observation that the vertical extent of the logarithmic region decreases as the strength of an adverse pressure gradient increases. The boundary layers considered in this report all developed in moderate to strong adverse pressure gradients and hence have small logarithmic regions with half-power regions extending down nearly to the wall. Consequently the Schofield and Perry model gives an accurate description of mean velocity data from the free stream down to about $y = 0{\cdot}02\delta$ (*see* Figures 2*b*, 6 and 8, also Schofield and Perry 1972). This description of the mean flow is the basis for the analysis presented in Section 3.

U_κ can be determined by adapting Clauser's methodology to the half-power law. The Clauser (1954) method determines the velocity ratio u_τ/U_1 from the logarithmic law, equation (9). This is done by rewriting equation (9) as

$$u/U_1 = (u_\tau/\kappa U_1)\log_e(yU_1/\nu) + (u_\tau/\kappa U_1)\log_e(u_\tau/U_1) + (u_\tau/U_1)A \tag{16}$$

† Obviously this can only be an approximation as no account of the laminar sublayer has been made.

then plotting the mean profile on co-ordinates u/U_1, $\log_e y(U_1/\nu)$ and comparing it with the family of straight lines given by equation (16) for different values of u_τ/U_1 (*see* Fig. 2*a*). In a similar manner the velocity ratio U_s/U_1 can be determined from equation (11b). The mean profile is plotted on co-ordinates u/U_1, $(y/\delta^*)^{1/2}$ and is compared with the family of straight lines given by equation (11b) for different values of U_s/U_1, as shown in Figure 2*b*. Note that in this example the Schofield and Perry model accurately describes the data down to a distance of only $0{\cdot}004\delta$ from the wall.

2.1 Defect Law and Large Turbulent Structure

The central equation to the theory of Schofield and Perry is equation (13) which was arrived at from a consideration of models for the shear stress distribution (*see* Perry and Schofield 1973). The equation is, however, consistent with current ideas on large turbulence structures in turbulent flows. Although the presence of large coherent structures in turbulent flows has long been discussed (Townsend 1956*b*; Grant 1958), the recent work of Brown and Roshko (1974) has strikingly demonstrated their existence. Brown and Roshko showed that a mixing layer consisted of a train of large roller eddies that did not change with Reynolds number. This large eddy pattern was shown to control the mean velocity distribution and the entrainment rate of the layer. Work by Bradshaw (1966) and Townsend (1979) implies that similar large coherent structures dominate boundary layer flow and that as the adverse pressure gradient of a layer is increased the proportion of the turbulence field occupied by large structures increases. Bradshaw (1966) showed that these large structures in adverse pressure gradient layers scaled on U_m^2/U_1. Thus it seems probable that in a boundary layer that is developing in a strong adverse pressure gradient there are large turbulent structures that:

(i) determine the entrainment of the layer and hence its overall thickness;

(ii) determine the mean velocity distribution;

(iii) have a velocity scale related to U_m.

It would seem reasonable therefore that for these types of layers a mean velocity scale should be described by the boundary layer thickness and U_m. This is what equation (13) does, viz.

$$U_s^2 = 64U_m^2(B/L).$$

Perry and Schofield show that equation (13) only applies to layers in which $\tau_m \geqslant (3/2)\tau_0$. This limit is consistent with Bradshaw's (1966) finding that large turbulence structures become increasingly more important as the pressure gradient (and hence τ_m/τ_0) of boundary layers increase.

3. ANALYSIS

Consider a two-dimensional turbulent boundary layer in an adverse pressure gradient sufficiently strong for τ_m to be at all times $\geqslant(3/2)\tau_0$. For such a layer the Schofield and Perry defect law will give an accurate description of the mean velocity profile from the free stream down to a small distance from the wall. Following Townsend, self-preserving forms for the mean and fluctuating flow are assumed. However, in this case the Schofield and Perry scales were used, viz.

$$u = U_1 - U_s f(y/B) \tag{12}$$

$$-\overline{u'v'} = -U_s^2 g(y/B) \tag{17}$$

These relations are substituted into the equation of motion

$$u(\partial u/\partial x) + v(\partial u/\partial y) + (\partial/\partial y)(\overline{u'v'}) = U_1(dU_1/dx) \tag{18}$$

where the viscous and quadratic turbulence terms have been omitted. The continuity equation

$$\partial u/\partial x + \partial v/\partial y = 0 \tag{19}$$

is used to eliminate the mean vertical velocity (v) leading to (*see* Appendix 1),

$$f\frac{d}{dx}(-U_1U_s)+\frac{U_s}{B}\frac{d}{dx}(U_1B)\eta f'+U_s\frac{dU_s}{dx}f^2-\frac{U_s}{B}f\frac{d}{dx}(U_sB)\int_0^\eta f d\eta=-\frac{U_s^2}{B}g' \tag{20}$$

where $f=f(y/B)$, $g=g(y/B)$, $\eta=y/B$ and the primes denote differentiation with respect to η. Integration gives

$$-\frac{d}{dx}(U_1U_s)\int_\mu^\eta f d\eta+\frac{Us}{B}\frac{d}{dx}(U_1B)\int_\mu^\eta \eta f' d\eta+U_s\frac{dU_s}{dx}\int_\mu^\eta f^2 d\eta$$
$$-\frac{U_s}{B}\frac{d}{dx}(U_sB)\int_\mu^\eta\left\{f'\int_0^\eta f d\eta\right\}d\eta=-\frac{U_s^2}{B}\int_\mu^\eta g' d\eta \tag{21}$$

where $\mu=\epsilon/B$ and is the limiting non-dimensional distance at which $f(\eta)$ describes the mean velocity within some prescribed accuracy band.† Introducing the following notations and substitutions:

$$\int_\mu^\eta f d\eta=I_1(\eta),\qquad \int_\mu^\eta f^2 d\eta=I_2(\eta),\qquad \int_0^\mu f(\eta)d\eta=I_\mu,$$
$$\int_\mu^\eta \eta f' d\eta=\eta f-I_1(\eta)-\mu f(\mu),$$
$$\int_\mu^\eta\left\{f'\int_\mu^\eta f d\eta\right\}d\eta=fI_1(\eta)-I_2(\eta)-f(\mu)I_1(\eta)$$

modifies equation (21) to

$$\frac{d}{dx}(U_1U_s)I_1(\eta)-\frac{U_s}{B}\frac{d}{dx}(U_1B)\left(\eta f-I_1(\eta)-\mu f(\mu)\right)-U_s\frac{dU_s}{dx}I_2(\eta)$$
$$+\frac{U_s}{B}\frac{d}{dx}(U_sB)\left(fI_1(\eta)-I_2(\eta)+\left(f-f(\mu)\right)I_\mu\right)=\frac{U_s^2}{B}\left(g(\eta)-g(\mu)\right) \tag{22}.$$

For self-preserving flow equation (22) must be identical in meaning for all x, that is coefficients of functions of η must be zero or in constant ratio. It is simply demonstrated (Appendix 1) that the relations:

$$U_1=aX^m=a(x-x_0)^m \tag{23a}$$
$$U_s=bX^m=b(x-x_0)^m \tag{23b}$$
$$B=cX=c(x-x_0) \tag{23c}$$

satisfy the condition, as substituting them into equation (22) leads to

$$2mabI_1(\eta)-mb^2I_2(\eta)-ab(m+1)\left(\eta f-\mu f(\mu)-I_1(\eta)\right)+$$
$$+b^2(m+1)\left(fI_1(\eta)-I_2(\eta)+\left(f-f(\mu)\right)I_\mu\right)=\frac{b^2}{c}\left(g(\eta)-g(\mu)\right) \tag{24}$$

which is independent of x. Equations (23) are thus the conditions for self-preserving or precise equilibrium flow.

3.1 Shear Stress Distribution

The shear stress distribution in these self-preserving layers may be obtained from equation (24). Rearranging equation (24) gives

† Set here at 3%.

$$g(\eta) = g(\mu) + \frac{ac}{b}(3m+1)I_1(\eta) - c(2m+1)I_2(\eta) - \frac{ac}{b}(m+1)\left(\eta f - \mu f(\mu)\right) +$$

$$+ c(m+1)\left[f I_1(\eta) + f I_\mu - f(\mu) I_\mu\right] \tag{25}$$

Now as

$$\frac{\tau(\eta)}{\frac{1}{2}\rho U_1^2} = -\frac{2(\overline{u'v'})}{U_1^2} = -\frac{2U_s^2}{U_1^2} g(\eta) = -\frac{2b^2}{a^2} g(\eta),$$

$$g(\eta) = -\frac{a^2}{2b^2}\left(\frac{\tau(\eta)}{\frac{1}{2}\rho U_1^2}\right) \tag{26}$$

Similarly

$$g(\mu) = -\frac{a^2}{2b^2}\left(\frac{\tau(\mu)}{\frac{1}{2}\rho U_1^2}\right).$$

The unknown $\tau(\mu)$ can be eliminated by evaluating equation (7) at $y = \mu B$ to give

$$\frac{\tau(\mu)}{\frac{1}{2}\rho U_1^2} \simeq c_f' + \frac{2B\alpha\mu}{U_1^2}$$

which will be an accurate approximation as μ is small.† Substitution gives

$$g(\mu) \simeq -\frac{a^2}{2b^2}\left(c_f' + \frac{2B\alpha\mu}{U_1^2}\right) \tag{27}$$

Finally $B\alpha/U_1^2$ is evaluated using the expression for the free stream velocity variation, equations (23). This gives

$$\frac{B\alpha}{U_1^2} = -\frac{1}{U_1}\frac{dU_1}{dx} B = -\frac{ma^2 X^{2m-1} cX}{a^2 X^{2m}} = -mc.$$

For $\mu = 0{\cdot}02$ (an average value used throughout this report‡) equation (27) becomes

$$g(\mu) = \frac{a^2}{2b^2}(0{\cdot}04mc - c_f').$$

Substituting this and equation (26) into equation (25) gives

$$\frac{\tau(\eta)}{\frac{1}{2}\rho U_1^2} = c_f' - 0{\cdot}04mc - \frac{2cb^2}{a^2}\left(\frac{a}{b}(3m+1)I_1(\eta) - (2m+1)I_2(\eta) - \frac{a}{b}(m+1)\left(\eta f - \mu f(\mu)\right) +\right.$$

$$\left. + (m+1)\left[f I_1(\eta) + f I_\mu - f(\mu) I_\mu\right]\right).$$

It is convenient to introduce the entrainment parameter (*see* Townsend 1976) defined as

$$\gamma = \frac{U_1 + \frac{1}{2}u_0}{|u_0|}\frac{dl_0}{dx}$$

which for the velocity and length scales used here becomes

$$\gamma = \left(\frac{U_1}{U_s} - \frac{1}{2}\right)\frac{dB}{dx} = \left(\frac{a}{b} - \frac{1}{2}\right)c.$$

† See Figure 3 which gives typical results for μ. Also shown are values of y_c, the height of the tangential junction between the logarithmic and half-power laws, which correlates with the theoretical relation, equation (15).

‡ The actual value adopted for μ, so long as it is small, has a very minor influence on subsequent calculations.

The equation for shear stress through the layer is then given by

$$\frac{\tau(\eta)}{\frac{1}{2}\rho U_1^2} = c_f' - \frac{0{\cdot}04m\gamma}{\left(\frac{a}{b}-\frac{1}{2}\right)} - \frac{2\gamma}{\frac{a^2}{b^2}\left(\frac{a}{b}-\frac{1}{2}\right)}\left\{\frac{a}{b}(3m+1)I_1(\eta)-(2m+1)I_2(\eta) - \frac{a}{b}(m+1)\right.$$
$$\left.\left(\eta f-\mu f(\mu)\right)+(m+1)\left(fI_1(\eta)+fI_\mu-f(\mu)I_\mu\right)\right\} \qquad (28).$$

3.2 Free Stream Velocity Variation

Equation (28) can be used to give an explicit equation for the free stream velocity variation exponent (m). Rearranging equation (26) gives

$$m = -\frac{\left[\frac{a}{b}I_1(\eta)-I_2(\eta) - \frac{a}{b}\left(\eta f-\mu f(\mu)\right)+fI_1(\eta)+fI_\mu-f(\mu)I_\mu\right] - \frac{a^2}{2\gamma b^2}\left(\frac{a}{b}-\frac{1}{2}\right)\left[c_f' - \frac{\tau(\eta)}{\frac{1}{2}\rho U_1^2}\right]}{\left[0{\cdot}02\frac{a^2}{b^2}+3\frac{a}{b}I_1(\eta)-2I_2(\eta) - \frac{a}{b}\left(\eta f-\mu f(\mu)\right)+fI_1(\eta)+fI_\mu-f(\mu)I_\mu\right]} \qquad (29).$$

For the case $\eta = 1, f(1) = 0$ and $\tau(1) = 0$, this equation becomes

$$m = -\left\{\frac{\frac{a}{b}\left(I_1(1)+\mu f(\mu)\right)-I_2(1)-f(\mu)I_\mu - \frac{c_f'a^2}{2\gamma b^2}\left(\frac{a}{b}-\frac{1}{2}\right)}{0{\cdot}02\frac{a^2}{b^2}+\frac{a}{b}\left(3I_1(1)+\mu f(\mu)\right)-2I_2(1)-f(\mu)I_\mu}\right\} \qquad (30).$$

For practical values of c_f'/γ, the influence of c_f'/γ in this equation is weak and thus m is essentially a function of U_1/U_s. Equations similar to (30) can be found in the literature based on the velocity ratio u_τ/U_1 (Townsend 1976). The difference and advantage of equation (30) is that it is based on the defect law given by Equation (12) which contains no empirical parameters and is invariant with pressure gradient. Thus the function f, the integrals I_1, I_2 and their products are functions of η alone. The functions are derived in Appendix 2, tabulated in Appendix 4, and are plotted in Figure 4.

Equations (28), (29) and (30) apply to all equilibrium layers in adverse pressure gradients of sufficient strength for $\tau_m/\tau_0 \geqslant 3/2$, which is the condition for equation (12) to be valid. Inspection of equation (30) shows that, for any equilibrium layer where m, a/b, c (and hence γ) are all constant, c_f' must also be constant. The appearance of c_f' in Equation (30) arises from the inner boundary condition of the half-power law (at approximately $0{\cdot}02\delta$). Unlike previous analyses the condition of constant c_f' is here a corollary to the analysis and not a central feature of it.

3.3 Pressure Gradient Parameter

Clauser's non-dimensional force ratio may be written

$$\beta_C = \frac{\delta^*}{\tau_0}\frac{dp}{dx} = -\frac{\delta^* U_1}{u_\tau^2}\frac{dU_1}{dx}$$

This is the relevant parameter for flows in pressure gradients near zero where τ_0 and the logarithmic region is large. For flows in moderate to strong pressure gradients where the influence of τ_0 is small and the logarithmic region is thin it is argued here that U_s replaces u_τ as the appropriate velocity scale of the mean flow. In this case the appropriate force ratio is

$$\beta^* = -\frac{\delta^*}{U_s^2}U_1\frac{dU_1}{dx} \qquad (31).$$

By using the definition for $\beta(=2{\cdot}86\delta^*(U_1/U_s))$ and the equations for self-preserving flow (equations (23)) equation (31) may be written

$$\beta^* = -\frac{cXma X^{m-1}}{2{\cdot}86bX^m} = -\frac{mca}{2{\cdot}86b} \qquad (32)$$

which is obviously constant for an equilibrium layer.

3.4 Existence Limits for Equilibrium Layers in Adverse Pressure Gradients

There are three existence conditions for the equilibrium layers analysed here. They are:

(i) $m < 0$, the condition for adverse pressure gradient flow;

(ii) $c_f' \geqslant 0$, the condition for attached flow;

(iii) $\tau_m/\tau_0 \geqslant 3/2$, the condition for moderate to strong adverse pressure gradient flow to which the Schofield and Perry defect law applies.

Condition (ii) can be made explicit in terms of the flow parameters m, a/b by substituting $c_f' = 0$ in Equation (30) which gives

$$m = -\frac{\frac{a}{b}\left(I_1(1)+\mu f(\mu)\right)-I_2(1)-f(\mu)I_\mu}{0{\cdot}02\frac{a^2}{b^2}+\frac{a}{b}\left(3I_1(1)+\mu f(\mu)\right)-2I_2(1)-f(\mu)I_\mu} \tag{33}$$

Condition (iii) can also be made explicit. At $\eta = \eta_m$ and $\tau(\eta_m) = \tau_m$. Equation (29) becomes

$$m = -\frac{\left\{\frac{a}{b}I_1(\eta_m)-I_2(\eta_m)-\frac{a}{b}\left(\eta_m f(\eta_m)-\mu f(\mu)\right)+f(\eta_m)I_1(\eta_m)+f(\eta_m)I_\mu-f(\mu)I_\mu\right\}-\frac{a^2}{2\gamma b^2}\left(\frac{a}{b}-\frac{1}{2}\right)\left(c_f'-\frac{\tau_m}{\frac{1}{2}\rho U_1^2}\right)}{\left\{0{\cdot}02\frac{a^2}{b^2}+3\frac{a}{b}I_1(\eta_m)-2I_2(\eta_m)-\frac{a}{b}\left(\eta_m f(\eta_m)-\mu f(\mu)\right)+f(\eta_m)I_1(\eta_m)+f(\eta_m)I_\mu-f(\mu)I_\mu\right\}} \tag{34}$$

Now for the limiting condition of

$$\tau_m = (3/2)\tau_0 \qquad \text{or} \qquad U_m^2 = (3/2)u_\tau^2 \tag{35}$$

equation (34) becomes

$$m = -\frac{\left\{\frac{a}{b}\left(I_1(\eta_m)-\eta_m f(\eta_m)+\mu f(\mu)\right)-I_2(\eta_m)+f(\eta_m)I_1(\eta_m)+f(\eta_m)I_\mu-f(\mu)I_\mu\right\}+\frac{c_f'}{\gamma}\frac{a^2}{4b^2}\left(\frac{a}{b}-\frac{1}{2}\right)}{0{\cdot}02\frac{a^2}{b^2}+\frac{a}{b}\left(3I_1(\eta_m)-\eta_m f(\eta_m)+\mu f(\mu)\right)-2I_2(\eta_m)+f(\eta_m)I_1(\eta_m)+f(\eta_m)I_\mu-f(\mu)I_\mu} \tag{36}$$

The value of η_m is given by equation (13), as

$$\eta_m = L/B = 64(U_m^2/U_s^2)$$

so that by using equation (35) this becomes

$$\eta_m = 48c_f'(a^2/b^2) \tag{37}$$

Equations (33) and (36) define a space with co-ordinates m, a/b within which all equilibrium layers based on scales U_s and B exist. The limit defined by equation (36) depends (fairly weakly) on c_f'/γ. Most of the "equilibrium layer" space is shown in Figure 5.

4. COMPARISON OF THEORY AND DATA

4.1 Mean Flow

The above analysis applies to attached flows with a free stream velocity variation of the form

$$U_1 = aX^m \tag{23a}$$

where m is sufficiently negative for

$$\tau_m \geqslant (3/2)\tau_0.$$

Consequently the literature was searched for flows with a free stream velocity distribution described by equation (23a). Nine such flows were found, analysed and compared with the theory.

Firstly the mean profiles were analysed to ensure they displayed half-power distributions of velocity near the wall. All 46 profiles exhibited extensively half-power regions. By comparing the data points with the family of lines given by equation (11b) the velocity ratio U_1/U_s was determined for each profile. Figure 7 shows that U_1/U_s $(= a/b)$ was closely constant for each layer and this is one of the requirements for the existence of an equilibrium layer (equations (23a,b)). Figure 6 confirms that the data is accurately described by the Schofield and Perry (1972) half-power law for values of y down to about $0{\cdot}02B$ from the wall. The only data where this limit is significantly exceeded is from a layer very close to separation (Stratford flow 6, layer IX) where the profiles show poor agreement with the half-power law close to the wall. Theoretical predictions for this layer must be less accurate than for other layers. Results for this layer are further discussed at the end of the Section.

Using values of U_s determined from the half-power distribution, the profiles were tested against the full defect law of Schofield and Perry (Equation (12)) as shown in Figure 8. The agreement was good and typical of previous results for non-equilibrium layers (*see* Perry and Schofield 1973; Simpson, Strickland and Barr 1977; Perry and Fairlie 1975).

As values for U_1/U_s had been determined the layer thicknesses (B) could be calculated and these are plotted against distance in Figure 9. The layer growth rate (c) was constant in all layers. Thus Equation (23c) was satisfied and with it all conditions for self-preserving flow for all nine layers. This result supports Townsend's contention (Townsend 1961) that if self-preserving flow is possible it usually occurs. Figure 9 was used to determined both c and the effective origin x_0 of each layer. Layer growth rates did not show the constancy for different layers assumed by Kader and Yaglom (1978), in fact they showed considerable variation† ($0{\cdot}03$ to $0{\cdot}10$) around the value of $0{\cdot}063$ used by Kader and Yaglom. The values of c were used to calculate the entrainment and pressure gradient parameters γ, β^*; these and values of c_f' determined using Clauser's method (equation (16)) are shown in Figure 7. They are substantially constant for each layer as required by the analysis.

Free stream velocity variations with distance are shown for all layers in Figure 10. Logarithmic co-ordinates are used to show the linear variation required by equation (23a). Values of x_0 determined from Figure 9 were used to calculate the abscissae $(x-x_0)$. The figure shows that all velocity variations have good linearity on these co-ordinates.‡ The lines joining the points on the figure have slopes predicted theoretically by equation (30) and the excellent agreement displayed in each case gives good support to the theory.

Values determined in this analysis of data, enable the layers to be positioned on the m, a/b co-ordinates and compared with the theoretical limits for existence of equilibrium layers. This is done in Figure 5 where it is shown that all nine layers fall within the limits set theoretically by Equations (33) and (37). It is seen that a wide range of equilibrium boundary layers has been observed and they all fall within the limits given by the analysis. It is obvious that different equilibrium layers can exist in the same pressure gradient; for instance layers II and IX have similar free stream velocity variations ($m = -0{\cdot}223$ and $-0{\cdot}219$) and yet have very different U_1/U_s velocity ratios. The equilibrium boundary layer that develops in a given pressure gradient will depend on the initial conditions of the layer on entry into the equilibrium pressure gradient, i.e. its initial velocity ratio and thickness.

Figure 5 shows that equilibrium layers can exist for values of m from above $-0{\cdot}10$ to about $-0{\cdot}30$ for practical flows. Thus Head's (1976) conclusion that no equilibrium layer was possible for $m = -0{\cdot}35$ is correct but the limiting value is too low. However, his conclusion that a wide range of equilibrium layers was possible for $m = -0{\cdot}255$ accords with Figure 5. It also

† All derived data is tabulated in Appendix 3.

‡ This fact is not very significant as plotting data on log-log co-ordinates is an undiscerning way to present data. Thus x_0 was not determined from these plots, as for each layer a wide range of values for x_0 gave results that showed good linearity on these co-ordinates.

follows from Figure 5 that two central conclusions of Mellor and Gibson (1966) are not supported by the present work. They are the conclusions that there is only one equilibrium layer for a given value of m and that this single sequence of equilibrium layers terminates at $m = -0{\cdot}23$.

Mellor and Gibson (1966) and Townsend (*see* Townsend 1960, 1976) have both made (approximate) calculations of the idealized Stratford flow ($\beta_C = \infty$, $c_f' = 0$) which give

$$m = -0{\cdot}255,\ u_0/U_1\dagger = 0{\cdot}81.$$

This result is in fair agreement with Figure 5 where the point $m = -0{\cdot}225$ on the $c_f' = 0$ curve corresponds to a U_1/U_8 velocity ratio of 0·96. The actual Stratford flow nearest the condition $c_f' = 0$ (layer IX) is very close to this point at $m = -0{\cdot}22$, $U_1/U_8 = 0{\cdot}96$, $c_f' = 0{\cdot}54\times10^{-3}$. Conclusions regarding measurements in this layer must, however, be somewhat guarded as the profiles show the poorest agreement with the Schofield and Perry defect law, particularly near the wall (*see* Figs. 3, 6 and 8). Because this layer was so close to separation it was an extremely difficult experimental situation in which to get reliable data near the wall. Any analysis of the wall flow is made additionally difficult by the sparsity of data points that were recorded near the wall by Stratford. In addition the dropping of the viscous and quadratic turbulence terms from the equation of motion means that the analysis will be at its most inaccurate for incipiently separating layers.

4.2 Shear Stress

Because the analysis presented here employs an invariant analytical expression for the mean flow profile, it is possible using equation (28) to obtain the (invariant) shear stress profile for any equilibrium layer from a knowledge of m, c_f', U_1/U_8 and c. As the experimentally derived values of c_f' and U_1/U_8 showed some (small) variation the following calculations are based on average values of c_f', U_1/U_8. Values of m were those predicted by equation (30).

Theoretically predicted shear stress profiles for all nine layers are shown in Figure 11. The profiles are of course forced to agree with the boundary conditions at the wall where $\tau(0)/\frac{1}{2}\rho U_1^2 = c_f'$. However, in all cases the calculated value of the shear stress at the free stream, where no agreement with the data is forced, was zero to a very high order of accuracy. Figure 11 shows that η_m, the position of maximum shear stress, moves away from the wall as the shear stress ratio τ_m/τ_0 increases. It varies from 0·3 for the limiting case of $\tau_m/\tau_0 = 1{\cdot}5$, to 0·45 for $\tau_m/\tau_0 = 30$, the largest shear stress ratio considered.

Fortunately shear stress profiles in four of the layers were measured allowing comparisons with measurements. Figure 12 compares predicted and measured profiles for moderate (Bradshaw 1966), medium (Samuel 1973) and strong (Bradshaw and Ferris 1967) adverse pressure gradient layers. In all cases agreement is good.‡ The agreement could be marginally improved in all three cases if the actual value for c_f' at the shear stress measuring station was used rather than the average layer value.

The remaining shear stress measurements are by Bradshaw (1967) (layer VI) for a flow that developed initially in zero pressure gradient before entering a strong equilibrium adverse pressure gradient. The approach of the shear stress profiles towards their new equilibrium form is strikingly shown in Figure 13 where successive experimental shear stress profiles are compared with the distribution the layer had in zero pressure gradient flow and its theoretical distribution for the equilibrium adverse pressure gradient. As with all turbulent boundary layers responding to a change in boundary conditions, the layer adjusts rapidly near the wall where the time scale of the turbulence is small. Further modification of the profile (through the large turbulence structure) is slower working outwards from the wall. In this case the process is all but complete at the last recorded profile.

† The assumed analytical form for the incipient separating mean velocity profiles was significantly different from equation (12). Thus u_0 though a similar type of velocity scale to U_s was not identical to it.

‡ The author is indebted to Professor Bradshaw for providing the original data points for two of these profiles.

5. CONCLUSIONS

(1) Self-preserving or precise equilibrium boundary layers based on the length and velocity scales proposed by Schofield and Perry exist in moderate to strong adverse pressure gradient flows. These scales are based on the maximum shear stress in the layer which is the dominant shear stress for flow approaching separation. These scales are the counterpart to u_τ and Δ for equilibrium boundary layers in pressure gradients near zero where the wall shear stress and the maximum shear stress in the layer are of similar magnitudes.

(2) The equilibrium layers are produced by moderate to strong adverse pressure gradient flows that have free stream velocity variations of the form

$$U_1 = aX^m.$$

Equilibrium boundary layers exist for values of m in the range $\sim 0{\cdot}3 > -m > \sim 0{\cdot}1$. This result does not agree with the Mellor and Gibson (1966) result that no equilibrium layers are possible in flows where $m < -0{\cdot}23$.

(3) For any equilibrium flow a range of equilibrium boundary layers can develop depending on the initial conditions of the layer entering the equilibrium pressure gradient. This result agrees with the calculations of Head (1976) but is contrary to those of Mellor and Gibson (1966) that predict a unique equilibrium layer for any particular pressure gradient.

(4) The flow parameters for all experimentally observed equilibrium boundary layers fall within limits theoretically derived using the Schofield and Perry defect law and the equations of motion. Approximate calculations of flow parameters by Townsend (1960), for an idealized flow in which the wall shear is held at zero throughout, agree with these results.

(5) As the Schofield and Perry defect law is invariant for any layer in which it is valid (i.e. for any layer in which $\tau_m/\tau_0 \geqslant 3/2$) the shear stress profile for any equilibrium boundary layer can be calculated from a knowledge of the initial conditions of the flow entering the equilibrium pressure gradient. Predicted shear stress profiles show good agreement with experimental data.

(6) The shear stress profile of a boundary layer moving from a zero to an adverse equilibrium pressure gradient adjusts outwards from the wall. The initial adjustment near the wall is rapid but is much slower in the outer layer.

REFERENCES

Abramowitz, M., and Stegun, I. A. (1965), *Handbook of Mathematical Functions*, Dover.

Bradshaw, P. (1966), NPL Aero. Rept. 1184; *see also* shortened version in *J. Fluid Mech.*, 1967, **29**, 625.

Bradshaw, P. (1967), NPL Aero. Rept. 1219.

Bradshaw, P., and Ferris, D. (1965), NPL Aero. Rept. 1145.

Brown, G. L., and Roshko, A. (1974), *J. Fluid Mech.* **64**, 775.

Coles, D. E., and Hirst, E. A. (1968), AFOSR—IFP—Stanford 1968 Conf. on Turbulent Boundary Layer Prediction, Vol 2.

Clauser, F. (1954), *Journal of the Aero. Sci.* **21**, 91.

Fairlie, B. D. (1973), Ph.D. Thesis, University of Melbourne.

Grant, H. L. (1958), *J. Fluid Mech.* **4**, 149.

Hama, F. R. (1954), *Trans. Soc. Naval Arch. and Mar. Eng'gs* **22**, 333.

Head, M. R. (1976), *J. Fluid Mech.* **73**, 1.

Head, M. R., and Patel, V. C. (1970), Aero. Res. Counc. R. & M. 3643.

Kader, B. A., and Yaglom, A. M. (1978), *J. Fluid Mech.* **89**, 305.

Klebanoff, P. S. (1954), NACA TN 3178.

Ludwieg, H., and Tillmann, W. (1949), *Ing.-Arch.* **17**, 288; transl. NACA TM 1285 (1950).

McDonald, H. (1969), *J. Fluid Mech.* **35**, 311.

Mellor, G. L., and Gibson, D. M. (1966), *J. Fluid Mech.* **24**, 225.

Perry, A. E. (1966), *J. Fluid Mech.* **26**, 481.

Perry, A. E., Bell, J. B., and Joubert, P. N. (1966), *J. Fluid Mech.* **25**, 299.

Perry, A. E., Schofield, W. H., and Joubert, P. N. (1969), *J. Fluid Mech.* **37**, 383.

Perry, A. E., and Schofield, W. H. (1973), *Phys. of Fluids* **16**, 2068.

Perry, A. E., and Fairlie, B. D. (1975), *J. Fluid Mech.* **69**, 657.

Rotta, J. C. (1962), *Prog. in Aero. Sci.* **2**, 3 (Ferri-Pergamon).

Samuel, A. E. (1973), Ph.D. Thesis, University of Melbourne; *see also* Samuel, A. E., and Joubert, P. N. (1974), *J. Fluid Mech.* **66**, 481.

Schofield, W. H. (1969), Ph.D. Thesis, University of Melbourne.

Schofield, W. H., and Perry, A. E. (1972), ARL/ME Report 134.

Simpson, R. L., Strickland, J. H., and Barr, P. W. (1977), *J. Fluid Mech.* **79**, 553.

Stratford, B. S. (1959), *J. Fluid Mech.* **5**, 17.

Townsend, A. A. (1956*a*), *J. Fluid Mech.* **1**, 561.

Townsend, A. A. (1956*b*), *The Structure of Turbulent Shear Flow*, 1st Ed., C.U.P.

Townsend, A. A. (1960), *J. Fluid Mech.* **8**, 143.

Townsend, A. A. (1961*a*), *J. Fluid Mech.* **11**, 97.

Townsend, A. A. (1961*b*), *J. Fluid Mech.* **12**, 536.

Townsend, A. A. (1965*a*), *J. Fluid Mech.* **22**, 773.

Townsend, A. A. (1965*b*), *J. Fluid Mech.* **23**, 767.

Townsend, A. A. (1976), *The Structure of Turbulent Shear Flow*, 2nd Ed., C.U.P.

Townsend, A. A. (1979), *J. Fluid Mech.* **95**, 515.

Yaglom, A. M. (1979), *Ann. Rev. of Fluid Mech.* **11**, 505.

APPENDIX 1

Derivation of Equilibrium Relations

The equation of motion without viscous and quadratic turbulence terms is

$$u(\partial u/\partial x)+v(\partial u/\partial y)+(\partial/\partial y)(\overline{u'v'}) = U_1(dU_1/dx) \tag{18}$$

The continuity equation is

$$(\partial u/\partial x)+(\partial v/\partial y) = 0 \tag{A1.1}$$

and Equation (12) gives

$$u = U_1-U_s f(\eta) \tag{12}$$

whence

$$(\partial u/\partial x) = (dU_1/dx)-(\partial U_s/\partial x)f-U_s f'(\partial\eta/\partial x) \tag{A1.2}$$

where $f = f(\eta)$ and primes denote differentiation with respect to η. Substitution of Equation (A1.2) into (A1.1) gives after integration

$$B\int_0^\eta \left\{U_s\, f'\frac{\partial\eta}{\partial x} + \frac{\partial U_s}{\partial x}f - \frac{\partial U_1}{dx}\right\}d\eta = v(\eta)-v(0) = v(\eta) \tag{A1.3}$$

as $v(0)$ the vertical velocity at the wall is zero. This last equation is inaccurate for the range $0 < \eta < \mu$ because Equation (12) is inaccurate in this range. However (A1.3) becomes very accurate for moderate to large values of η.

From Equation (12) we may also write

$$\partial u/\partial y = -(U_s/B)f' \tag{A1.4}$$

Substitution of equations (12), (17), (A1.2), (A1.3) and (A1.4) into (18) gives

$$(U_1-U_s f)\left(\frac{dU_1}{dx} - \frac{dU_s}{dx}f - U_s f'\frac{\partial\eta}{\partial x}\right) - U_s f'\left(\int_0^\eta U_s f'\frac{\partial\eta}{\partial x}d\eta + \int_0^\eta \frac{dU_s}{dx}f\,d\eta - \int_0^\eta \frac{dU_1}{dx}d\eta\right) =$$

$$= U_1\frac{dU_1}{dx} - \frac{\partial}{\partial y}\left(U_s^2 g(\eta)\right)$$

$$\therefore U_1\frac{dU_1}{dx} - U_1\frac{dU_s}{dx}f - U_s U_1 f'\frac{\partial\eta}{\partial x} - U_s f\frac{dU_1}{dx} + U_s f\frac{\partial U_s}{\partial x}f + U_s^2 ff'\frac{\partial\eta}{\partial x} - U_s^2 f'\int_0^\eta f'\frac{\partial\eta}{\partial x}d\eta$$

$$-U_s f'\int_0^\eta \frac{\partial U_s}{\partial x}f\,d\eta + U_s f'\int_0^\eta \frac{dU_1}{dx}d\eta = U_1\frac{dU_1}{dx} - \frac{U_s^2}{B}g'$$

as U_s, U_1 are not functions of y (nor, therefore, of η)

$$-f\frac{\partial}{\partial x}[U_1U_s] + U_s\frac{dU_s}{dx}f^2 - U_s U_1 f'\frac{\partial\eta}{dx} + U_s^2 ff'\frac{\partial\eta}{dx} - U_s^2 f'\int_0^\eta f'\frac{\partial\eta}{\partial x}d\eta$$

$$-U_s\frac{\partial U_s}{\partial x}f'\int_0^\eta f\,d\eta + U_s f'\eta\frac{dU_1}{dx} = -\frac{U_s^2}{B}g' \tag{20}$$

This equation may be simplified as follows. Integration by parts gives

$$\int_0^\eta f'\frac{\partial\eta}{\partial x}d\eta = \left[\frac{\partial\eta}{\partial x}f\right]_0^\eta - \int_0^\eta f\frac{\partial}{\partial\eta}\left(\frac{\partial\eta}{\partial x}\right)d\eta.$$

Thus two terms in Equation (20) may be combined thus

$$U_s^2 ff'\frac{\partial\eta}{\partial x} - U_s^2 f'\int_0^\eta \frac{\partial\eta}{\partial x}f'd\eta = U_s^2 f'\int_0^\eta f\frac{\partial}{\partial\eta}\left(\frac{\partial\eta}{\partial x}\right)d\eta$$

As $\partial\eta/\partial x = -(y/B^2)(dB/dx) = -(\eta/B)(dB/dx)$ two more terms may be combined thus

$$-U_s U_1 f' \frac{\partial \eta}{\partial x} + U_s f' \eta \frac{dU_1}{dx} = f' U_s \left[U_1 \frac{\eta}{B} \frac{dB}{dx} + \eta \frac{dU_1}{dx} \right] = \eta \frac{U_s}{B} f' \frac{d}{dx}(BU_1).$$

Hence equation (20) becomes

$$-f\frac{d}{dx}[U_1U_s] + U_s\frac{dU_s}{dx}f^2 + f'\frac{U_s}{B}\eta\frac{d}{dx}[BU_1] + U_s^2 f' \int_0^\eta f \frac{\partial}{\partial \eta}\left(\frac{\partial \eta}{\partial x}\right) d\eta$$
$$- U_s \frac{dU_s}{dx} f' \int_\mu^\eta f d\eta = -\frac{U_s^2}{B} g' \qquad \text{(A1.5).}$$

Now, using the expression for $\partial\eta/\partial x$ above, two more terms can be combined thus

$$U_s^2 f' \int_0^\eta f \frac{\partial}{\partial \eta}\left[\frac{-\eta}{B}\frac{dB}{dx}\right] d\eta - U_s \frac{dU_s}{dx} f' \int_0^\eta f d\eta$$
$$= -\frac{U_s f'}{B}\left\{ U_s \frac{dB}{dx}\int_0^\eta f d\eta + B\frac{dU_s}{dx}\int_0^\eta f d\eta \right\}$$
$$= -\frac{U_s}{B} f' \frac{d}{dx}(BU_s)\int_0^\eta f d\eta.$$

Using this identity equation (A1.5) becomes

$$-f\frac{d}{dx}[U_1U_s] + U_s\frac{dU_s}{dx}f^2 + \eta f'\frac{U_s}{B}\frac{d}{dx}(U_1B) - \frac{U_s f'}{B}\frac{d}{dx}[BU_s]\int_0^\eta f d\eta = -\frac{U_s^2}{B}g'$$

and integration with respect to η over the range of validity of equation (12) (μ to η)† gives

$$-\frac{d}{dx}[U_1U_s]\int_\mu^\eta f d\eta + U_s\frac{dU_s}{dx}\int_\mu^\eta f^2 d\eta + \frac{U_s}{B}\frac{d}{dx}(U_1B)\int_\mu^\eta \eta f' d\eta$$
$$-\frac{U_s}{B}\frac{d}{dx}[BU_s]\int_\mu^\eta f'\int_0^\eta f d\eta d\eta = -\frac{U_s^2}{B}\int_\mu^\eta g' d\eta \qquad (21).$$

To simplify equation (21) we introduce the definitions

$$\int_\mu^\eta f d\eta = I_1(\eta) \text{ and } \int_\mu^\eta f^2 d\eta = I_2(\eta)$$

and perform integration by parts on two terms, viz.

$$\int_\mu^\eta \eta \frac{d}{d\eta}\Big(f(\eta)\Big) d\eta = \eta f - \mu f(\mu) - I_1(\eta)$$

$$\int_\mu^\eta \frac{df}{d\eta}\int_0^\eta f d\eta d\eta = fI_1(\eta) - I_2(\eta) + [f - f(\mu)]\int_0^\eta f(\eta) d\eta$$
$$= fI_1(\eta) - I_2(\eta) + [f - f(\mu)]I_\mu.$$

Also

$$\int_\mu^\eta \frac{dg}{d\eta} d\eta = g(\eta) - g(\mu).$$

Substitution of these relations into equation (21) gives

$$\frac{d}{dx}(U_1U_s)I_1(\eta) - \frac{U_s}{B}\frac{d}{dx}(U_1B)\Big(\eta f - I_1(\eta) - \mu f(\mu)\Big) - U_s\frac{dU_s}{dx}I_2(\eta)$$
$$+ \frac{U_s}{B}\frac{d}{dx}(U_sS)\Big(fI_1(\eta) - I_2(\eta) + \Big(f - f(\mu)\Big)I_\mu\Big) = \frac{U_s^2}{B}\Big(g(\eta) - g(\mu)\Big) \qquad (22).$$

† Integration over the range 0 to η (as in equation (A1.3)) gives inaccurate values of τ in in the range 0 to μ and these inaccuracies affect values of τ at large η. For this reason the integration here is limited to $\eta > \mu$ and an (accurate) estimate of $\tau(\mu)$ is used; see main text.

The conditions for self-preserving flow (equation (23)) when substituted into equation (22) give

$$2mabX^{2m-1}I_1(\eta) - \frac{bac(m+1)}{c}X^{2m-1}\Big(\eta f - I_1(\eta) - \mu f(\mu)\Big) - mb^2X^{2m-1}I_2(\eta) + \frac{b^2c(m+1)}{c}X^{2m-1}$$

$$\Big(fI_1(\eta) - I_2(\eta) + \Big(f - f(\mu)\Big)I_\mu\Big) = \frac{b^2X^{2m-1}}{c}\Big(g(\eta) - g(\mu)\Big)$$

which simplifies to

$$2mabI_1(\eta) - ab(m+1)\Big(\eta f - I_1(\eta) - \mu f(\mu)\Big) - mb^2I_2(\eta) + b^2(m+1)\Big(fI_1(\eta) - I_2(\eta) +$$

$$+\Big(f - f(\mu)\Big)I_\mu\Big) = \frac{b^2}{c}\Big(g(\eta) - g(\mu)\Big) \qquad (24).$$

APPENDIX 2

Derivation of Functions

We have

$$f(\eta) = 1 - 0\cdot 4\eta^{1/2} - 0\cdot 6 \sin\left(\frac{\pi}{2}\eta\right)$$

hence

$$\eta f(\eta) = \eta - 0\cdot 4\eta^{3/2} - 0\cdot 6\eta \sin\left(\frac{\pi}{2}\eta\right).$$

By definition

$$I_1(\eta) = \int_\mu^\eta f d\eta = \int_\mu^\eta \left(1 - 0\cdot 4\eta^{1/2} - 0\cdot 6 \sin\left(\frac{\pi}{2}\eta\right)\right) d\eta$$

$$= \eta - 0\cdot 267\eta^{3/2} + 0\cdot 382 \cos\left(\frac{\pi\eta}{2}\right) - \mu + 0\cdot 267\mu^{3/2} - 0\cdot 382 \cos\left(\frac{\pi}{2}\mu\right).$$

Also by definition

$$I_2(\eta) = \int_\mu^\eta f^2 d\eta = \int_\mu^\eta \left(1 - 0\cdot 4\eta^{1/2} - 0\cdot 6 \sin\left(\frac{\pi}{2}\eta\right)\right)^2 d\eta$$

$$= \int_\mu^\eta \left(1 - 0\cdot 8\eta^{1/2} + 0\cdot 16\eta - 1\cdot 2 \sin\left(\frac{\pi}{2}\eta\right) + 0\cdot 48\eta^{1/2} \sin\left(\frac{\pi}{2}\eta\right) + 0\cdot 36 \sin^2\left(\frac{\pi}{2}\eta\right)\right) d\eta$$

$$= \left[\eta\right]_\mu^\eta - 0\cdot 8\left[\frac{2}{3}\eta^{3/2}\right]_\mu^\eta + 0\cdot 16\left[\frac{\eta^2}{2}\right]_\mu^\eta - 1\cdot 2\int_\mu^\eta \sin\left(\frac{\pi}{2}\eta\right) d\eta + 0\cdot 48\int_\mu^\eta \eta^{1/2} \sin\left(\frac{\pi}{2}\eta\right) d\eta +$$

$$+ 0\cdot 36\int_\mu^\eta \sin^2\left(\frac{\pi}{2}\eta\right) d\eta.$$

Consider the integral

$$\int_\mu^\eta \sin\left(\frac{\pi}{2}\eta\right) d\eta = \frac{2}{\pi}\int_{\frac{\mu\pi}{2}}^{\frac{\eta\pi}{2}} \sin t\, dt = \frac{2}{\pi}\Big[-\cos t\Big]_{\frac{\mu\pi}{2}}^{\frac{\pi\eta}{2}} = \frac{2}{\pi}\left(\cos\left(\frac{\pi}{2}\mu\right) - \cos\left(\frac{\pi}{2}\eta\right)\right).$$

Consider the integral

$$\int_\mu^\eta \sin^2\left(\frac{\pi}{2}\eta\right) d\eta = \frac{2}{\pi}\int_{\frac{\mu\pi}{2}}^{\frac{\eta\pi}{2}} \sin^2 t\, dt = \frac{2}{\pi}\Big[-\frac{1}{4}\sin 2t + \frac{t}{2}\Big]_{\frac{\pi}{2}\mu}^{\frac{\pi}{2}\eta} = \frac{\eta}{2} - \frac{1}{2\pi}\sin(\pi\eta) = \frac{\mu}{2} + \frac{1}{2\pi}\sin(\mu\pi).$$

Consider the integral

$$\int_\mu^\eta \eta^{1/2} \sin\left(\frac{\pi}{2}\eta\right) d\eta = J_1$$

by using the substitution $t^2 = (\pi/2)\eta$ we get

$$J_1 = \frac{4\sqrt{2}}{\pi\sqrt{\pi}}\int_{(\frac{\pi}{2}\mu)^{1/2}}^{(\frac{\pi}{2}\eta)^{1/2}} t^2 \sin t^2 dt.$$

As

$$\frac{d}{dt}(t\cos t^2) = \cos t^2 - 2t^2 \sin t^2$$

then

$$t^2 \sin t^2 = \tfrac{1}{2}\cos t^2 - \tfrac{1}{2}\frac{d}{dt}(t\cos t^2).$$

Substituting this relation into J_1 gives

$$J_1 = \frac{2\sqrt{2}}{\pi\sqrt{\pi}}\int_{(\frac{\mu}{2}\pi)^{1/2}}^{(\frac{\pi}{2}\eta)^{1/2}} \cos t^2 dt - \frac{2\sqrt{2}}{\pi\sqrt{\pi}}\int_{(\frac{\pi}{2}\mu)^{1/2}}^{(\frac{\pi}{2}\eta)^{1/2}} \frac{d}{dt}(t\cos t^2)dt$$

$$= \frac{2\sqrt{2}}{\pi\sqrt{\pi}}\int_{(\frac{\pi\eta}{2})^{1/2}}^{(\frac{\pi}{2}\eta)^{1/2}} \cos t^2\, dt - \frac{2\eta^{1/2}}{\pi}\cos\frac{\pi}{2}\eta + \frac{2\mu^{1/2}}{\pi}\cos\frac{\pi}{2}\mu$$

Consider the integral

$$J_2 = \int_{(\frac{\pi}{2}\mu)^{1/2}}^{(\frac{\pi}{2}\eta)^{1/2}} \cos\ t^2 dt$$

By using the substitution $t^2 = (\pi/2)s^2$

$$J_2 = \sqrt{\frac{\pi}{2}}\int_{\mu^{1/2}}^{\eta^{1/2}} \cos\left(\frac{\pi}{2}s^2\right)ds$$

hence

$$J_1 = \frac{2}{\pi}\int_{\mu^{1/2}}^{\eta^{1/2}} \cos\left(\frac{\pi}{2}s^2\right)ds - \frac{2\eta^{1/2}}{\pi}\cos\frac{\pi}{2}\eta + \frac{2\mu^{1/2}}{\pi}\cos\frac{\pi}{2}\mu$$

$$= \frac{2}{\pi}C(\eta^{1/2}) - \frac{2}{\pi}\eta^{1/2}\cos\frac{\pi}{2}\eta - \frac{2}{\pi}C(\mu^{1/2}) - \frac{2}{\pi}\mu^{1/2}\cos\frac{\pi}{2}\mu$$

where $C(\eta)$ is Fresnel's cosine integral which is tabulated in Abramowitz and Stegun (1965).

$$\therefore I_2(\eta) = 1\cdot18\eta - 0\cdot533\eta^{3/2} + 0\cdot08\eta^2 - 0\cdot0573\sin(\eta\pi)$$
$$+0\cdot7639\cos\left(\eta\frac{\pi}{2}\right) - 0\cdot3056\eta^{1/2}\cos\left(\frac{\pi}{2}\eta\right) + 0\cdot3056C(\eta^{1/2})$$
$$-1\cdot18\mu + 0\cdot5333\mu^{3/2} - 0\cdot08\mu^2 + 0\cdot0573\sin(\mu\pi)$$
$$-0\cdot7639\cos\left(\mu\frac{\pi}{2}\right) + 0\cdot3056\mu^{1/2}\cos\left(\frac{\pi}{2}\mu\right) - 0\cdot3056C(\mu^{1/2}).$$

Finally

$$fI_1(\eta) = 1 - 0\cdot4\eta^{3/2} - 0\cdot6\eta\sin\left(\frac{\pi}{2}\eta\right) + 0\cdot1067\eta^3 - 0\cdot1528\eta^{3\cdot2}\cos\left(\frac{\pi}{2}\eta\right)$$
$$-\mu + 0\cdot2667\mu^{3/2} - 0\cdot382\cos\left(\frac{\pi}{2}\mu\right) - 0\cdot4\eta^{5/2} + 0\cdot4\eta^{3\cdot2}\mu$$
$$-0\cdot1067\eta^{3/2}\mu^{3/2} + 0\cdot1528\eta^{3\cdot2}\cos\left(\frac{\pi}{2}\mu\right) - 0\cdot6\eta^2\sin\left(\frac{\pi}{2}\eta\right)$$
$$+0\cdot16\eta^{5/2}\sin\left(\frac{\pi}{2}\eta\right) - 0\cdot2292\eta\sin\left(\frac{\pi}{2}\eta\right)\cos\left(\frac{\pi}{2}\eta\right) + 0\cdot6\eta\mu\sin\left(\frac{\pi}{2}\eta\right)$$
$$-0\cdot16\mu^{3/2}\eta\sin\left(\frac{\pi}{2}\eta\right) + 0\cdot2292\eta\sin\left(\frac{\pi}{2}\eta\right)\cos\left(\frac{\pi}{2}\mu\right).$$

APPENDIX 3

Equilibrium Layer Data

Profile (xm.)	U_1 (m/s.)	U_1/U_s (a/b)	B (m.)	c_f' ($\times 10^3$)	γ ($\times 10^3$)	β^* ($\times 10^3$)	c_f'/γ	X (m.)
	I. Ludwieg and Tillman (1949)				*Mild Adverse Pressure Gradient Flow*			
3·332	25·75	1·818	0·1112	1·60	88·59	10·69		1·600
3·532	24·85	1·7241	0·1208	1·53	82·28	10·14		1·800
3·732	24·50	1·6667	0·1304	1·52	78·42	9·80		2·000
3·932	24·05	1·6129	0·1448	1·34	74·80	9·48		2·200
4·132	23·60	1·5873	0·1625	1·26	73·08	9·33		2·400
4·332	23·10	1·5152	0·1772	1·17	58·24	8·91		2·600
Average	—	1·6540	—	1·403	77·568	9·73	0·018	—
	$c = 67{\cdot}21 \times 10^{-3}$; $x_0 = 1{\cdot}732$ m; $m = -0{\cdot}259873$							
			II. Clauser (1954)	*Flow 1*				
2·1092	9·906	1·7857	0·0679	2·10	42·75	4·46		1·9728
3·3528	8·870	1·6949	0·1056	2·14	39·73	4·23		3·1264
3·8867	8·534	1·7241	0·1243	2·08	40·70	4·31		3·7498
5·6632	7·681	1·8518	0·1792	1·93	44·95	4·62		5·5268
7·2634	7·193	1·9608	0·2418	1·75	48·57	4·90		7·1270
8·2052	6·858	1·8868	0·2683	1·83	46·11	4·71		8·0688
9·0678	6·645	2·0000	0·2963	1·73	49·87	5·00		8·9314
9·8298	6·462	1·9608	0·3220	1·76	48·57	4·94		9·6934
Average	—	1·8581	—	1·915	45·156	4·65	0·042	—
	$c = 33{\cdot}25 \times 10^{-3}$; $x_0 = 0{\cdot}1364$ m; $m = -0{\cdot}223708$							
			III. Clauser (1954)	*Flow 2*				
2·2860	7·955	1·3514	0·1041	1·30	67·23	8·65		1·0444
2·7432	7·559	1·2821	0·1311	1·20	61·18	8·20		1·5016
3·3528	7·163	1·2987	0·1571	1·15	63·07	8·31		2·1112
3·8618	6·950	1·2987	0·1910	1·04	63·07	8·31		2·6202
4·9286	6·492	1·3333	0·2800	1·05	65·80	8·53		3·6870
5·8430	6·157	1·3333	0·3459	1·05	65·80	8·53		4·6014
7·2908	5·761	1·3333	0·4712	0·95	65·80	8·53		6·0492
8·1290	5·516	1·3333	0·5700	0·85	65·80	8·53		6·8874
Average	—	1·3205	—	1·074	64·719	8·45	0·017	—
	$c = 78{\cdot}96 \times 10^{-3}$; $x_0 = 1{\cdot}2416$ m; $m = -0{\cdot}252664$							
			IV. Bradshaw (1966)	a = *0·15*				
0·610	43·71	2·0000	0·02702	2·24	46·88	4·50		0·8740
1·2192	39·35	2·0833	0·046809	2·11	49·48	4·68		1·4832
1·6764	37·64	2·0833	0·060717	2·03	49·484	4·68		1·9404
2·1336	36·27	2·0833	0·07470	1·88	49·484	4·68		2·3976
Average	—	2·0625	—	2·065	48·832	4·64	0·042	—
	$c = 31{\cdot}2538 \times 10^{-3}$; $x_0 = -0{\cdot}26397$ m; $m = -0{\cdot}212891$							

APPENDIX 3—continued

Profile (xm.)	U_1 (m/s.)	U_1/U_s (a/b)	B (m.)	c_f' ($\times 10^3$)	γ ($\times 10^3$)	β^* ($\times 10^3$)	c_f'/γ	X (m.)
			V. Bradshaw and Ferris (1965)		a = *0·255*			
0·5843	41·61	1·4706	0·0349	1·45	58·14	7·77		0·5993
1·1939	34·66	1·5626	0·0750	1·32	63·64	8·44		1·2089
1·6511	31·97	1·6129	0·0979	1·25	66·66	8·81		1·6661
2·1083	29·96	1·6129	0·1275	1·23	66·66	8·82		2·1233
Average	—	1·5647	—	1·313	63·775	8·46	0·021	—
		$c = 59{\cdot}90\times10^{-3}$; $x_0 = -0{\cdot}015$ m; $m = -0{\cdot}256245$						
			VI. Bradshaw (1967)		a = *0 → −0·255*			
1·0668	33·76	1·9231	0·04593	1·87	55·00	5·99		1·1928
1·2192	32·65	1·8868	0·05118	1·80	53·60	5·88		1·3452
1·5240	30·91	1·7857	0·06554	1·66	49·69	5·56		1·6500
1·8288	29·51	1·7241	0·07485	1·53	47·31	5·37		1·9548
2·1336	28·33	1·7241	0·08715	1·47	47·31	5·37		2·2596
Average	—	1·8088	—	1·666	50·58	5·63	0·033	—
		$c = 38{\cdot}65\times10^{-3}$; $x_0 = -0{\cdot}126$ m; $m = -0{\cdot}239261$						
			VII. Stratford (1959)		*Flow 5*			
0·9260	15·19	1·2195	0·01750	1·42	45·24	5·97		0·3099
1·0763	13·43	1·2048	0·03205	1·19	44·32	5·90		0·4601
1·2506	12·81	1·3158	0·04121	1·45	51·30	6·44		0·6344
1·6221	11·295	1·3333	0·05976	1·36	52·40	6·52		1·0059
1·9007	10·387	1·2987	0·08236	1·21	50·22	6·36		1·2845
Average	—	1·2744	—	1·326	48·696	6·24	0·027	—
		$c = 62{\cdot}883\times10^{-3}$; $x_0 = 0{\cdot}6162$ m; $m = -0{\cdot}243127$						
			VIII. Samuel (1973)		*Flow 2*			
2·90	22·1	1·92	0·1022	1·85	57·69	6·70		3·284
3·38	21·0	1·82	0·1217	1·66	53·63	6·35		3·764
Average	—	1·87	—	1·755	55·66	6·53	0·032	—
		$c = 40{\cdot}625\times10^{-3}$; $x_0 = -0{\cdot}3843$; $m = -0{\cdot}239586$						
			IX. Stratford (1959)		*Flow 6*			
0·926	15·00	1·064	0·01686	0·99	59·74	8·65		0·1647
1·0763	13·00	0·9804	0·03493	0·55	50·85	8·67		0·3150
1·2506	11·98	0·9709	0·05002	0·53	49·84	8·59		0·4893
1·6221	10·28	0·9091	0·09277	0·33	43·30	8·04		0·8608
1·9007	9·45	0·8772	0·1199	0·31	39·93	7·76		1·1394
Average	—	0·9603	—	0·54	48·73	8·34	0·0111	—
		$c = 105{\cdot}921\times10^{-3}$; $x_0 = 0{\cdot}76133$; $m = -0{\cdot}219426$						

APPENDIX 4

Tabulation of Functions

η	$f(\eta)$	$\eta f(\eta)$	$I_1(\eta)$	$I_2(\eta)$	$f(\eta)I_1(\eta)$
0·02	0·924585	0·018492	0·000000	0·000000	0·000000
0·03	0·902454	0·027074	0·009133	0·008342	0·008242
0·04	0·882326	0·035293	0·018056	0·016303	0·015931
0·05	0·863482	0·043174	0·026784	0·023922	0·023127
0·06	0·845555	0·050733	0·035328	0·031223	0·029872
0·07	0·828329	0·057983	0·043697	0·038227	0·036196
0·08	0·811663	0·064933	0·051897	0·044950	0·042123
0·09	0·795459	0·071591	0·059932	0·051407	0·047673
0·10	0·779648	0·077965	0·067807	0·057609	0·052866
0·11	0·764178	0·084060	0·075526	0·063568	0·057715
0·12	0·749007	0·089881	0·083092	0·069292	0·062236
0·13	0·734106	0·095434	0·090507	0·074791	0·066442
0·14	0·719448	0·100723	0·097775	0·080073	0·070344
0·15	0·705013	0·105752	0·104897	0·085145	0·073954
0·16	0·690786	0·110526	0·111876	0·090016	0·077282
0·17	0·676752	0·115048	0·118713	0·094691	0·080339
0·18	0·662900	0·119322	0·125411	0·099178	0·083135
0·19	0·649220	0·123352	0·131972	0·103482	0·085679
0·20	0·635704	0·127141	0·138396	0·107609	0·087979
0·21	0·622347	0·130693	0·144686	0·111566	0·090045
0·22	0·609141	0·134011	0·150844	0·115358	0·091885
0·23	0·596082	0·137099	0·156870	0·118989	0·093507
0·24	0·583166	0·139960	0·162766	0·122466	0·094919
0·25	0·570390	0·142597	0·168533	0·125792	0·096130
0·26	0·557750	0·145015	0·174174	0·128974	0·097146
0·27	0·545245	0·147216	0·179689	0·132016	0·097975
0·28	0·532872	0·149204	0·185079	0·134921	0·098624
0·29	0·520630	0·150983	0·190347	0·137696	0·099100
0·30	0·508517	0·152555	0·195492	0·140344	0·099411
0·31	0·496532	0·153925	0·200518	0·142869	0·099563
0·32	0·484674	0·155096	0·205423	0·145276	0·099563
0·33	0·472942	0·156071	0·210211	0·147569	0·099418
0·34	0·461337	0·156855	0·214883	0·149751	0·099133
0·35	0·499858	0·157450	0·219439	0·151827	0·098716
0·36	0·438504	0·157861	0·223880	0·153800	0·098172
0·37	0·427276	0·158092	0·228209	0·155674	0·097508
0·38	0·416173	0·158146	0·232426	0·157452	0·096730
0·39	0·405197	0·158027	0·236533	0·159139	0·095842
0·40	0·394347	0·157739	0·240531	0·160737	0·094852
0·41	0·383623	0·157285	0·244420	0·162250	0·093765
0·42	0·373026	0·156671	0·248203	0·163681	0·092586
0·43	0·362557	0·155899	0·251881	0·165034	0·091321
0·44	0·352216	0·154975	0·255455	0·166311	0·089975
0·45	0·342003	0·153901	0·258926	0·167516	0·088553
0·46	0·331920	0·152683	0·262295	0·168652	0·087061
0·47	0·321966	0·151324	0·265565	0·169721	0·085503
0·48	0·312144	0·149829	0·268735	0·170726	0·083884
0·49	0·302452	0·148202	0·271808	0·171670	0·082209
0·50	0·292893	0·146447	0·274785	0·172556	0·080483

APPENDIX 4—continued

η	$f(\eta)$	$\eta f(\eta)$	$I_1(\eta)$	$I_2(\eta)$	$f(\eta)I_1(\eta)$
0·51	0·283467	0·144568	0·277666	0·173387	0·078709
0·52	0·274175	0·142571	0·280454	0·174164	0·076894
0·53	0·265017	0·140459	0·283150	0·174891	0·075040
0·54	0·255995	0·138237	0·285755	0·175570	0·073152
0·55	0·247108	0·135910	0·288271	0·176202	0·071234
0·56	0·238359	0·133481	0·290698	0·176792	0·069291
0·57	0·229748	0·130957	0·293038	0·177339	0·067325
0·58	0·221276	0·128340	0·295293	0·177848	0·065341
0·59	0·212943	0·125637	0·297464	0·178319	0·063343
0·60	0·204751	0·122851	0·299553	0·178756	0·061334
0·61	0·196700	0·119987	0·301560	0·179158	0·059317
0·62	0·188791	0·117051	0·303487	0·179530	0·057296
0·63	0·181025	0·114046	0·305336	0·179872	0·055274
0·64	0·173403	0·110978	0·307108	0·180186	0·053254
0·65	0·165926	0·107852	0·308805	0·180474	0·051239
0·66	0·158593	0·104672	0·310427	0·180737	0·049232
0·67	0·151407	0·101443	0·311977	0·180977	0·047235
0·68	0·144368	0·098170	0·313456	0·181196	0·045253
0·69	0·137476	0·094858	0·314865	0·181395	0·043286
0·70	0·130732	0·091512	0·316206	0·181574	0·041338
0·71	0·124137	0·088138	0·317480	0·181737	0·039411
0·72	0·117693	0·084739	0·318689	0·181883	0·037507
0·73	0·111398	0·081320	0·319834	0·182014	0·035629
0·74	0·105254	0·077888	0·320917	0·182132	0·033778
0·75	0·099262	0·074447	0·321940	0·182236	0·031956
0·76	0·093422	0·071001	0·322903	0·182329	0·030166
0·77	0·087735	0·067556	0·323809	0·182411	0·028409
0·78	0·082201	0·064117	0·324658	0·182483	0·026687
0·79	0·076821	0·060689	0·325453	0·182546	0·025002
0·80	0·071595	0·057276	0·326195	0·182602	0·023354
0·81	0·066524	0·053885	0·326886	0·182649	0·021746
0·82	0·061608	0·050519	0·327526	0·182690	0·020178
0·83	0·056848	0·047184	0·328118	0·182725	0·018653
0·84	0·052244	0·043885	0·328864	0·182755	0·017171
0·85	0·047796	0·040627	0·329164	0·182780	0·015733
0·86	0·043505	0·037414	0·329620	0·182801	0·014340
0·87	0·039371	0·034253	0·330034	0·182818	0·012994
0·88	0·035394	0·031147	0·330408	0·182832	0·011695
0·89	0·031575	0·028102	0·330743	0·182843	0·010443
0·90	0·027914	0·025122	0·331040	0·182852	0·009241
0·91	0·024410	0·022213	0·331302	0·182859	0·008087
0·92	0·021065	0·019379	0·331529	0·182864	0·006984
0·93	0·017877	0·016626	0·331723	0·182868	0·005930
0·94	0·014848	0·013958	0·331887	0·182871	0·004928
0·95	0·011978	0·011379	0·322021	0·182872	0·003977
0·96	0·009266	0·008895	0·332127	0·182874	0·003077
0·97	0·006712	0·006510	0·332207	0·182874	0·002230
0·98	0·004316	0·004230	0·332262	0·182875	0·001434
0·99	0·002079	0·002058	0·332293	0·182875	0·000691
1·00	0·000000	0·000000	0·332304	0·182875	0·000000

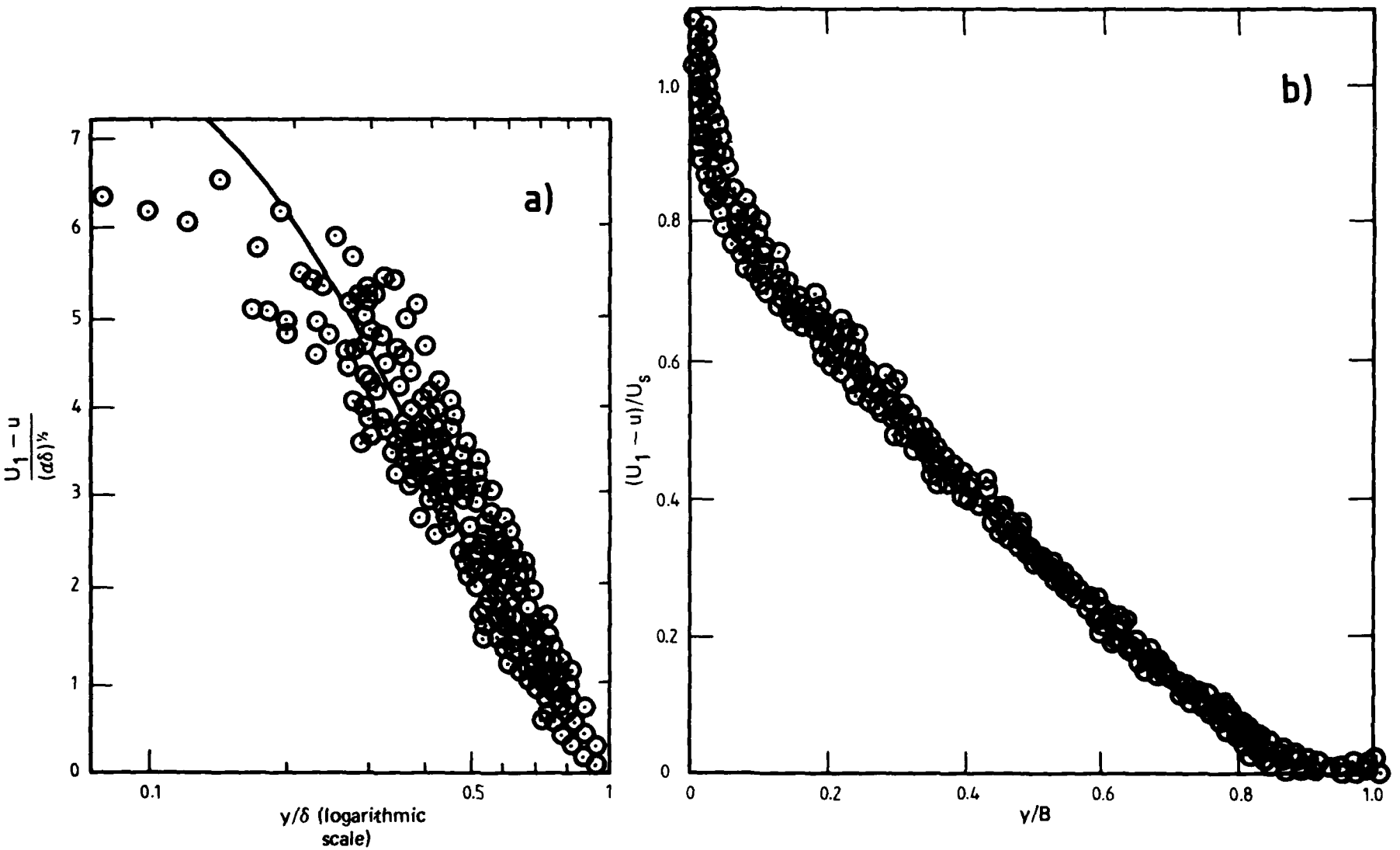

FIG. 1 DEFECT LAWS FOR BOUNDARY LAYERS IN ADVERSE PRESSURE GRADIENTS
(a) Defect law by Kader & Yaglom (from Kader & Yaglom (1978))
(b) Defect law by Schofield & Perry (from Schofield & Perry (1972)).

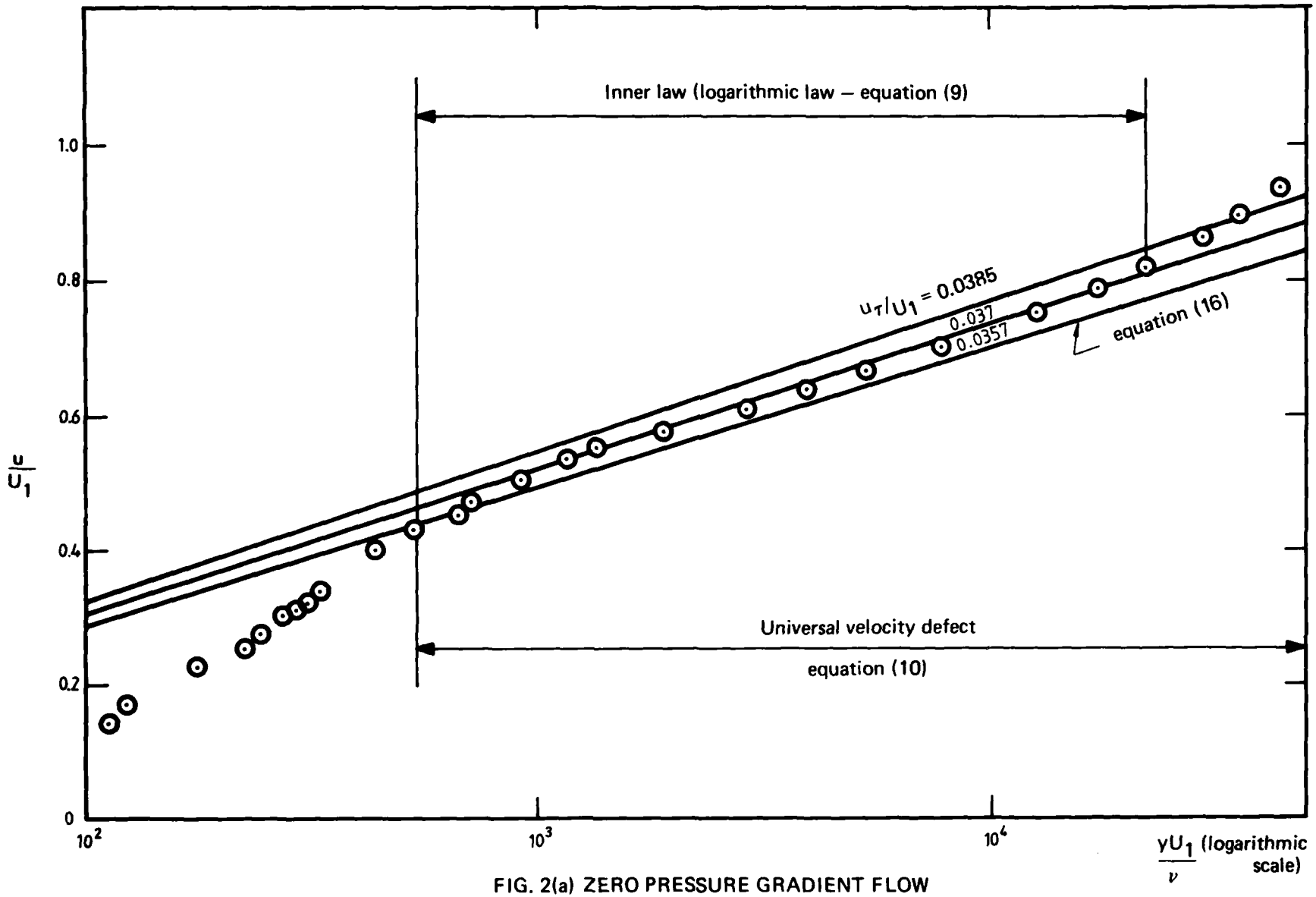

FIG. 2(a) ZERO PRESSURE GRADIENT FLOW
Data taken from Fig. 3 in Klebanoff (1954)

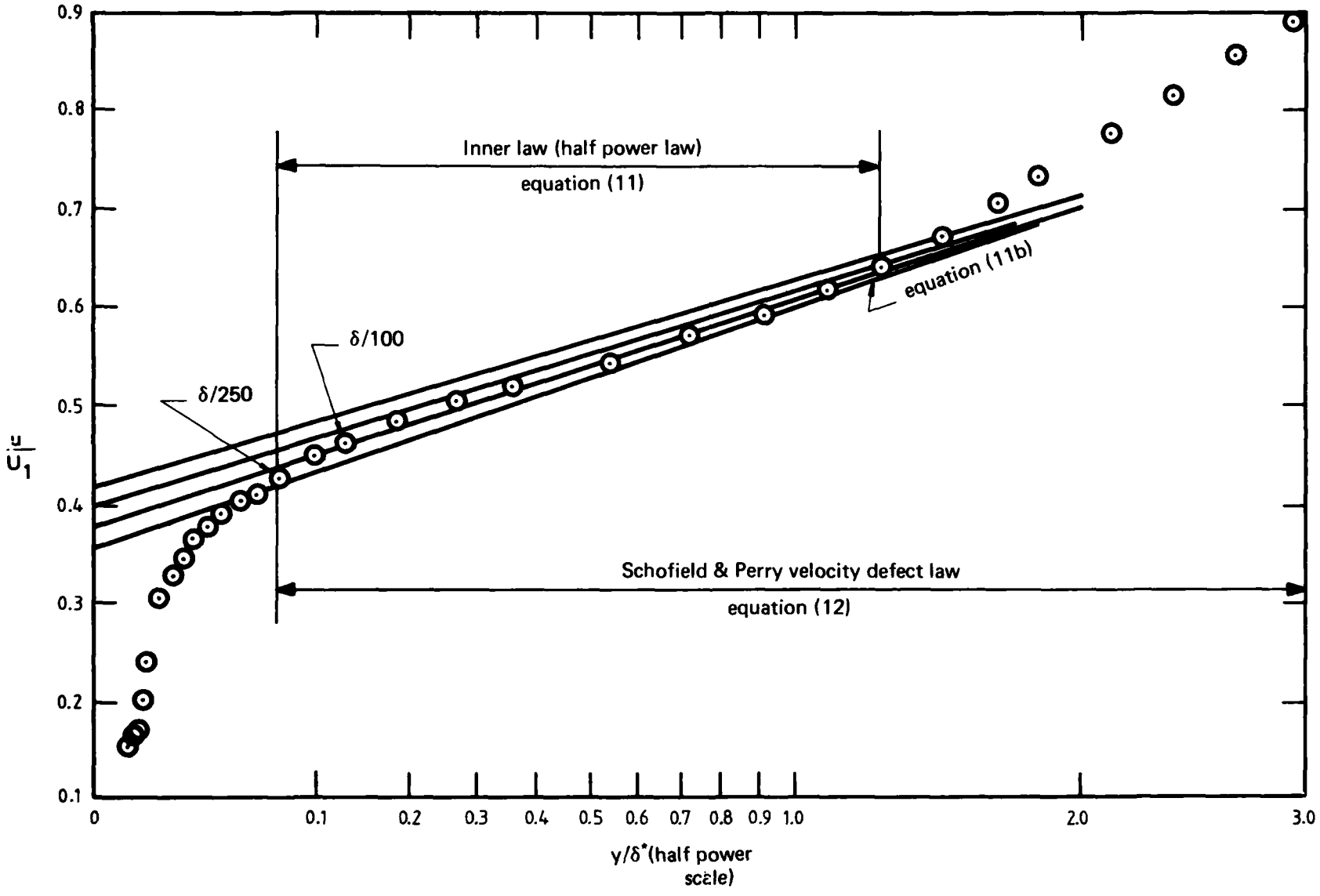

FIG. 2(b) ADVERSE PRESSURE GRADIENT FLOW
Data of Bradshaw & Ferriss (1965),"a = 0.255" flow, profile at x = 2.1083 m.

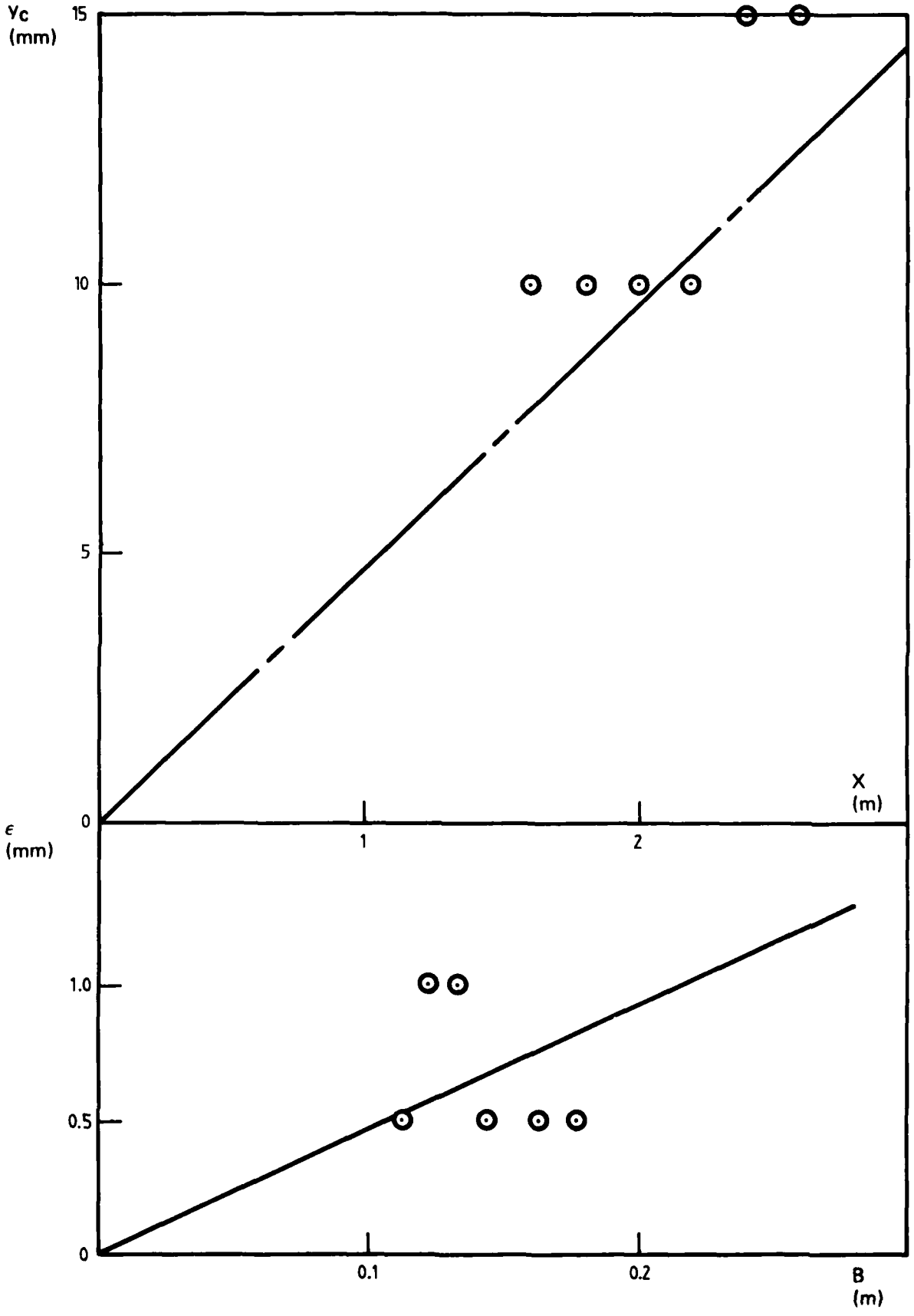

FIG. 3 Y_c VERSUS X AND ϵ VERSUS B FOR LAYER I

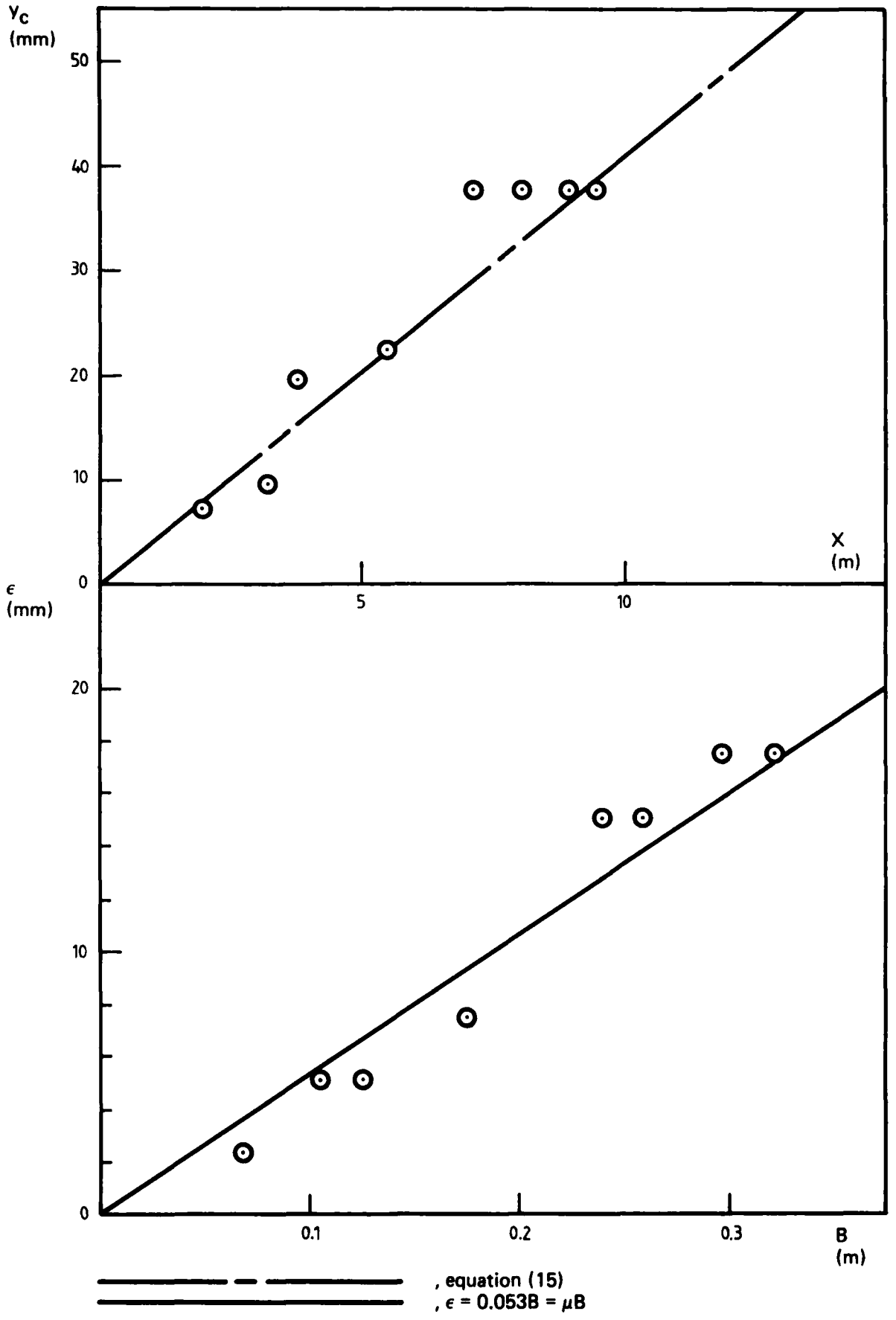

FIG. 3 Continued. LAYER II

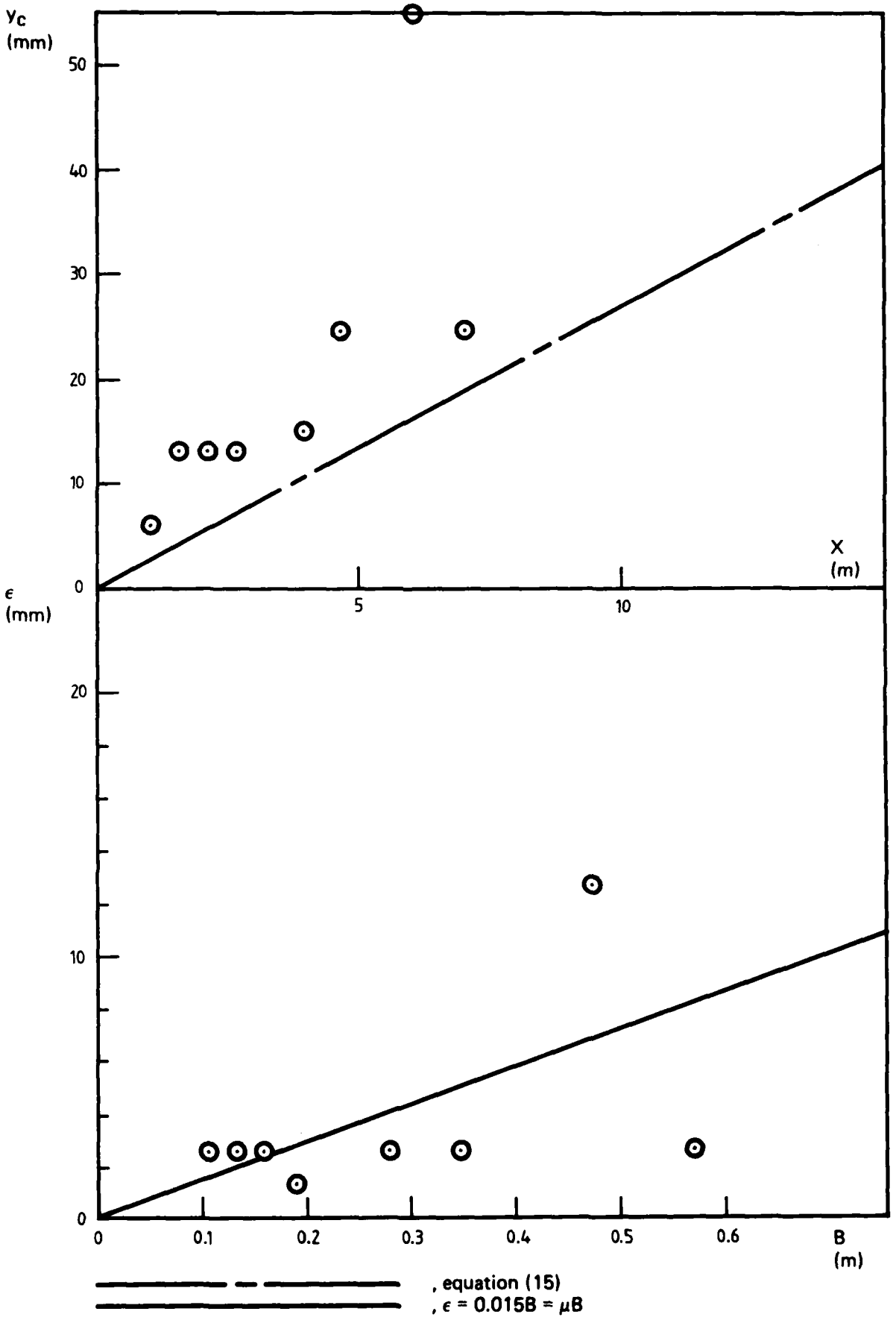

FIG. 3 Continued. LAYER III

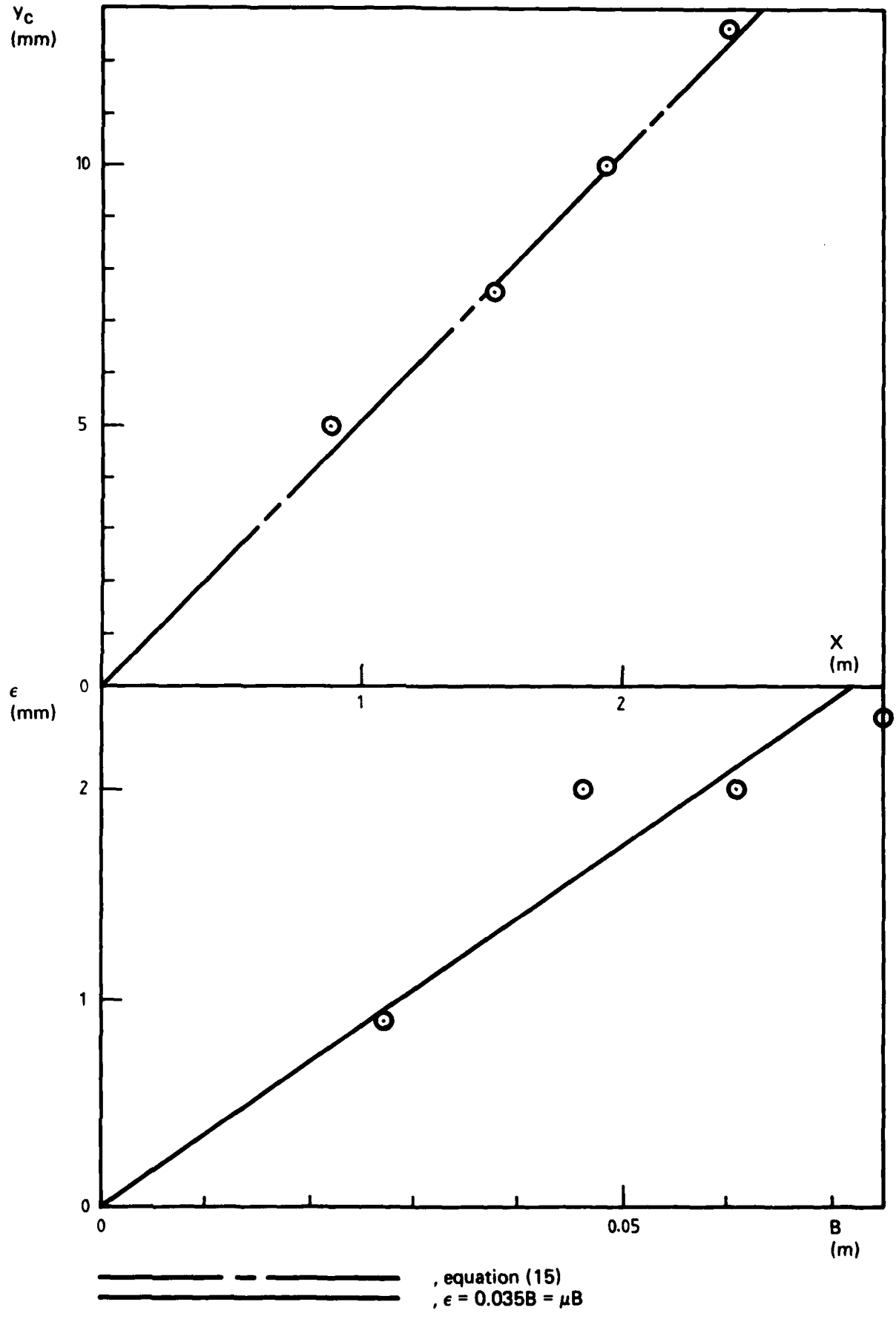

FIG. 3 Continued. LAYER IV

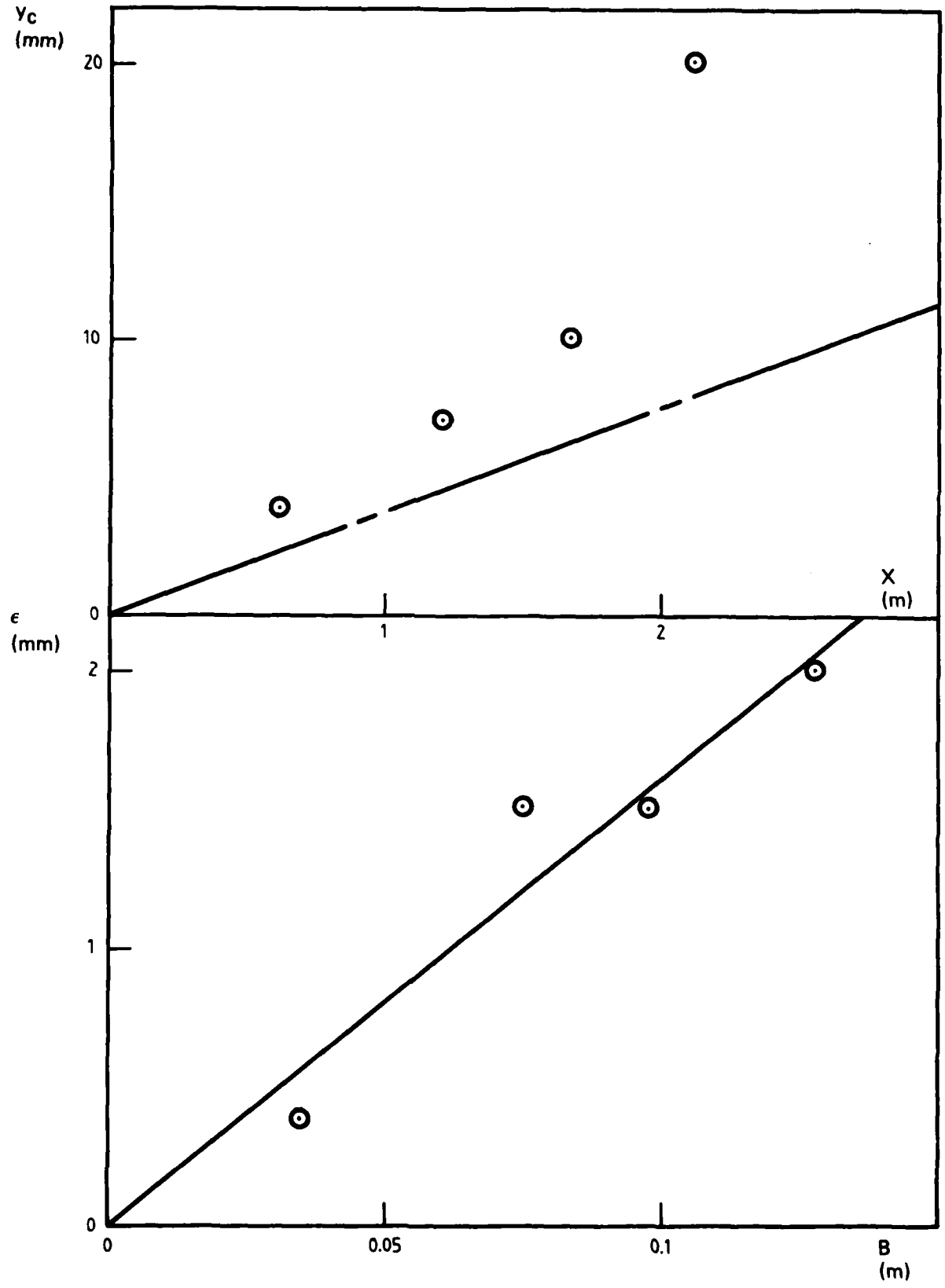

FIG. 3 Continued. LAYER V

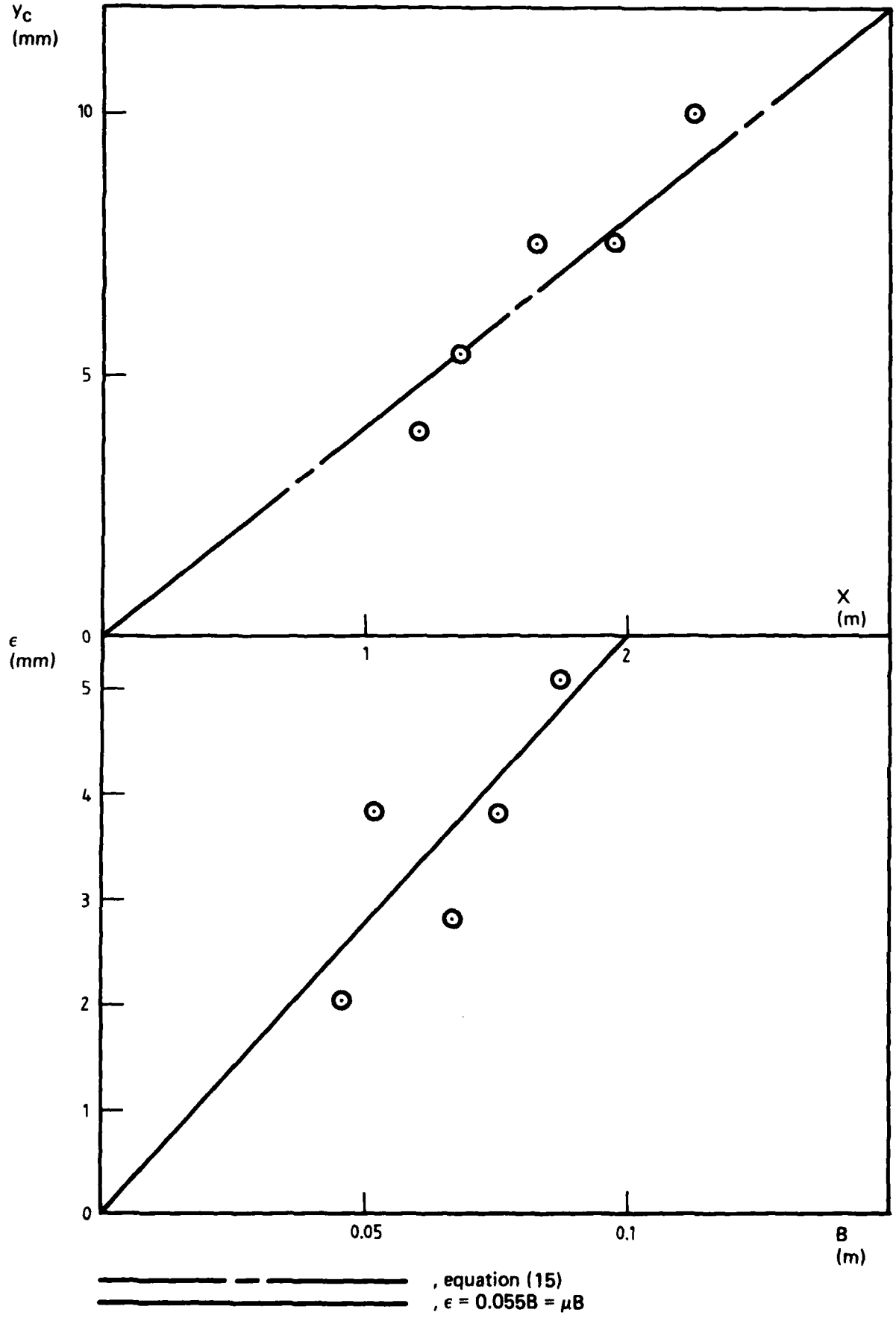

FIG. 3 Continued. LAYER VI

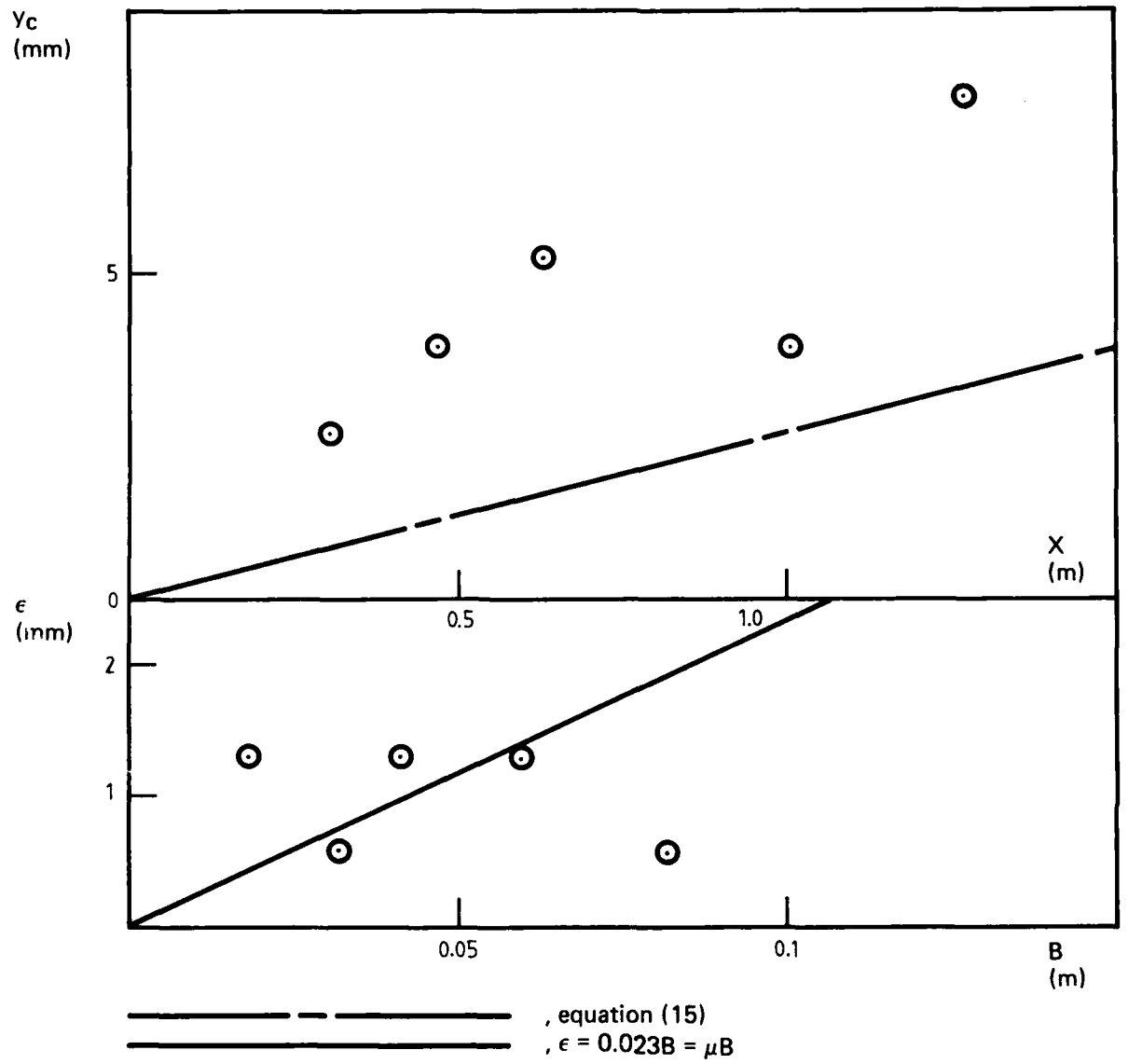

FIG. 3 Continued. LAYER VII

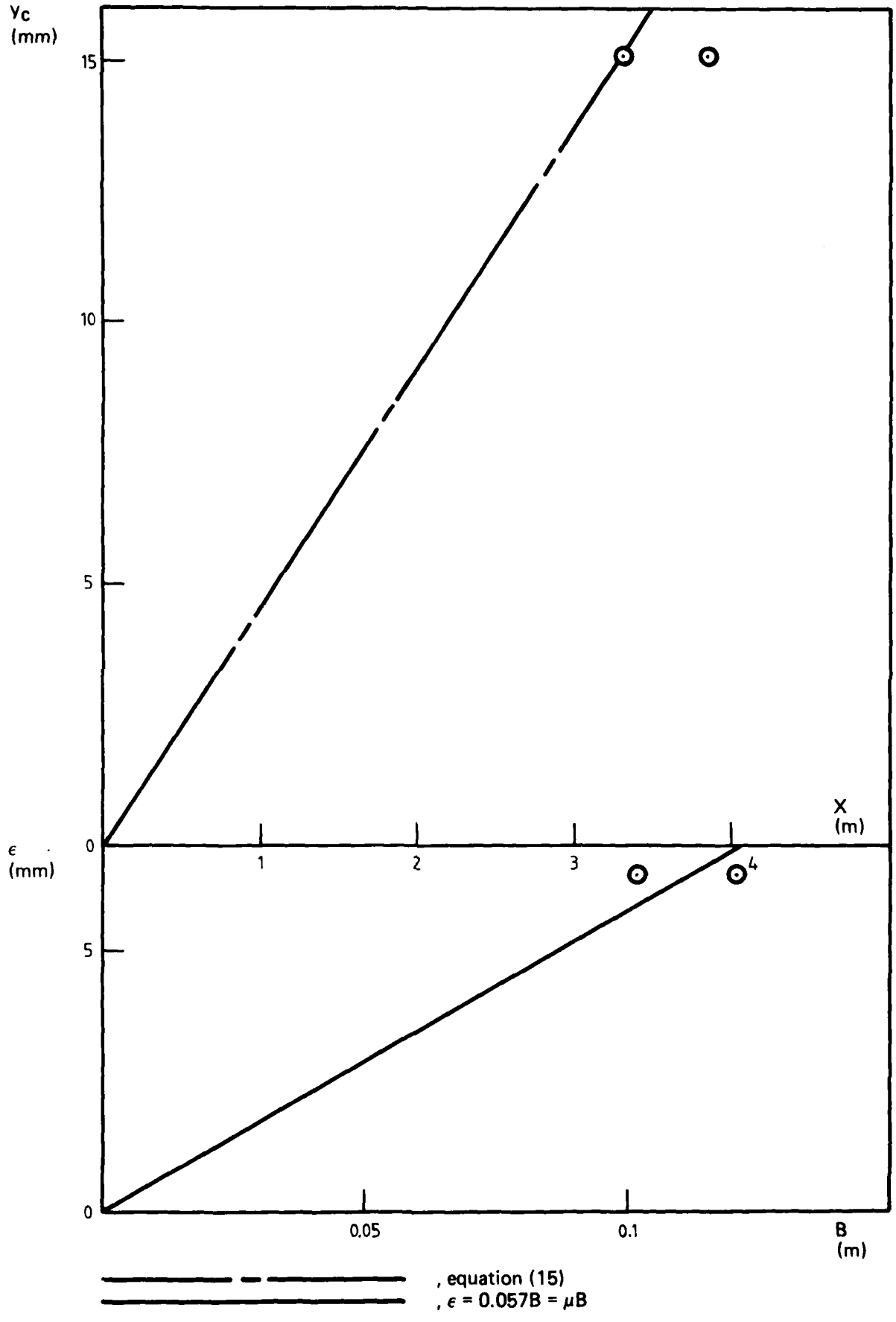

FIG. 3 Continued. LAYER VIII

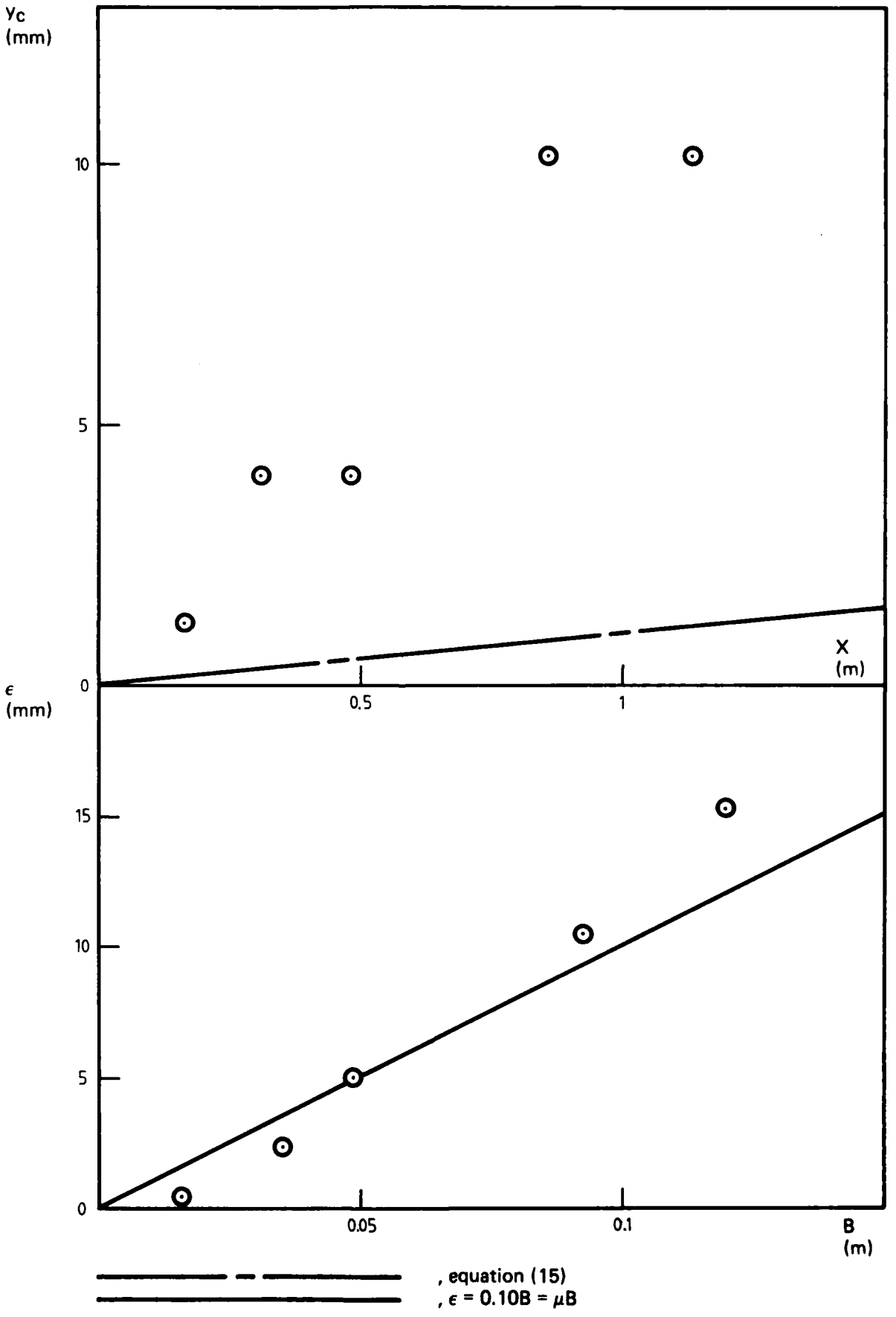

FIG. 3 Continued. LAYER IX

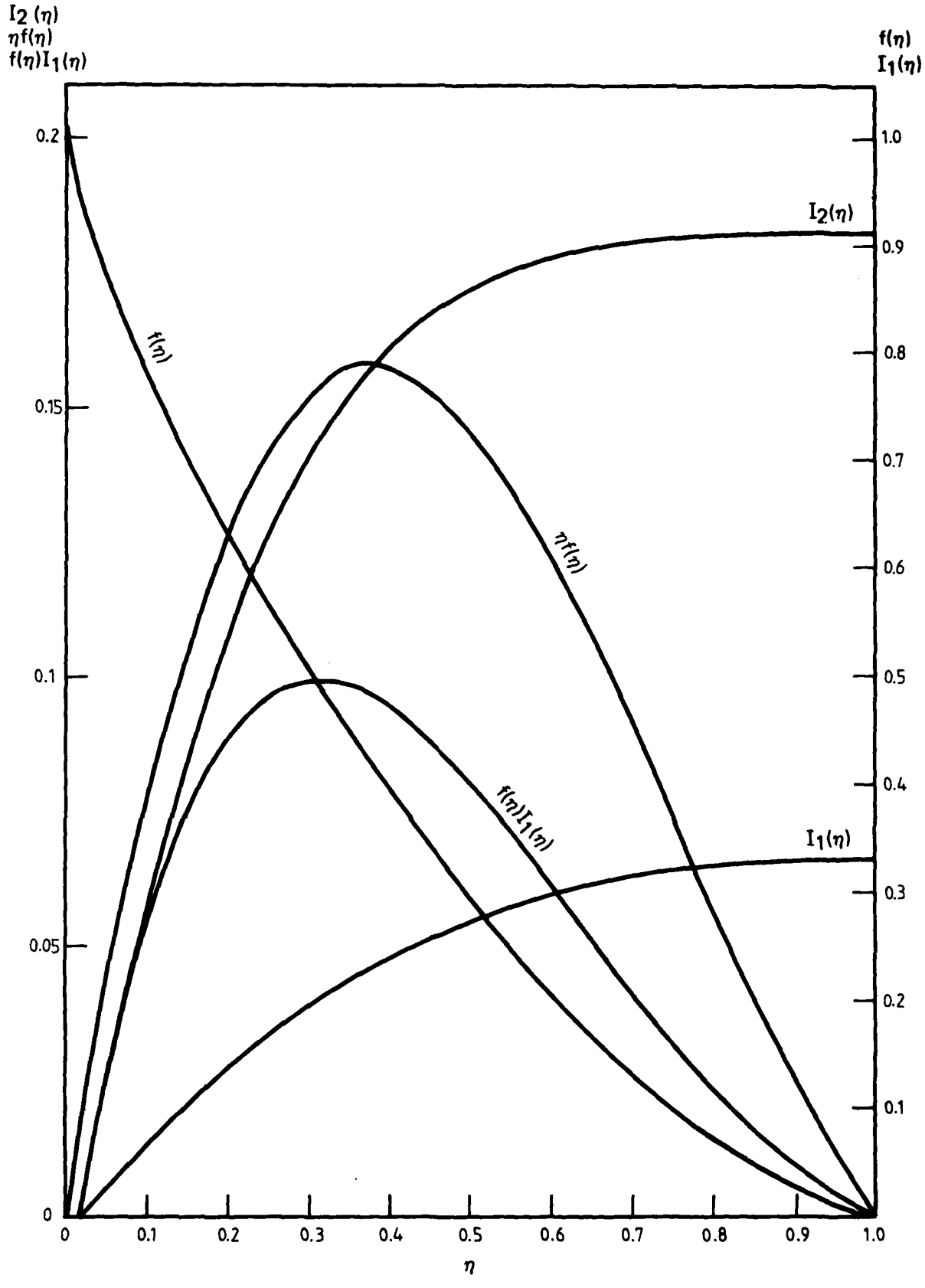

FIG. 4 FUNCTIONS OF η.

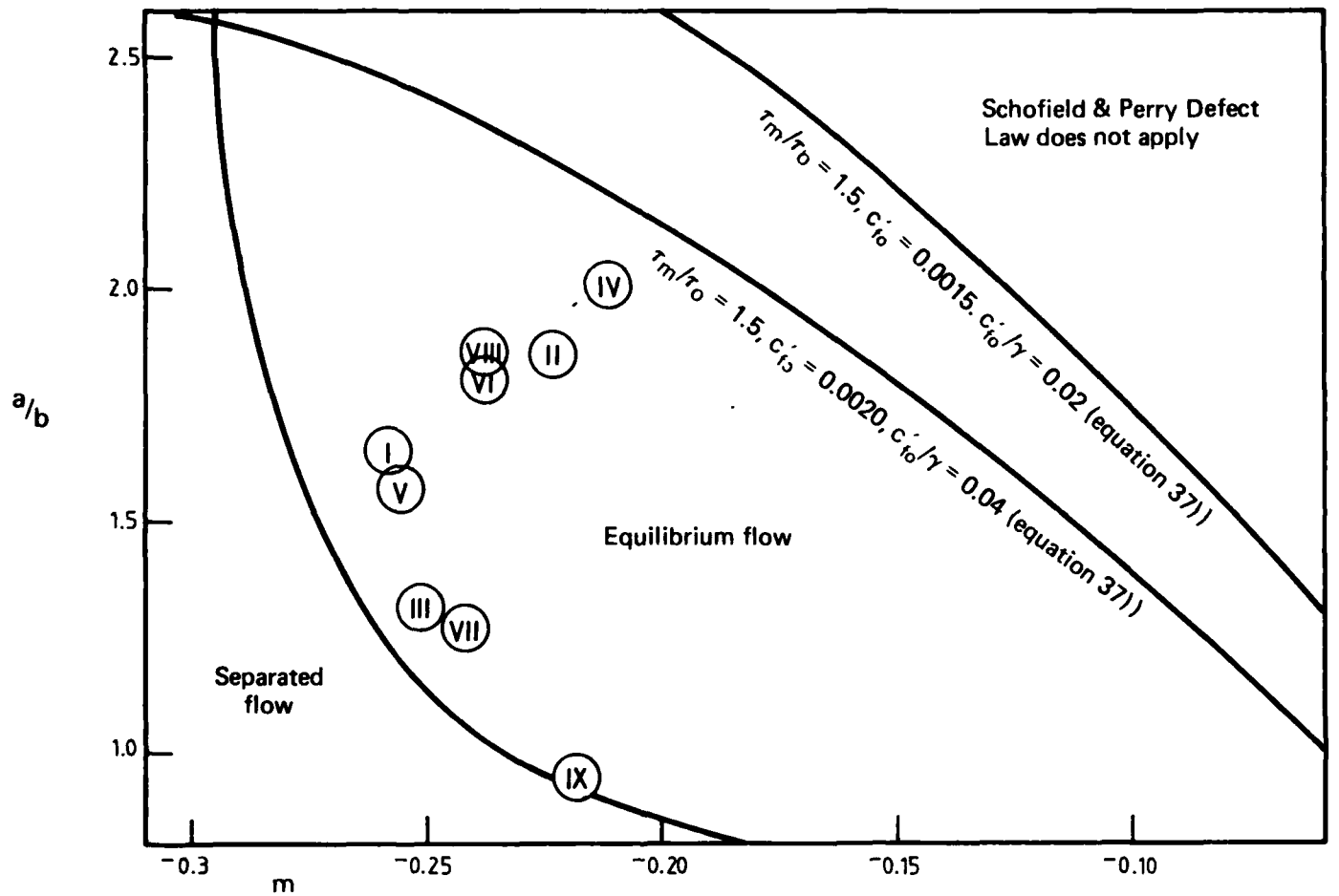

FIG. 5 LIMITS FOR EQUILIBRIUM FLOW
I, Ludwieg & Tillmann (1949) Mild Adverse Pressure Gradient Flow; II, Clauser (1954) Flow 1; III Clauser (1954) Flow 2; IV, Bradshaw (1966) a=−0.15; V, Bradshaw & Ferriss (1965) a=−0.255; VI, Bradshaw (1967) a = 0 → −0.255; VII, Stratford (1959) Flow 5; VIII, Samuel (1973) Flow 2; IX, Stratford (1959) Flow 6.

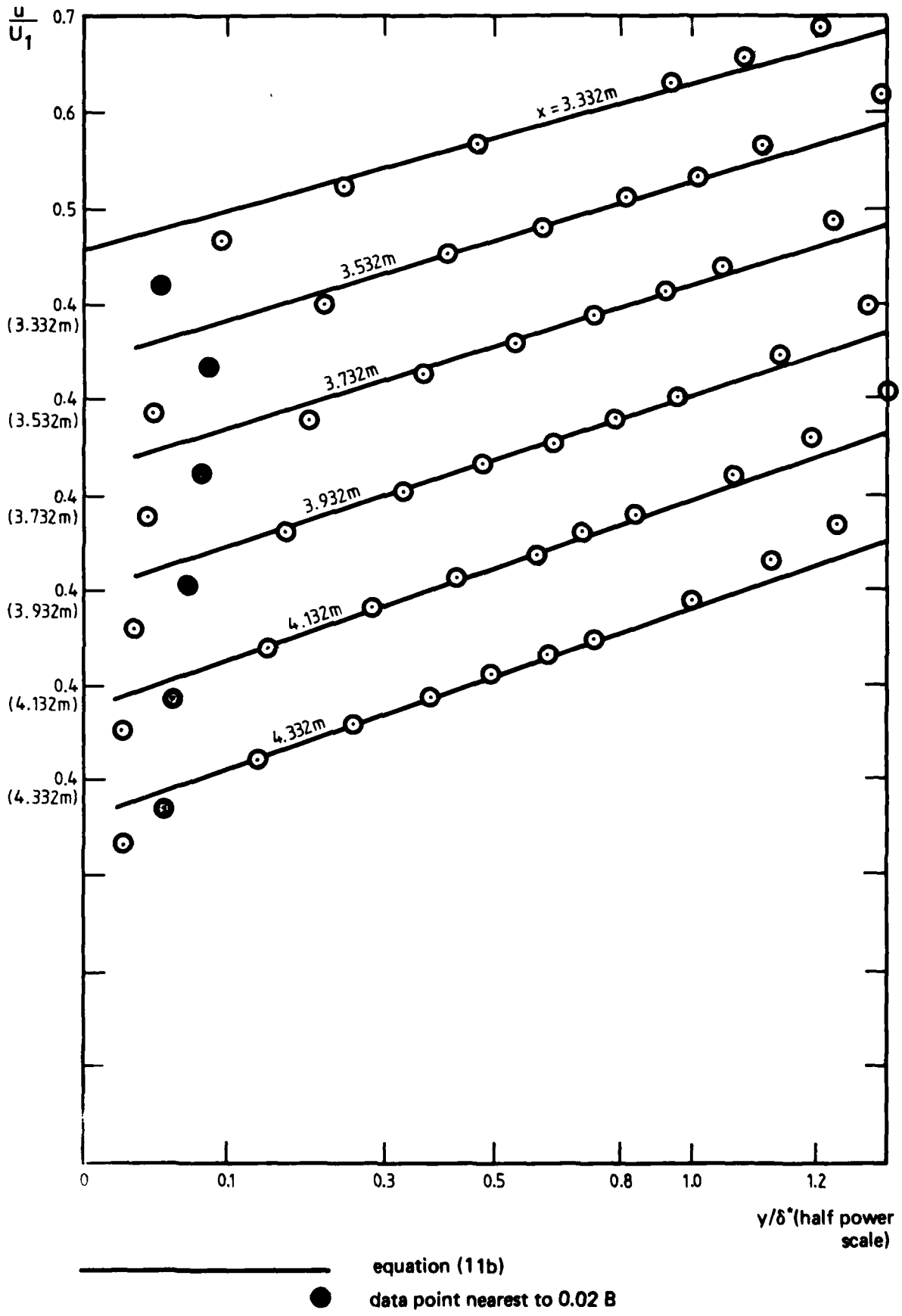

FIG. 6 HALF POWER DISTRIBUTIONS OF MEAN VELOCITY IN EQUILIBRIUM LAYERS
I, Data of Ludwieg & Tillmann (1949) mild adverse pressure gradient flow.

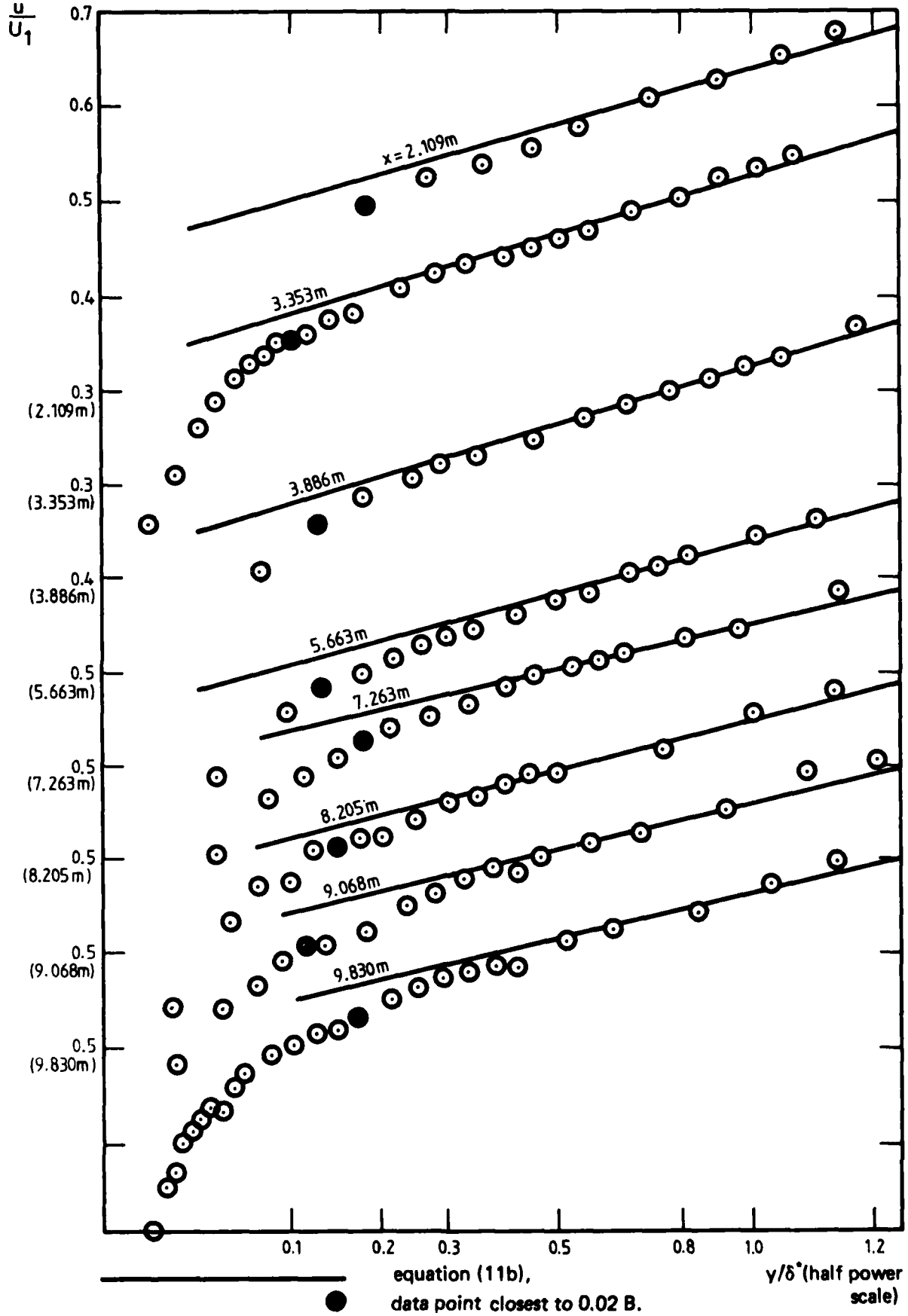

FIG. 6 Continued.
Π, Data of Clauser (1954) Flow 1.

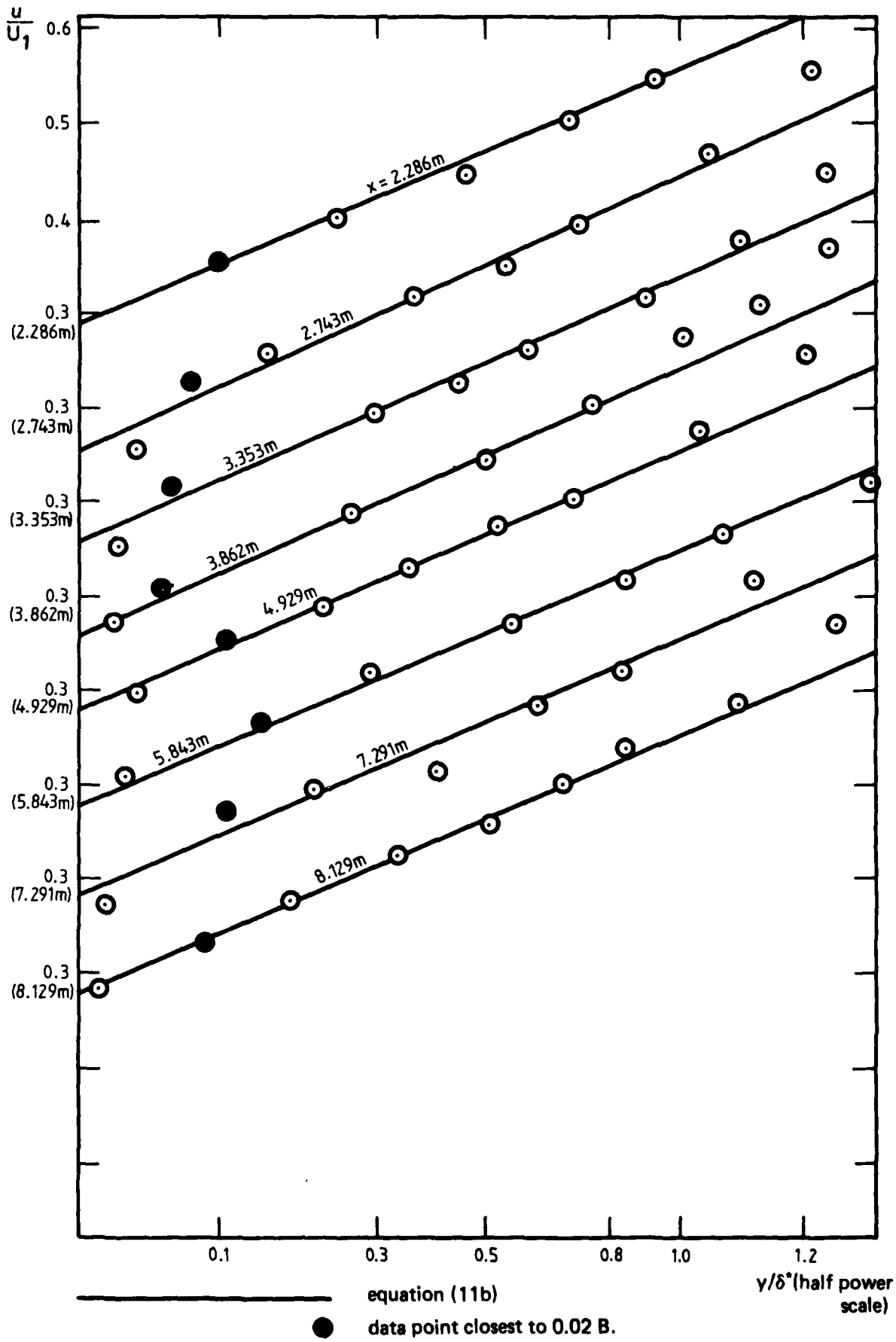

FIG. 6 Continued.
III, Data of Clauser (1954) Flow 2

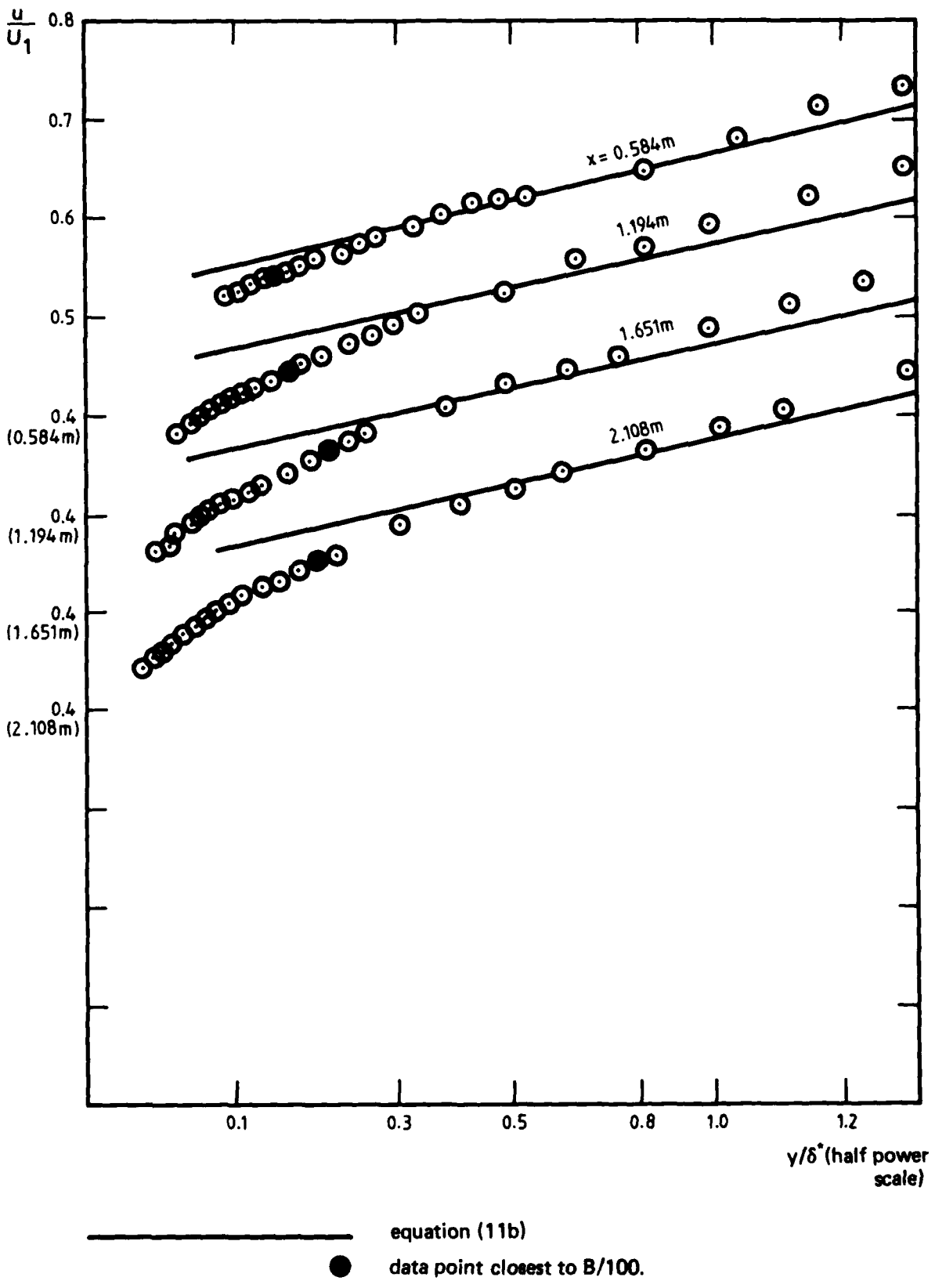

FIG. 6 Continued.
IV, Data of Bradshaw (1966) a = –0.15, .

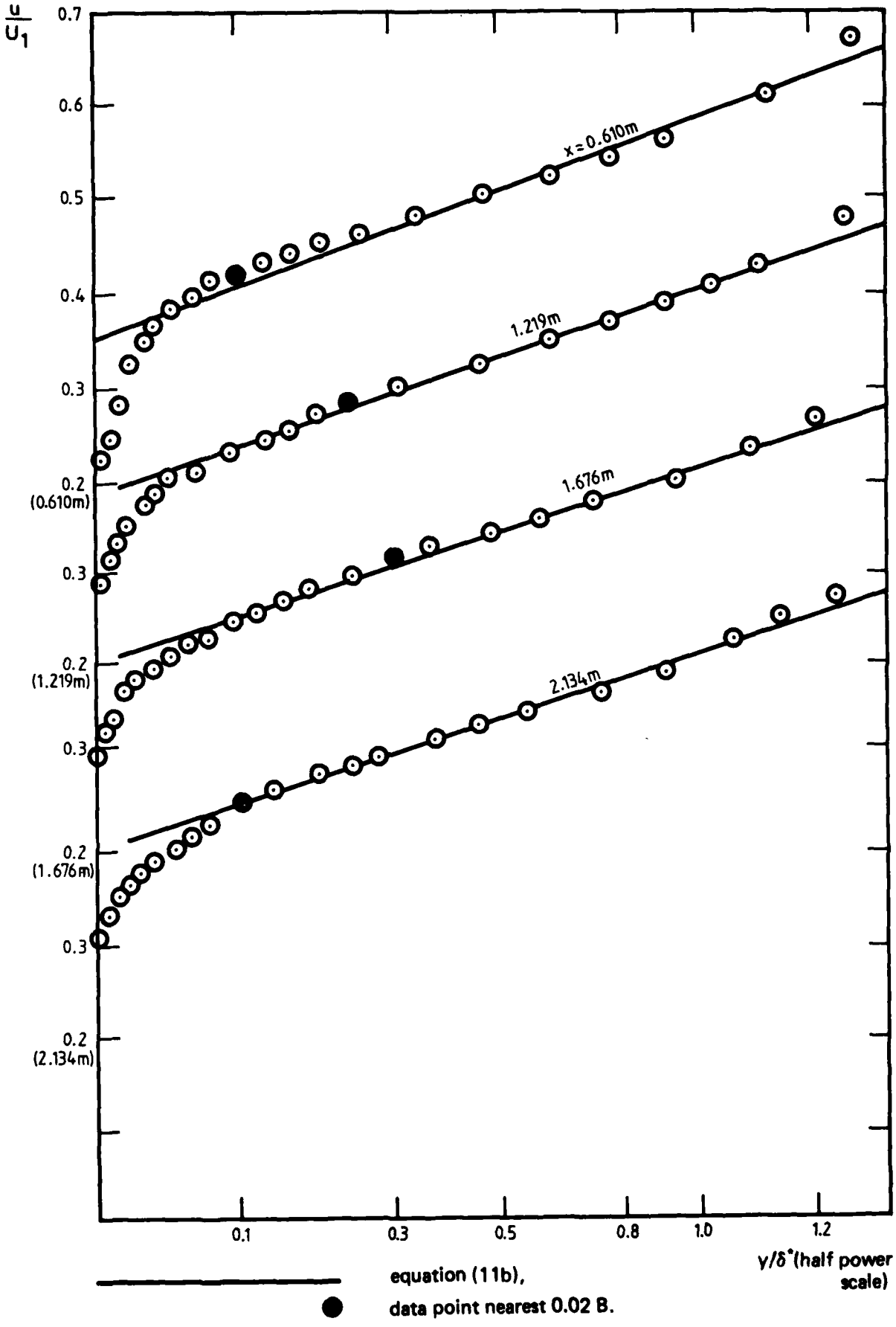

FIG. 6 Continued.
V, Data of Bradshaw & Ferriss (1965).

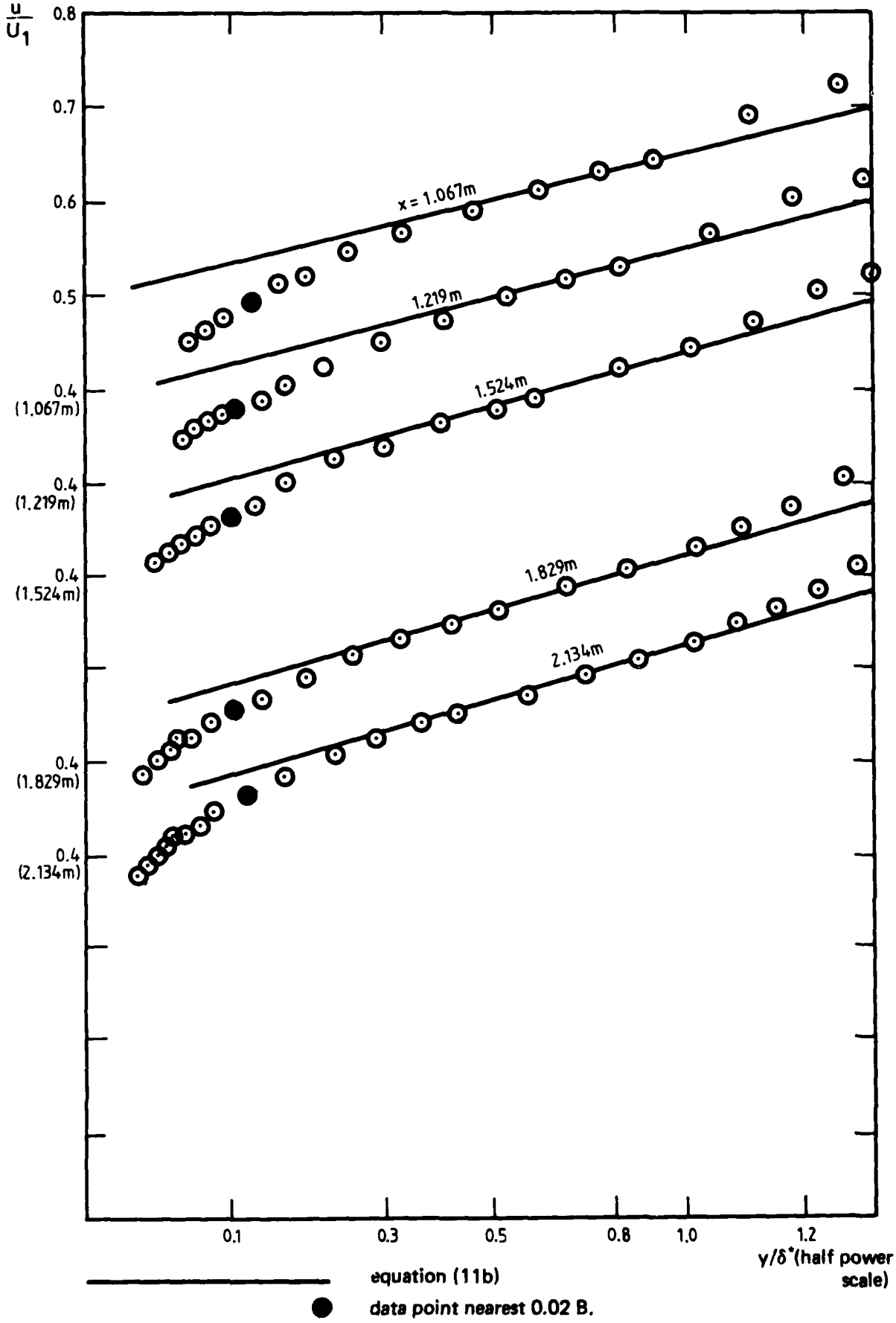

FIG. 6 Continued.
VI, Data of Bradshaw (1967) $a = 0 \rightarrow -0.255$.

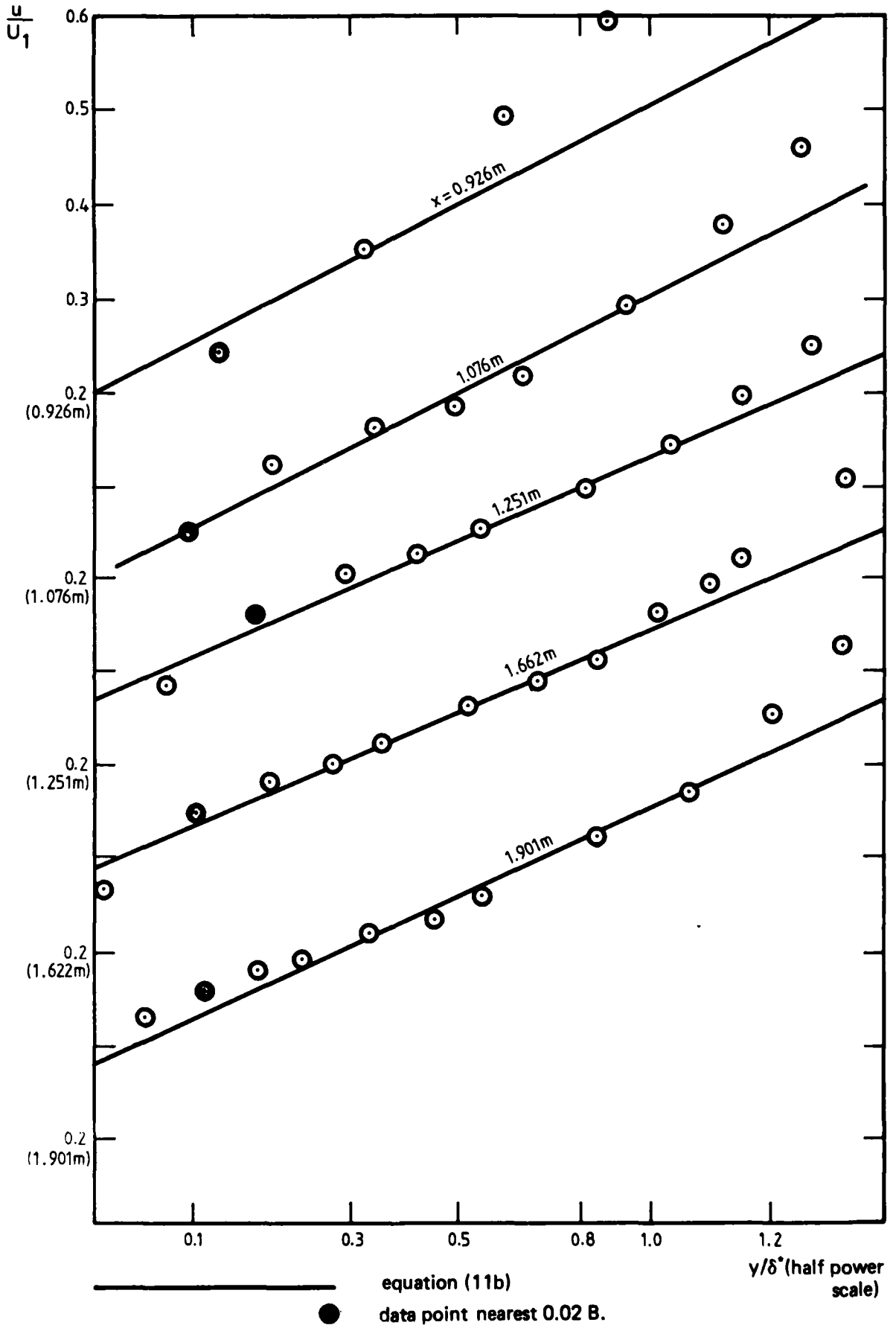

FIG. 6 Continued.
VII, Data of Stratford (1959) Flow 5.

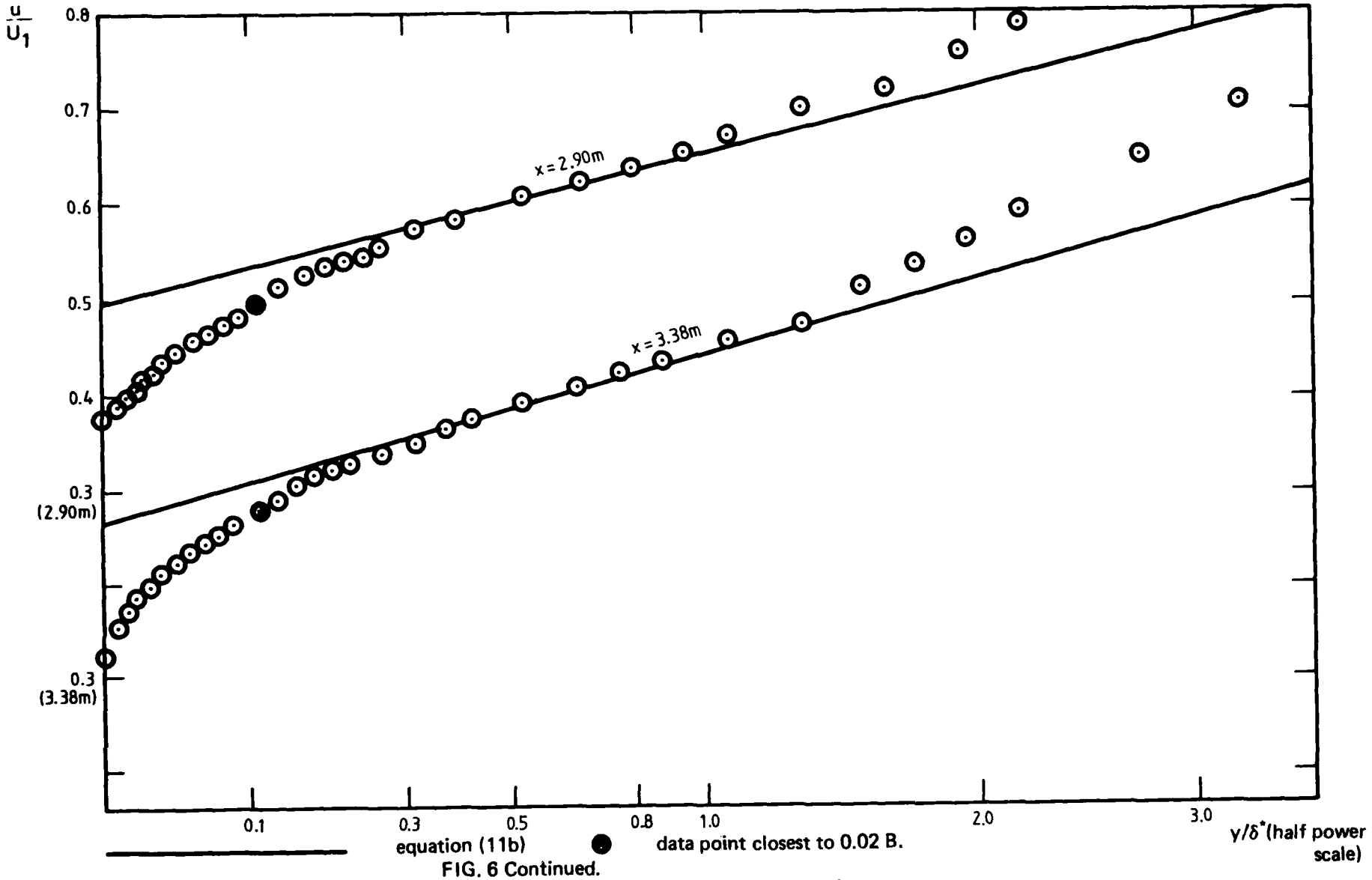

FIG. 6 Continued.
VIII, Data of Samuel (1973) Flow 2.

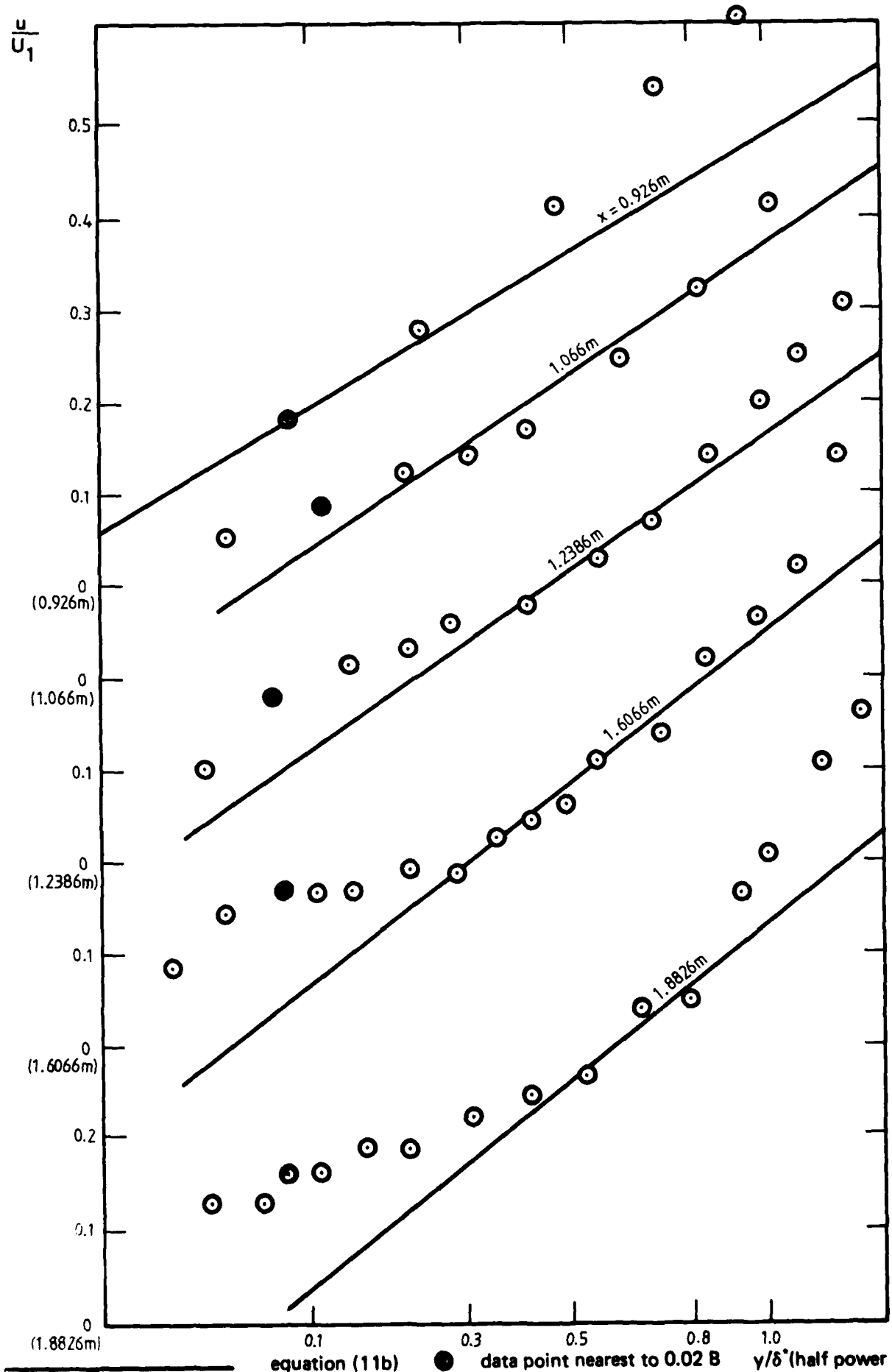

equation (11b) ● data point nearest to 0.02 B

FIG. 6 Continued.

IX. Data of Stratford (1959) Flow 6

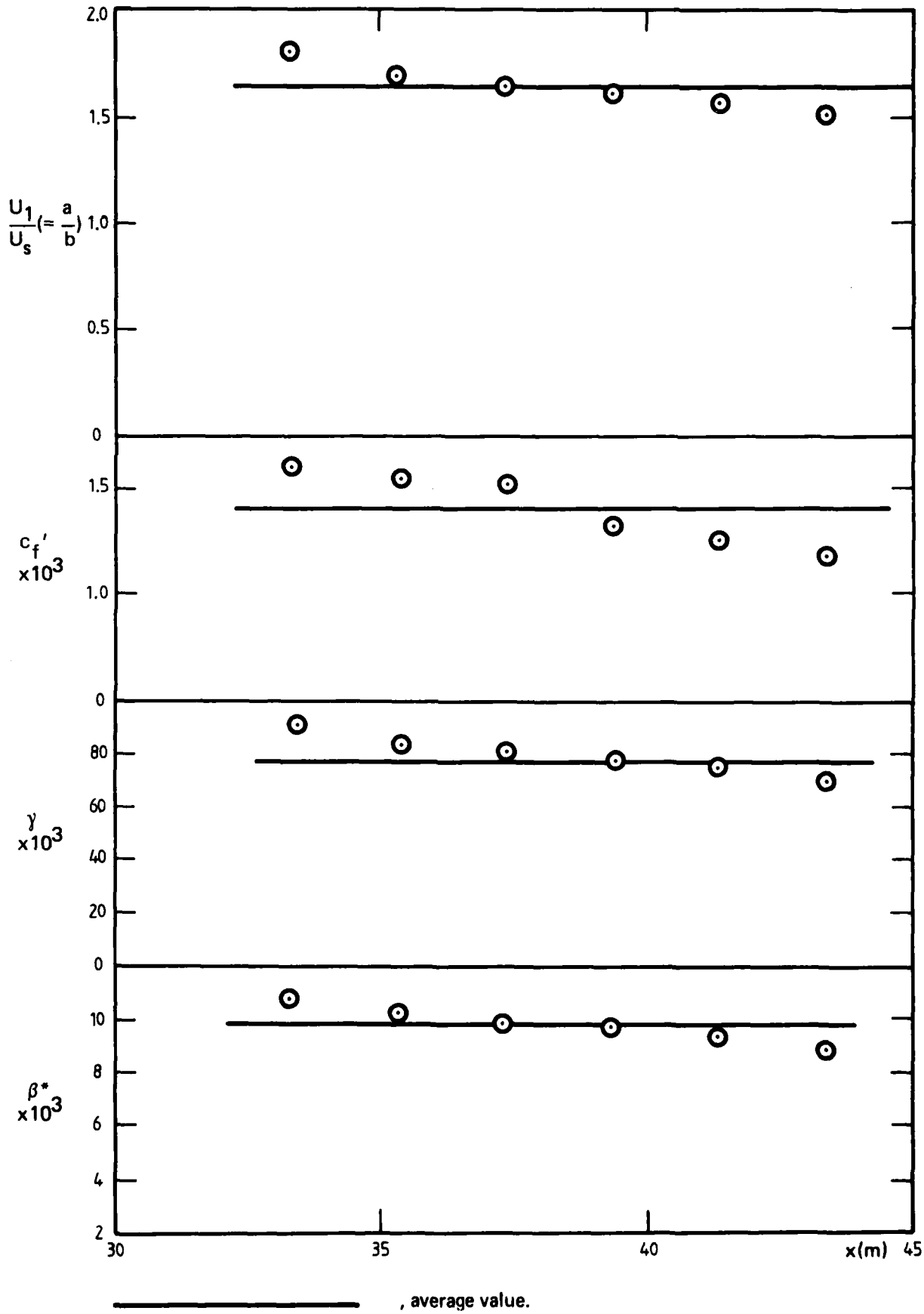

FIG. 7 PARAMETERS FOR EQUILIBRIUM LAYERS
I, Data for Ludwieg & Tillmann (1949) mild adverse pressure gradient

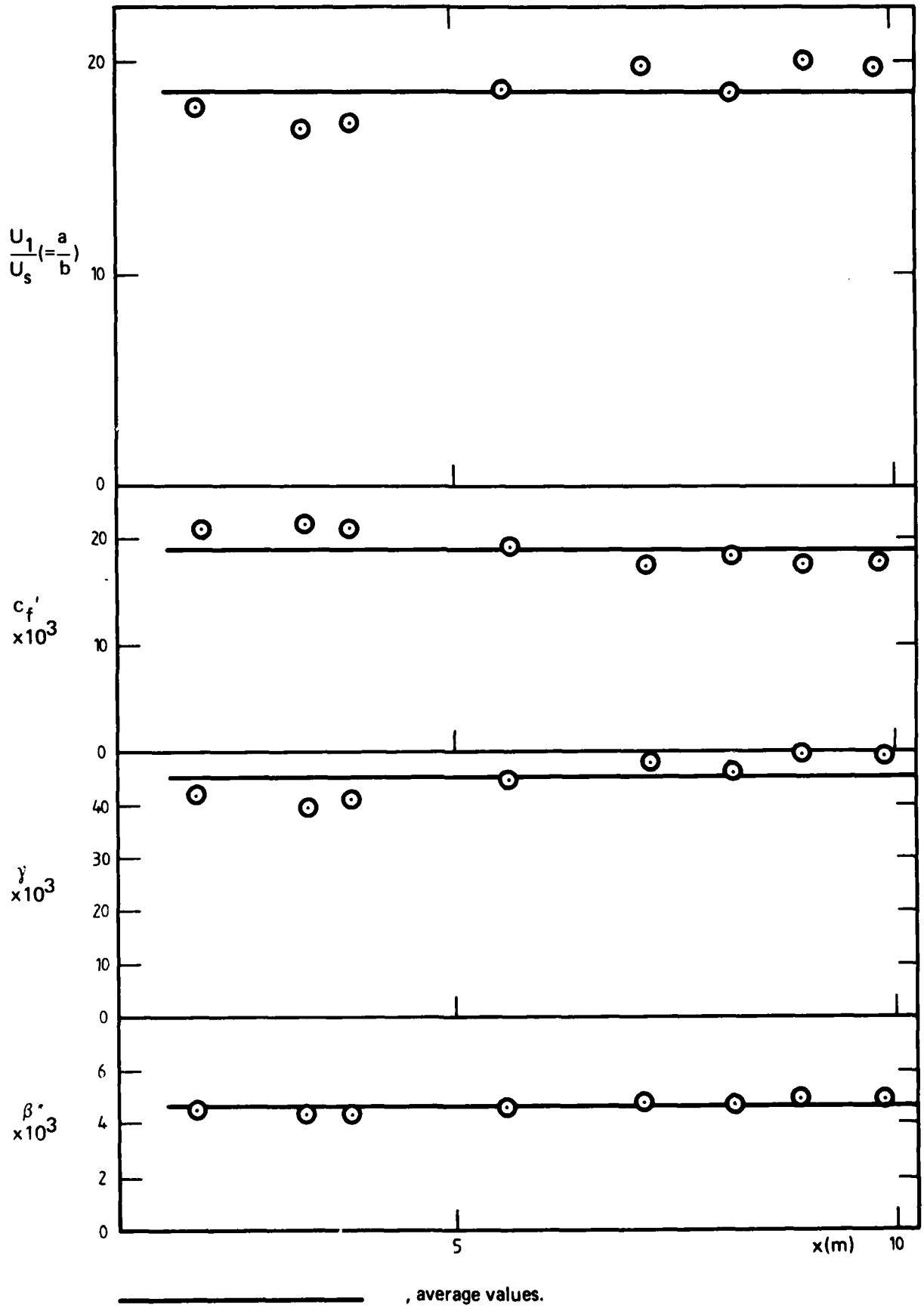

FIG. 7 Continued.
II, Data of Clauser (1954) Flow 1

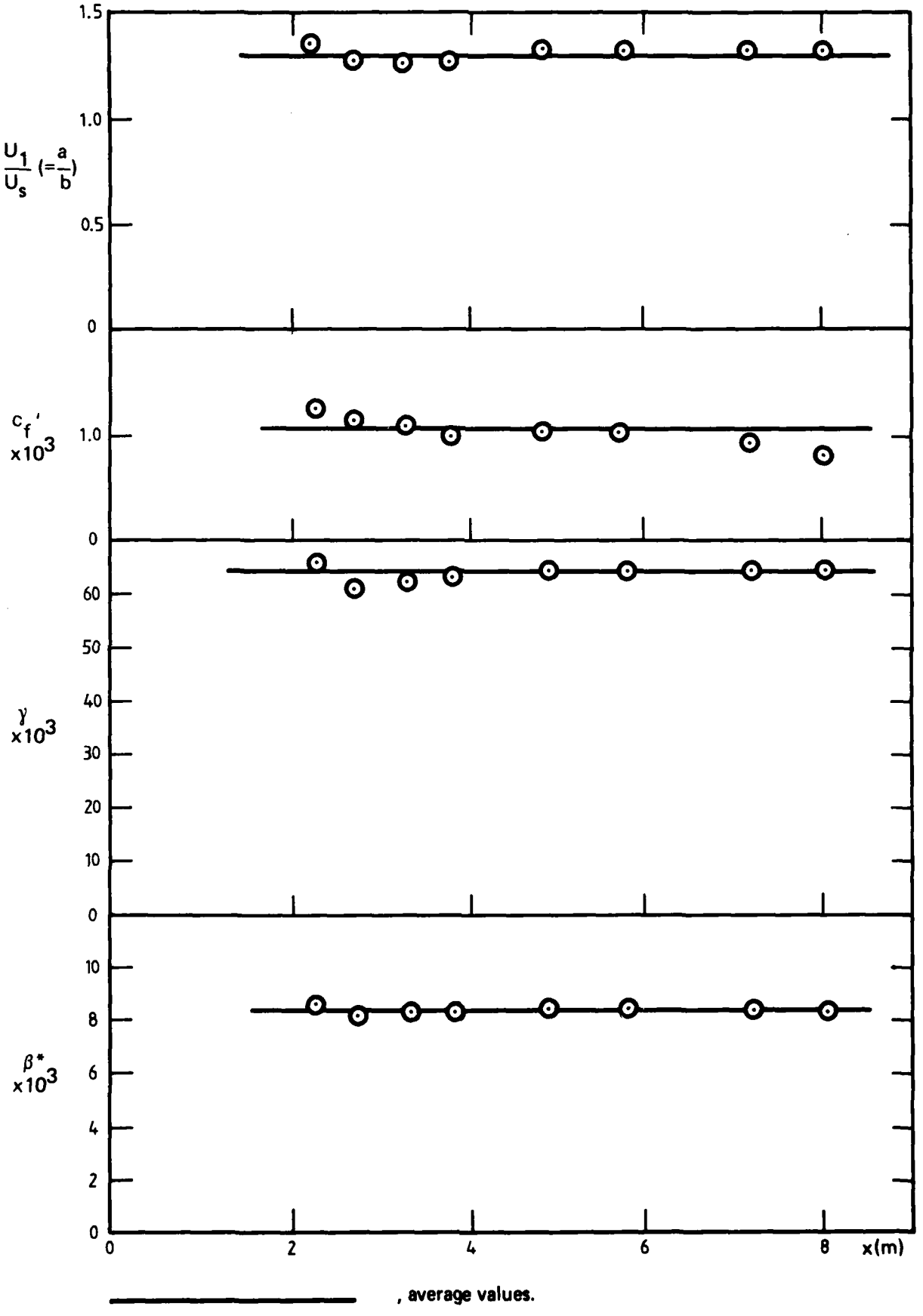

FIG. 7 Continued.
III, Data for Clauser (1954) Flow 2

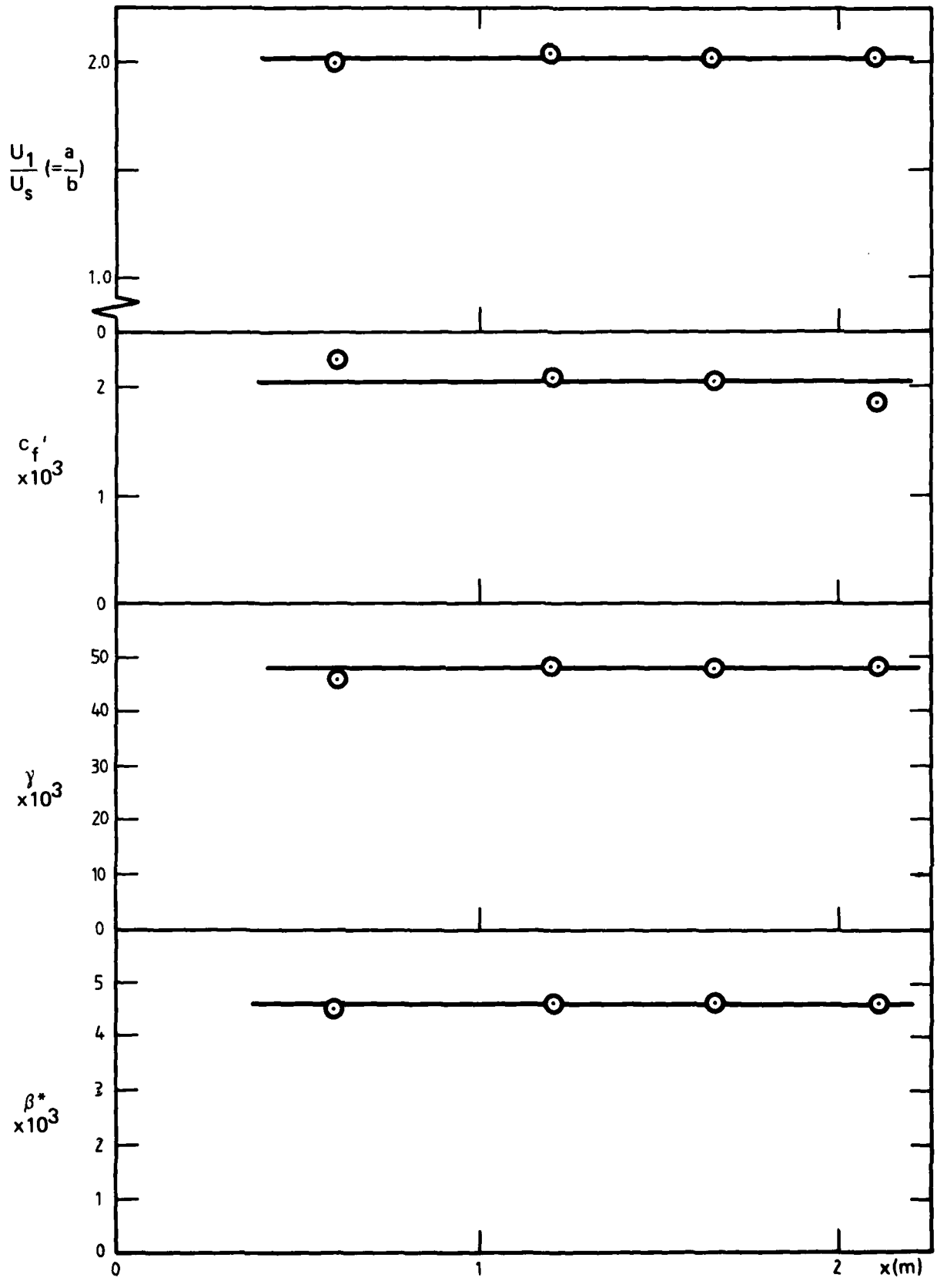

FIG. 7 Continued.
IV, Data of Bradshaw (1966) a = −0.15

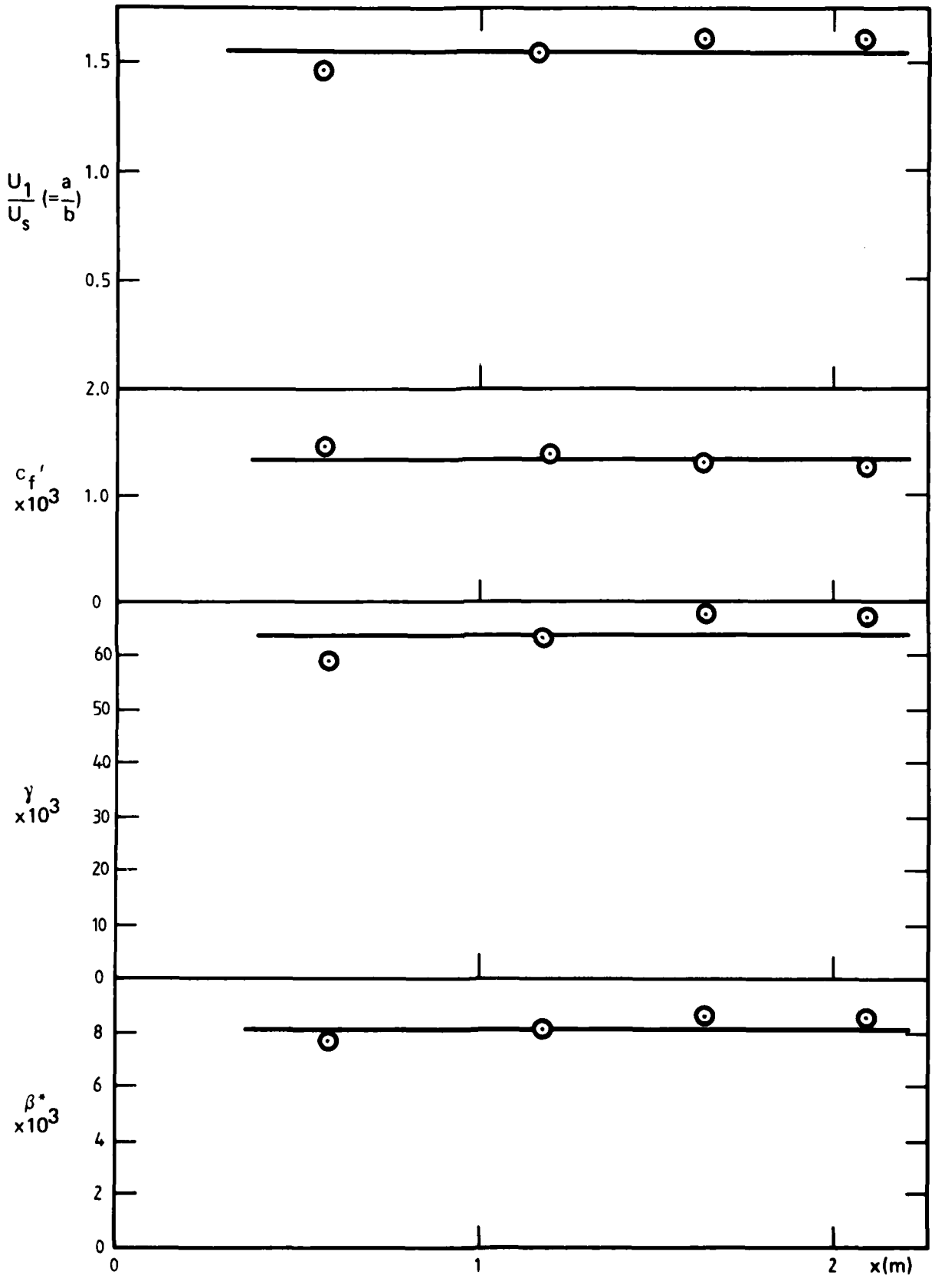

———— , average value.

FIG. 7 Continued.
V, Data of Bradshaw & Ferriss (1965) a = –0.255,

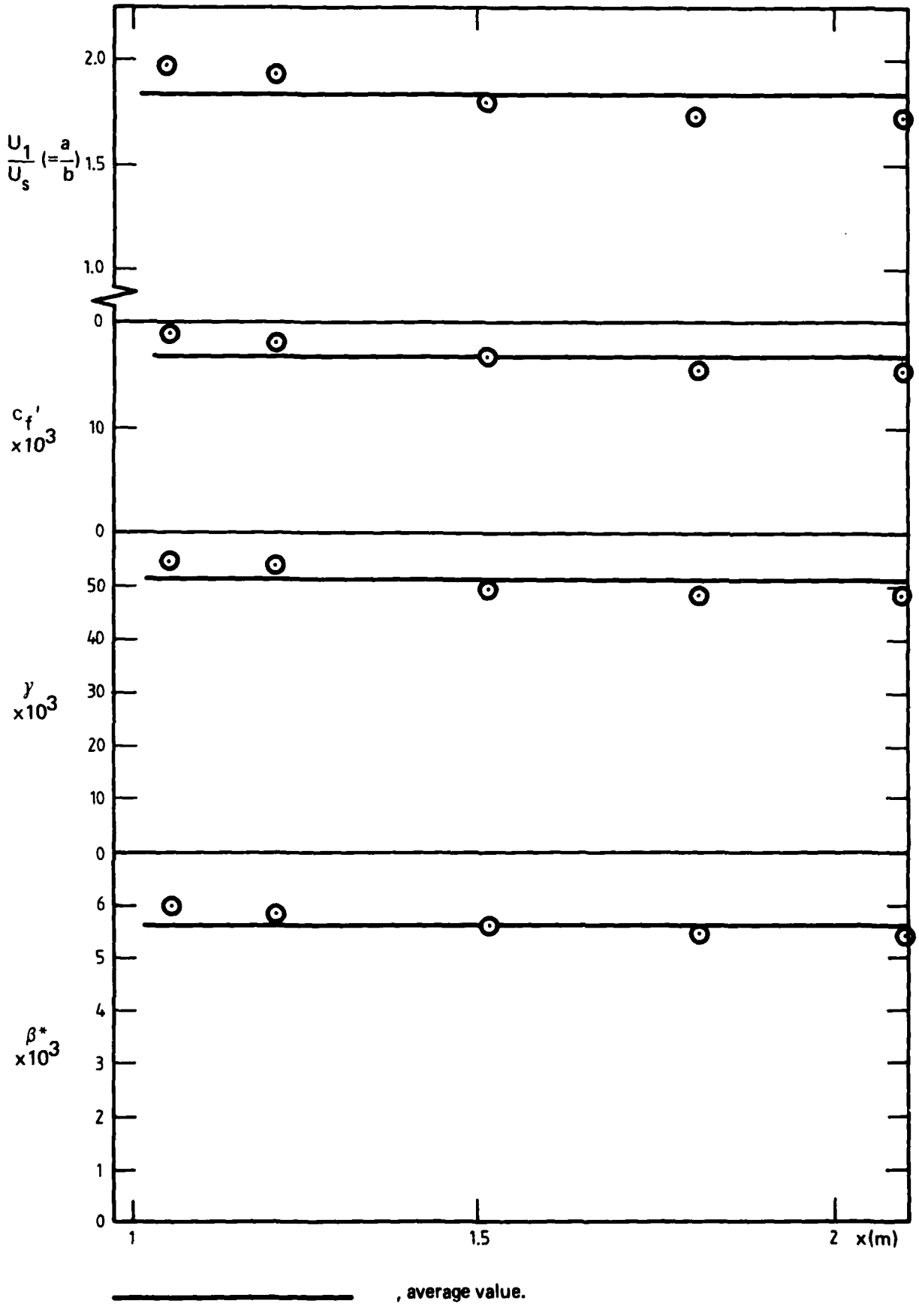

FIG. 7 Continued.
VI, Data of Bradshaw (1967) a = 0→– 0.255

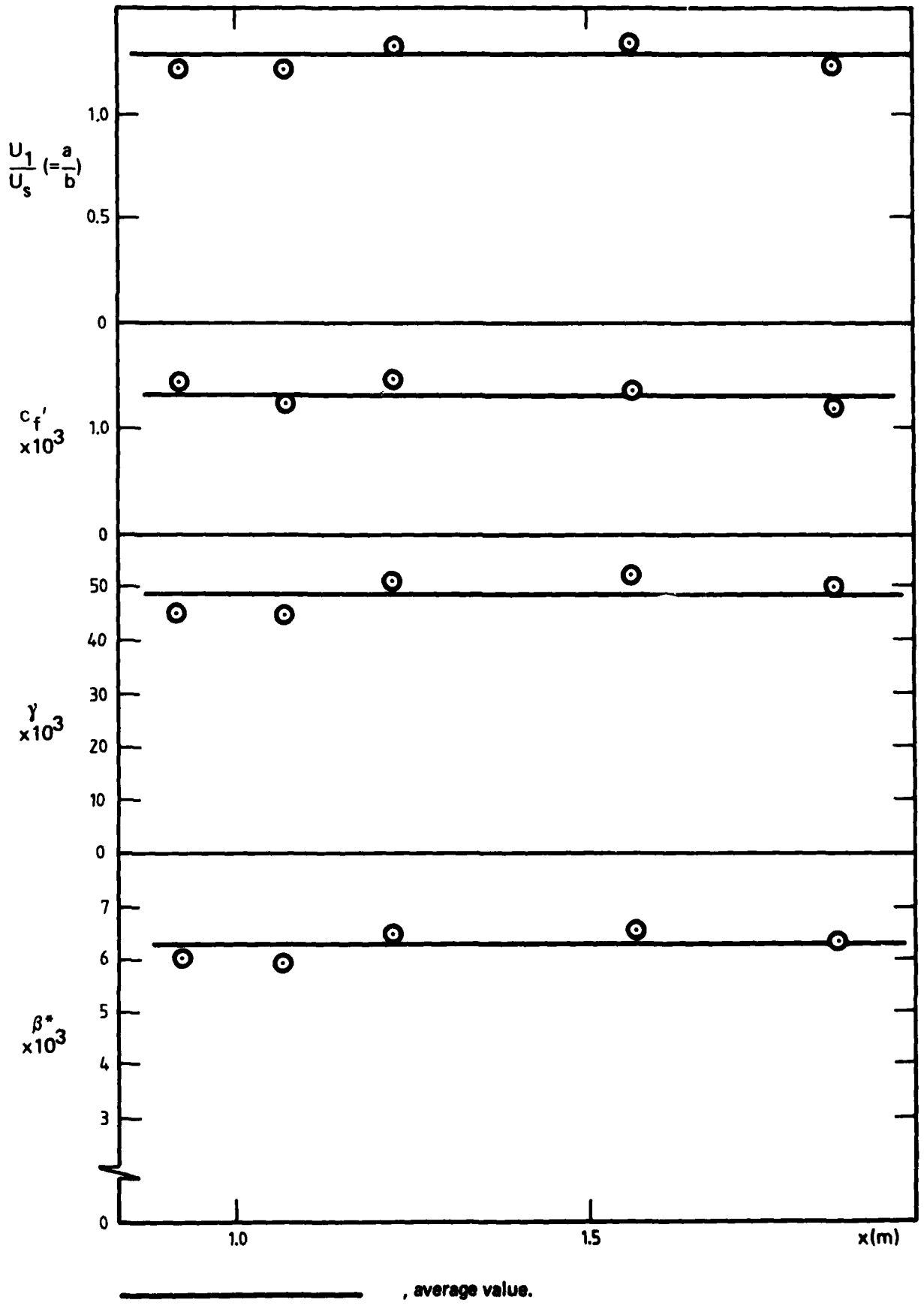

FIG. 7 Continued.
VII, Data of Stratford (1959) Flow 5

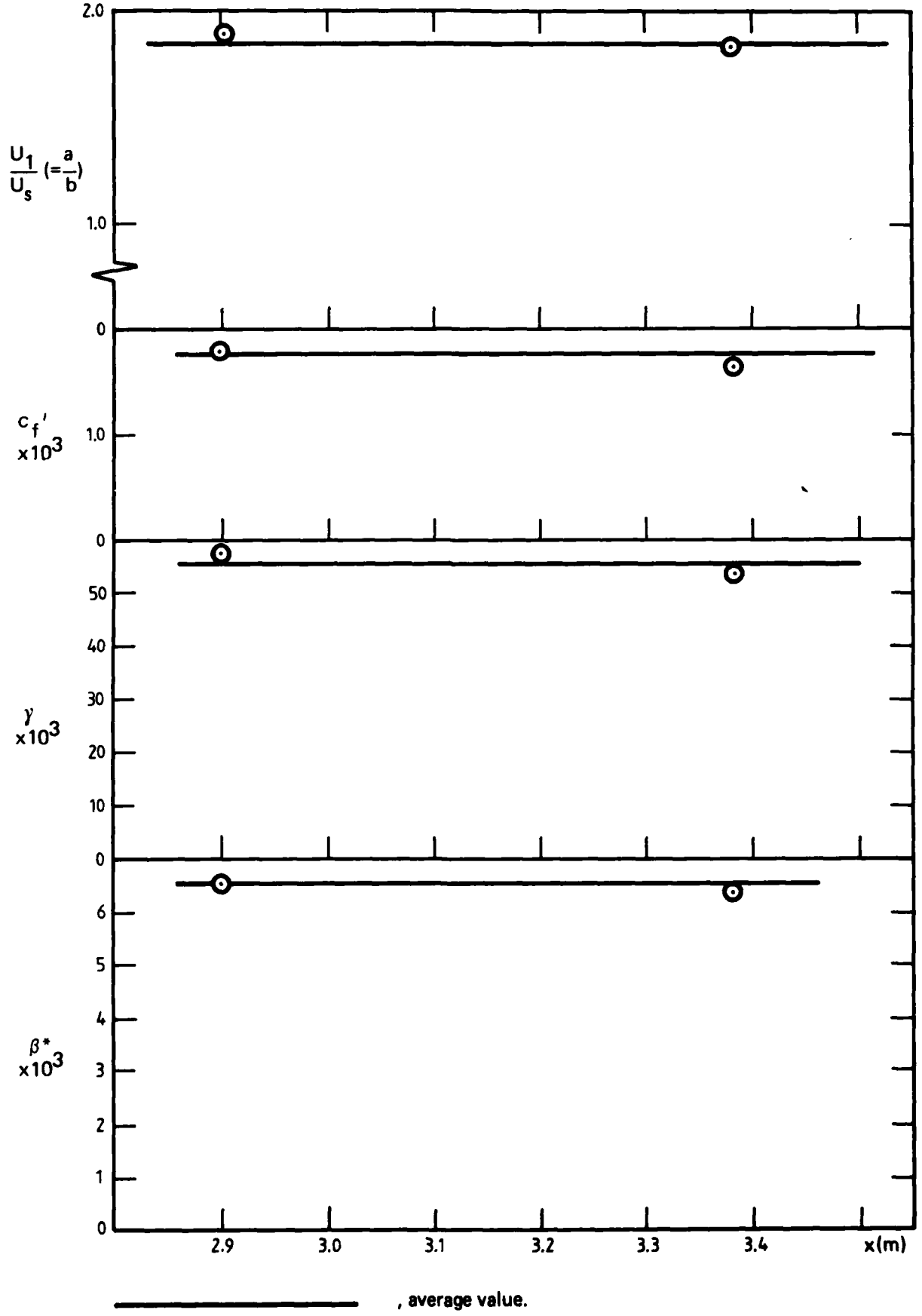

FIG. 7 Continued.
VIII, Data of Samuel (1973) Flow 2

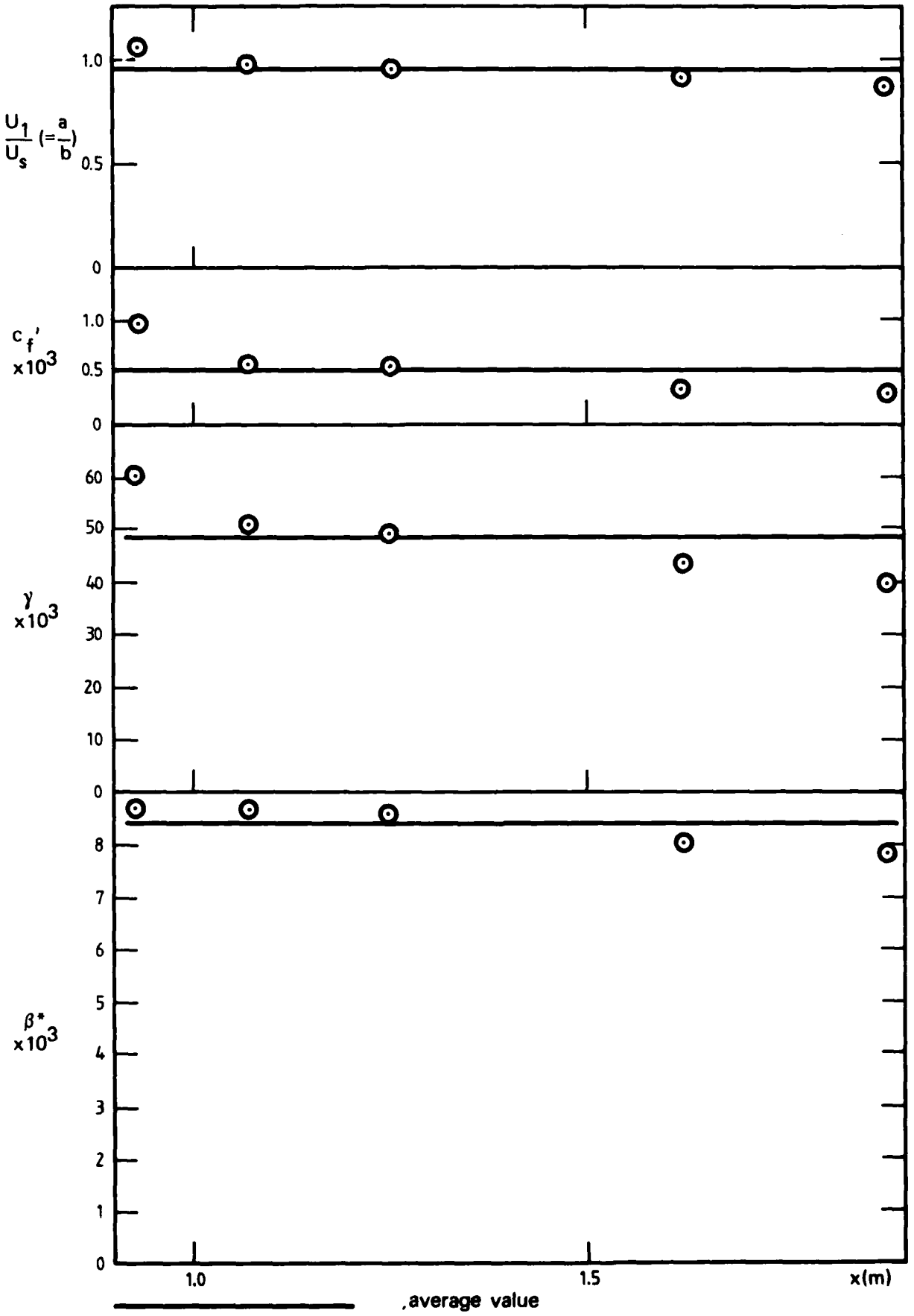

FIG. 7 Continued.
IX, Data of Stratford (1959) Flow 6.

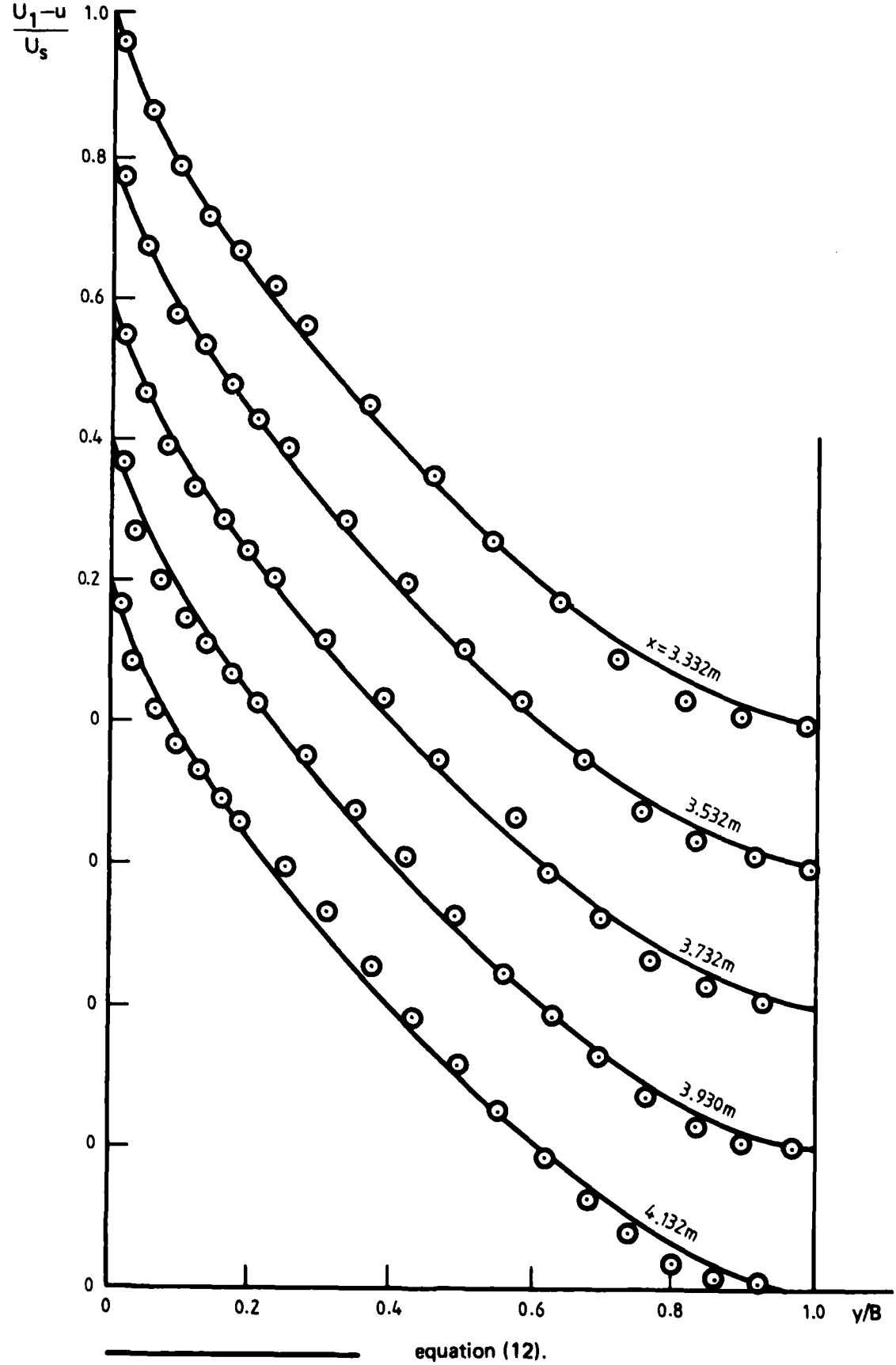

FIG. 8 MEAN VELOCITY PROFILES – SCHOFIELD & PERRY DEFECT CO-ORDINATES.
I Data of Ludwieg & Tillmann (1949) mild adverse pressure gradient layers.

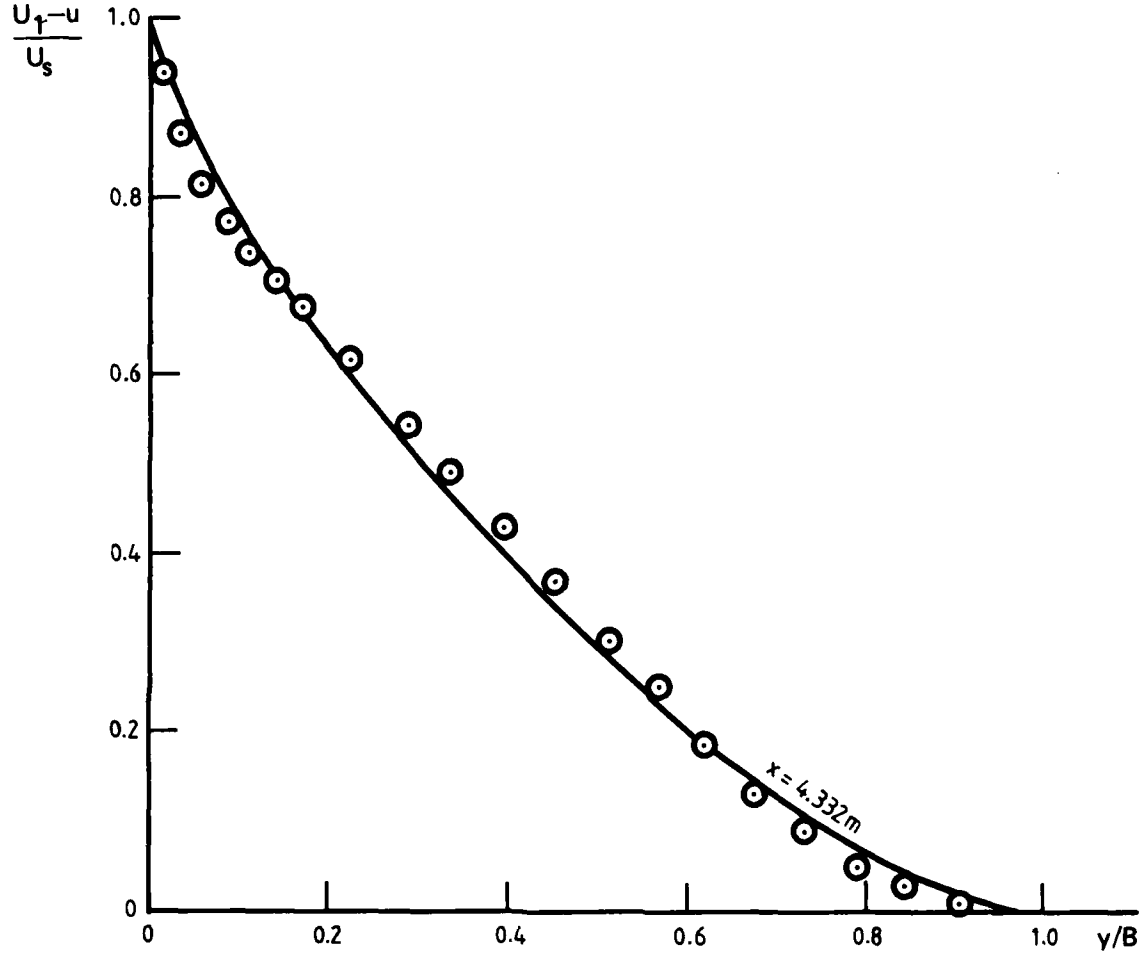

———————— , equation (12).

FIG. 8 Continued.
I Data of Ludwieg & Tillmann concluded.

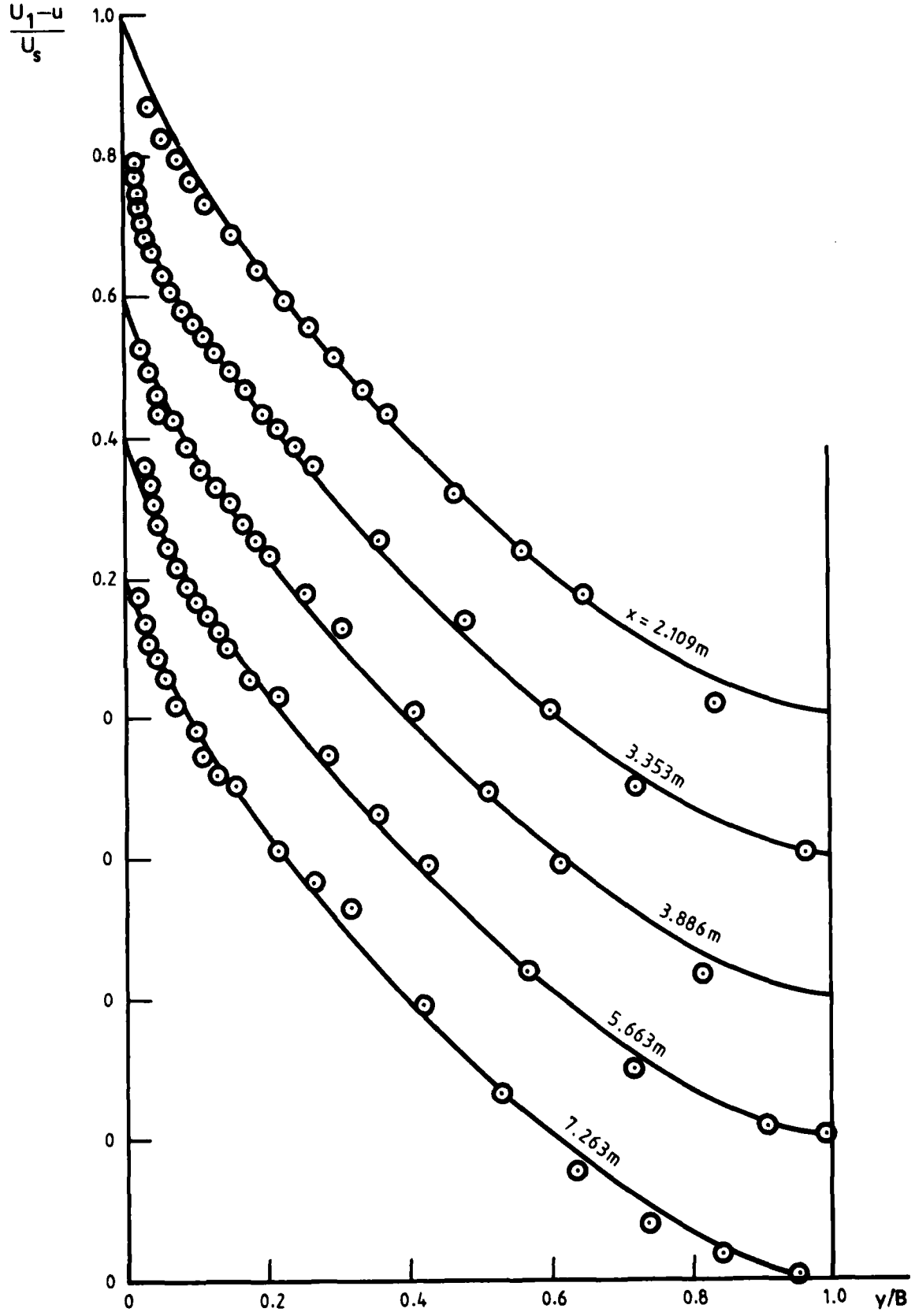

———————— , equation (12).

FIG. 8 Continued.
II Data of Clauser (1954) Flow 1

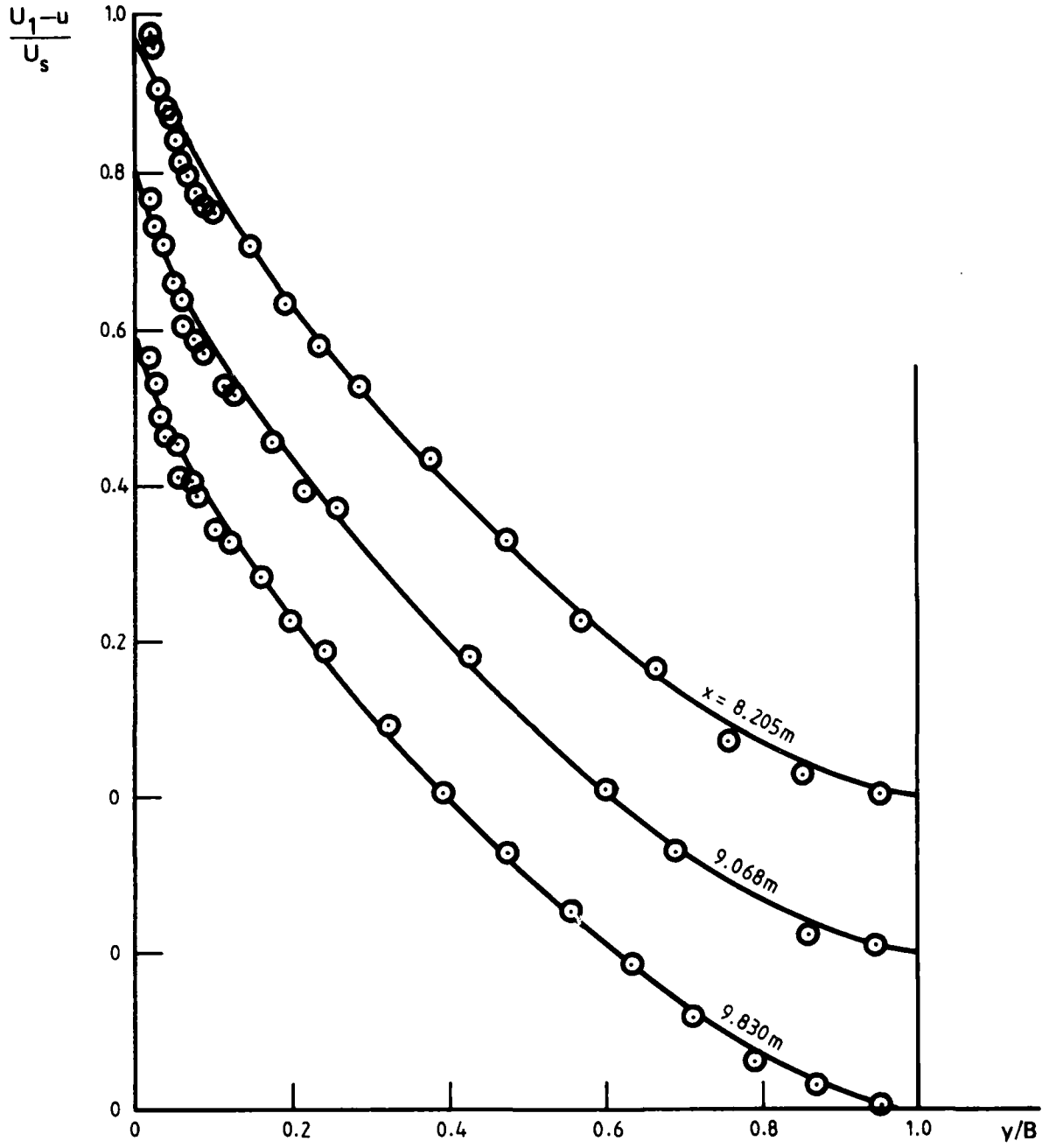

, equation (12).

FIG. 8 Continued.
Data of Clauser (1954) Flow 1 concluded.

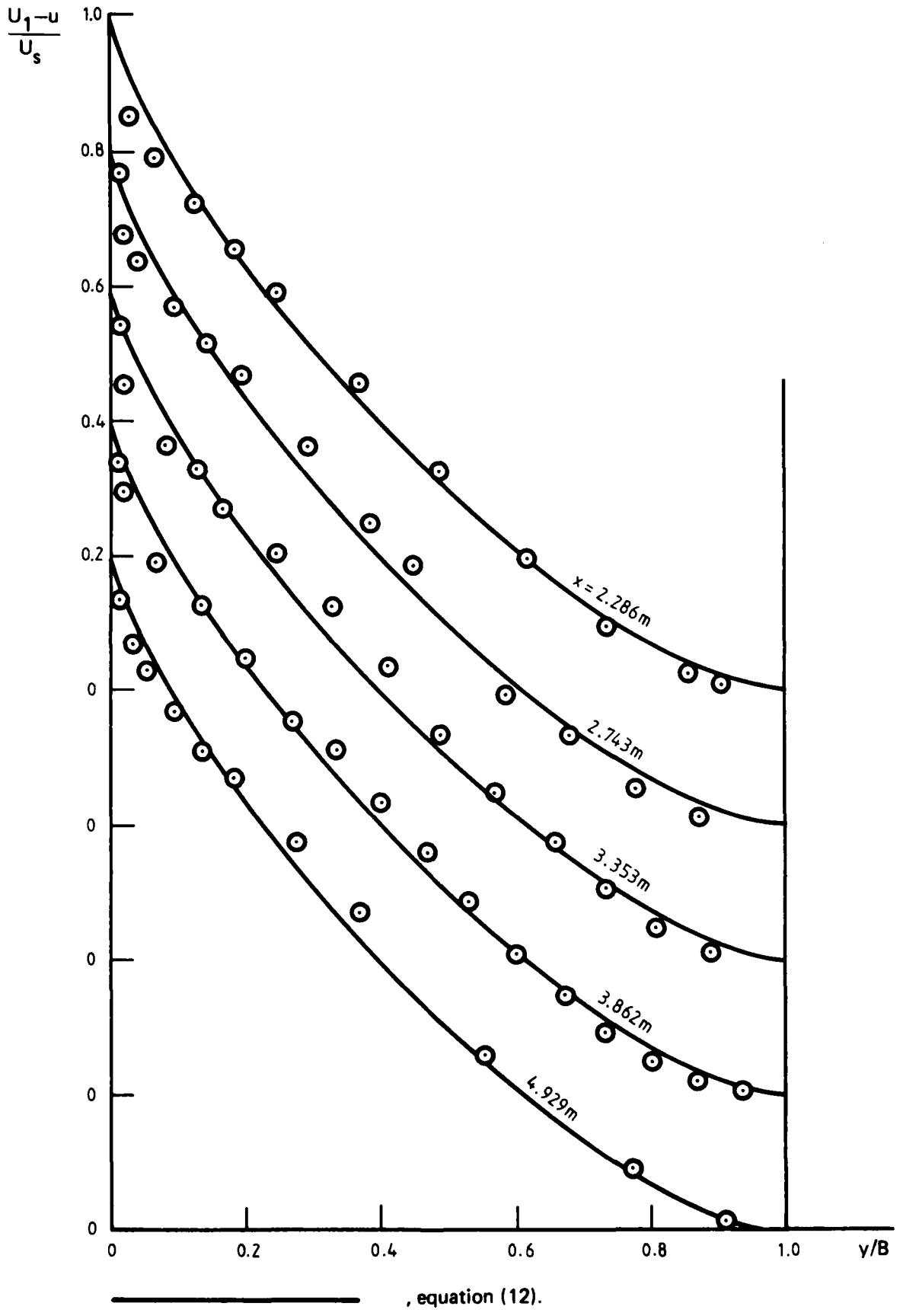

FIG. 8 Continued.
III Data of Clauser (1954) Flow 2

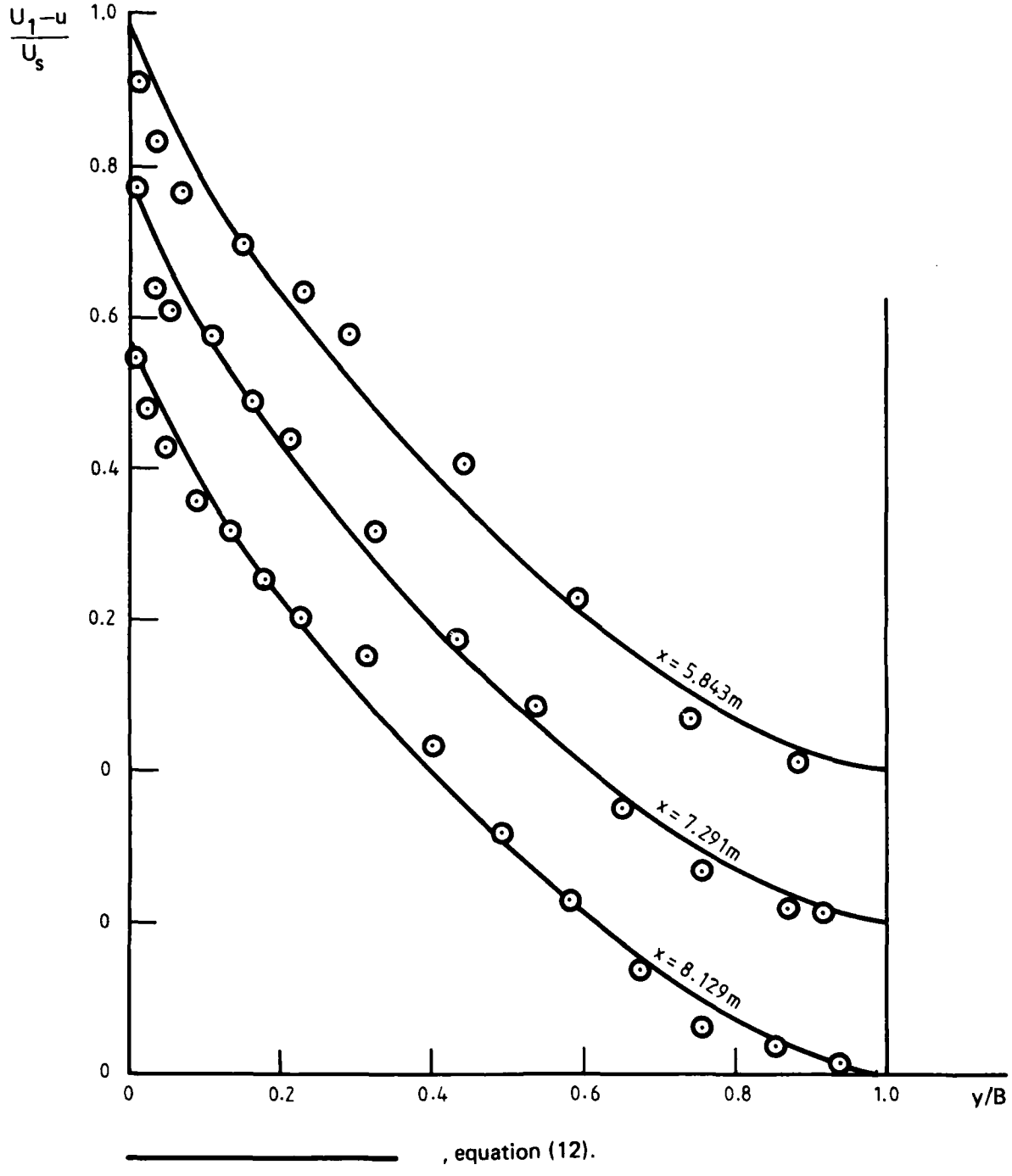

FIG. 8 Continued.
Data of Clauser (1954) Flow 2 concluded.

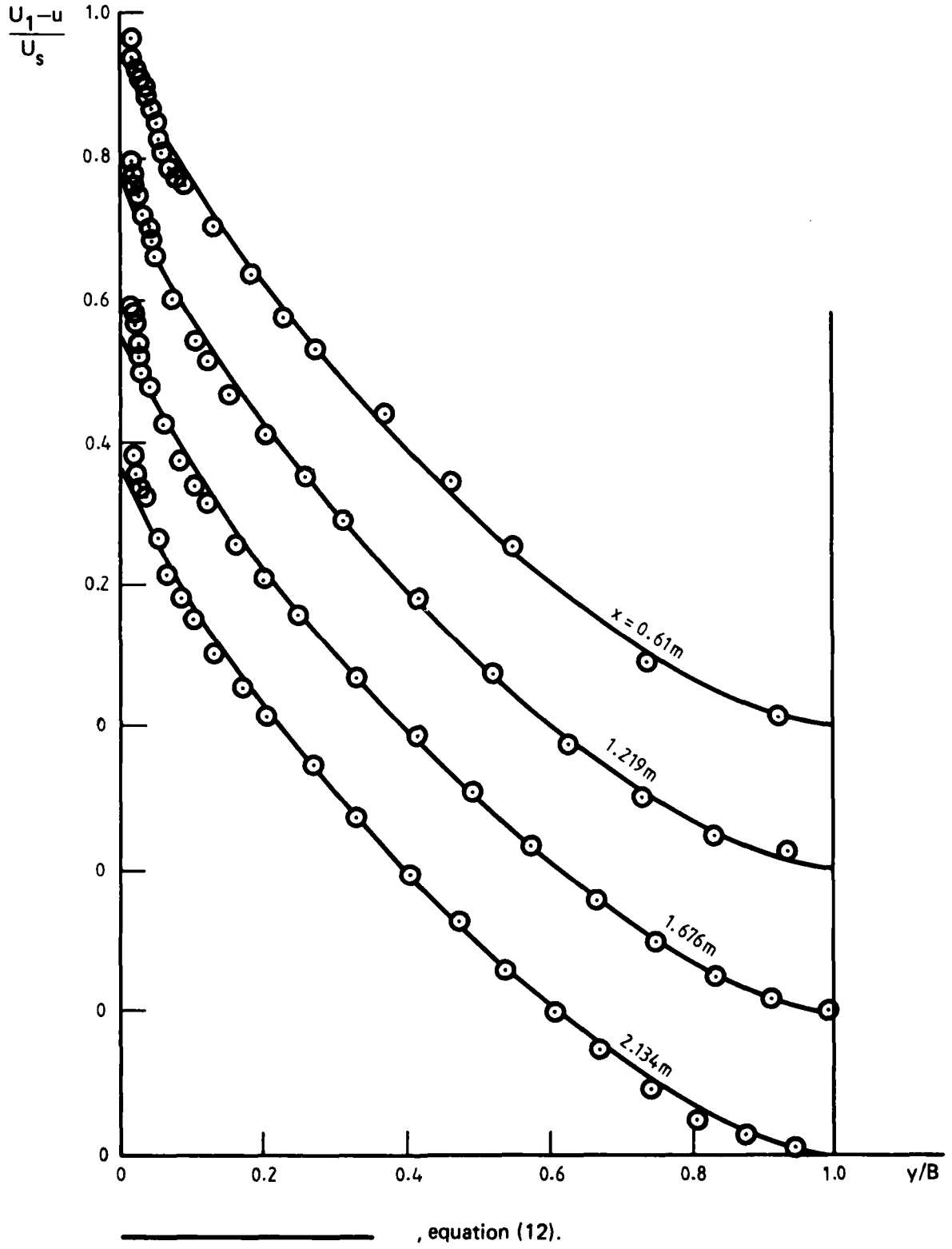

FIG. 8 Continued.
IV. Data of Bradshaw (1966) a = –0.15.

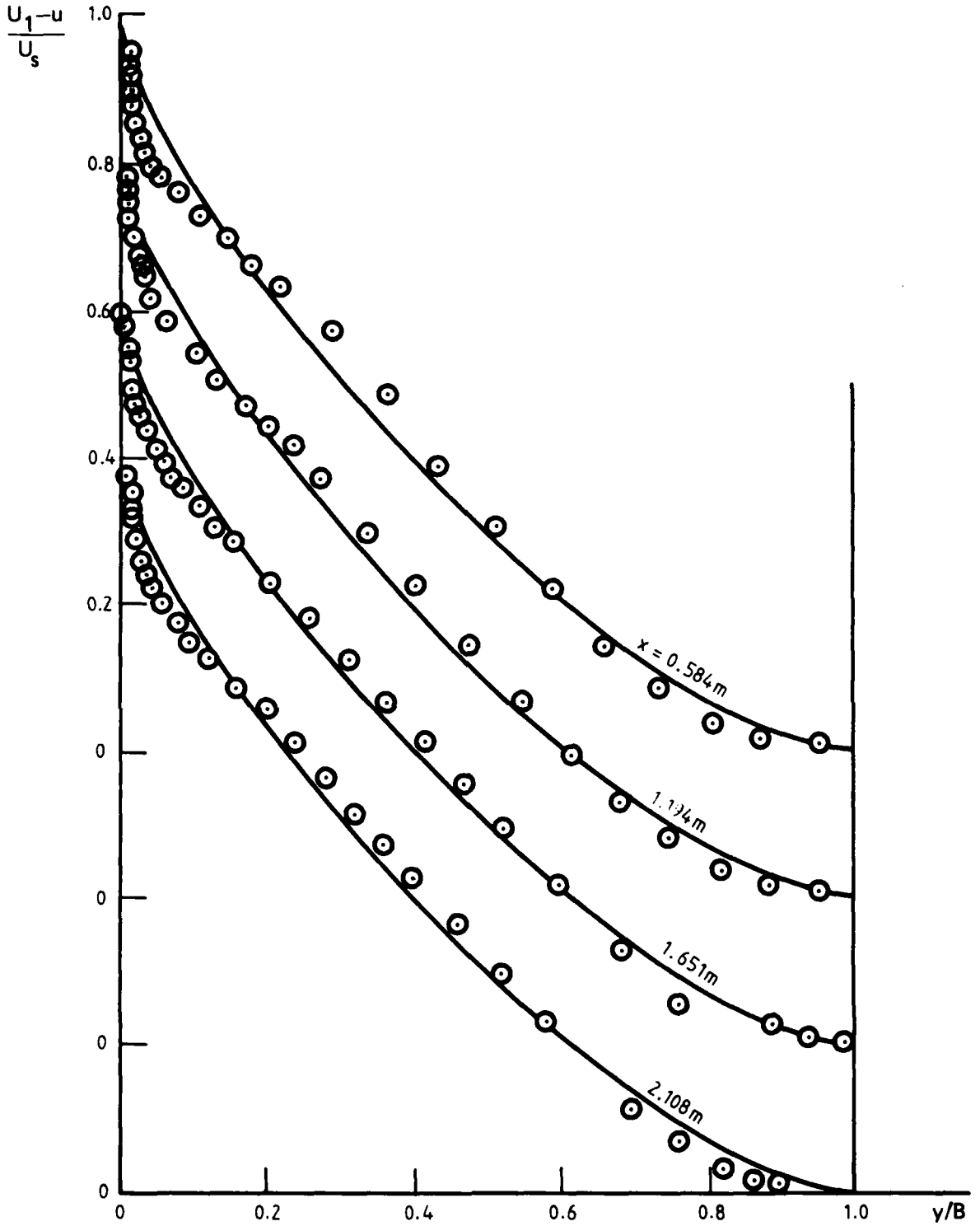

, equation (12).

FIG. 8 Continued.

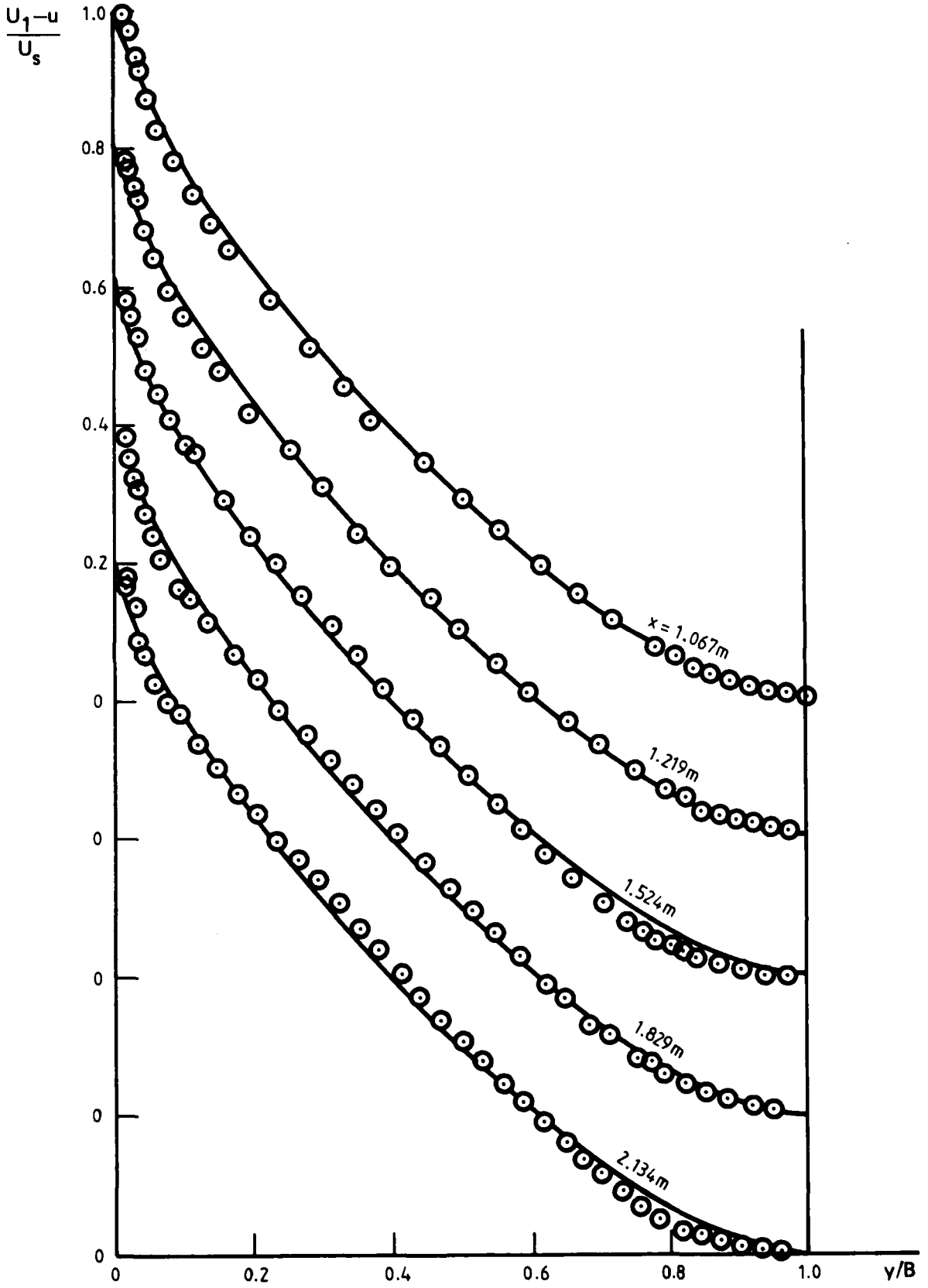

, equation (12).

FIG. 8 Continued.
VI. Data of Bradshaw (1967) $\alpha = 0 - 0.255$

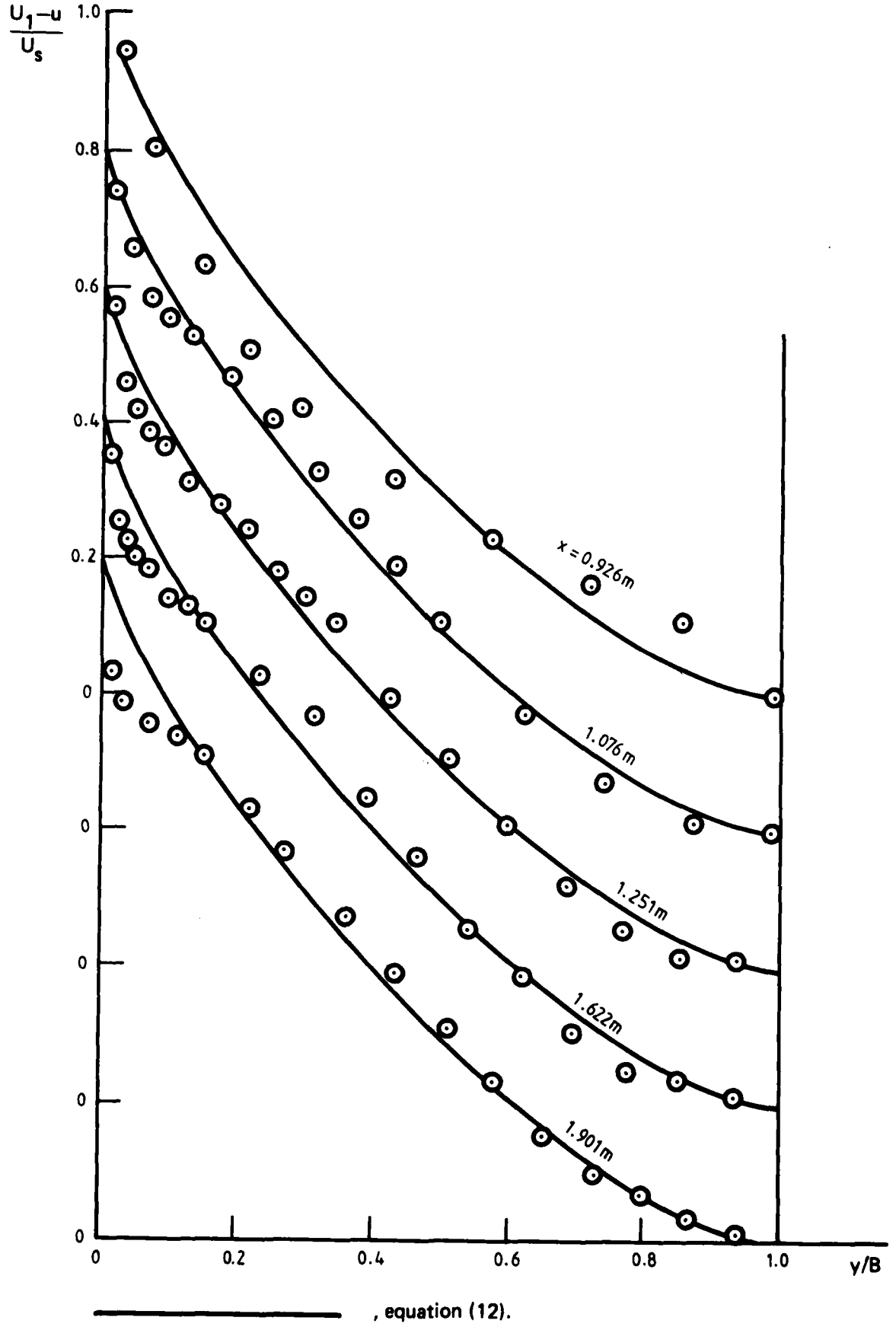

———————— , equation (12).

FIG. 8 Continued.
VII Data of Stratford (1969) Flow 5

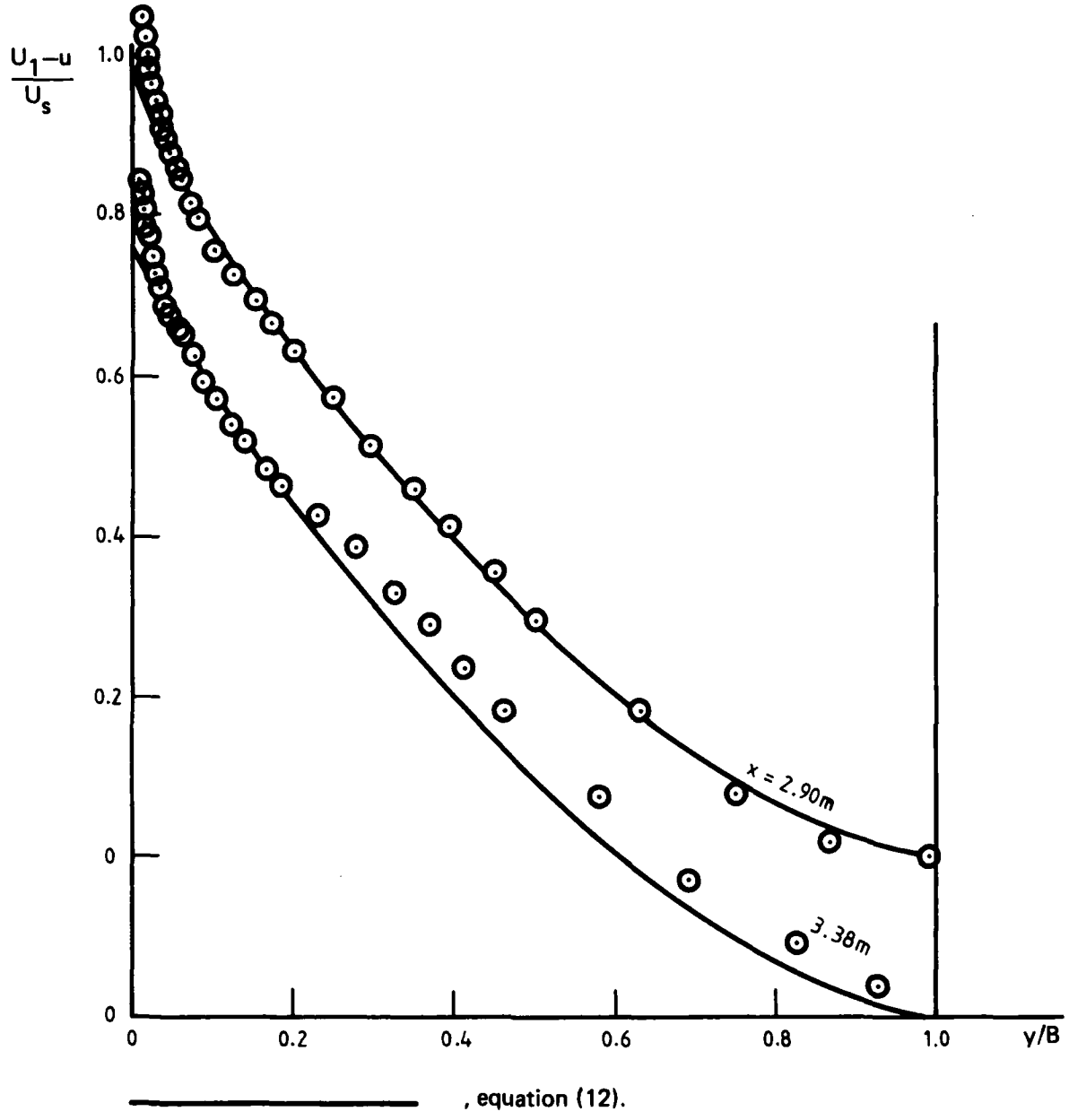

FIG. 8 Continued.
VIII. Data of Samuel (1973) Flow 2

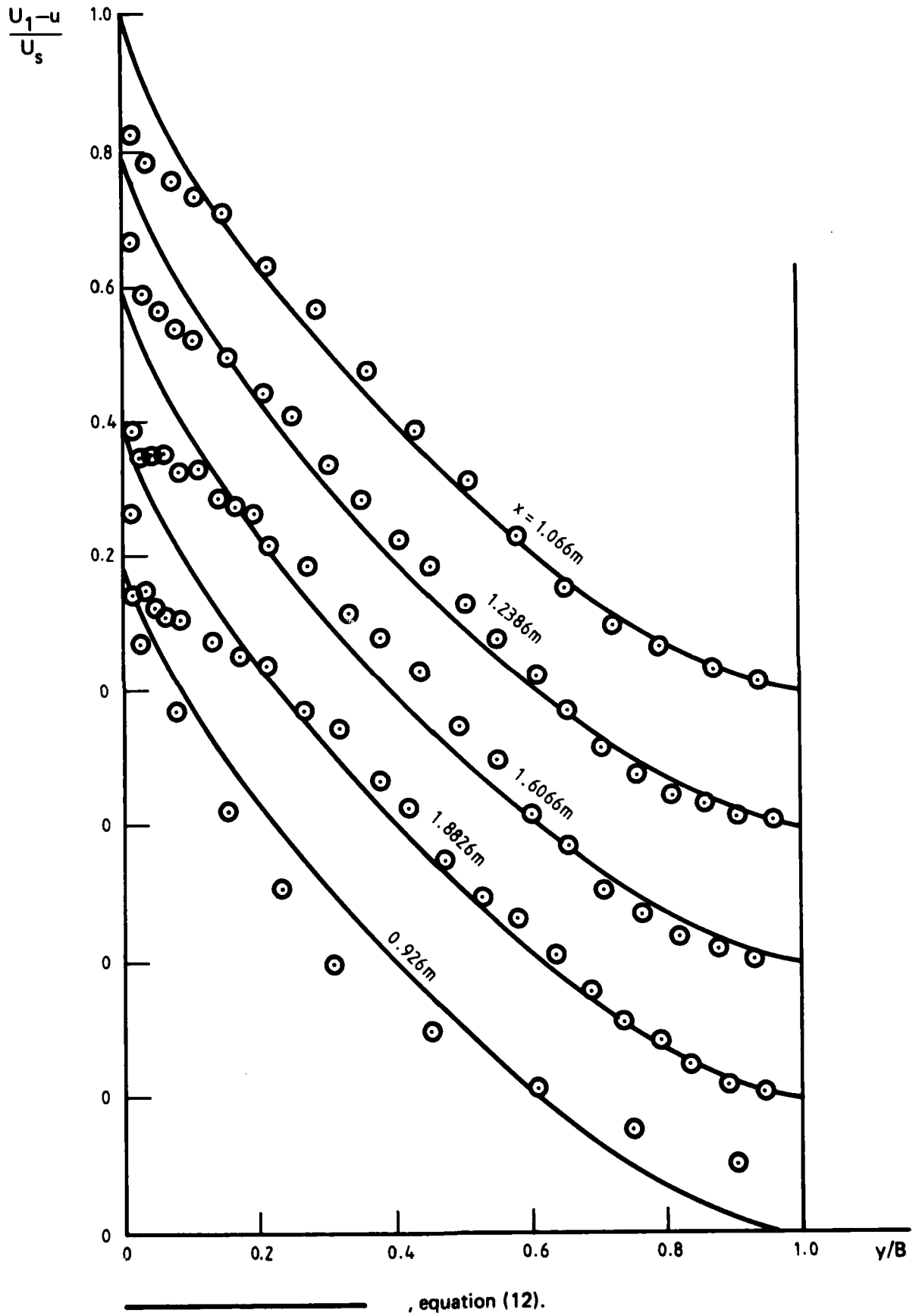

FIG. 8 Continued.
IX. Data of Stratford (1959) Flow 6

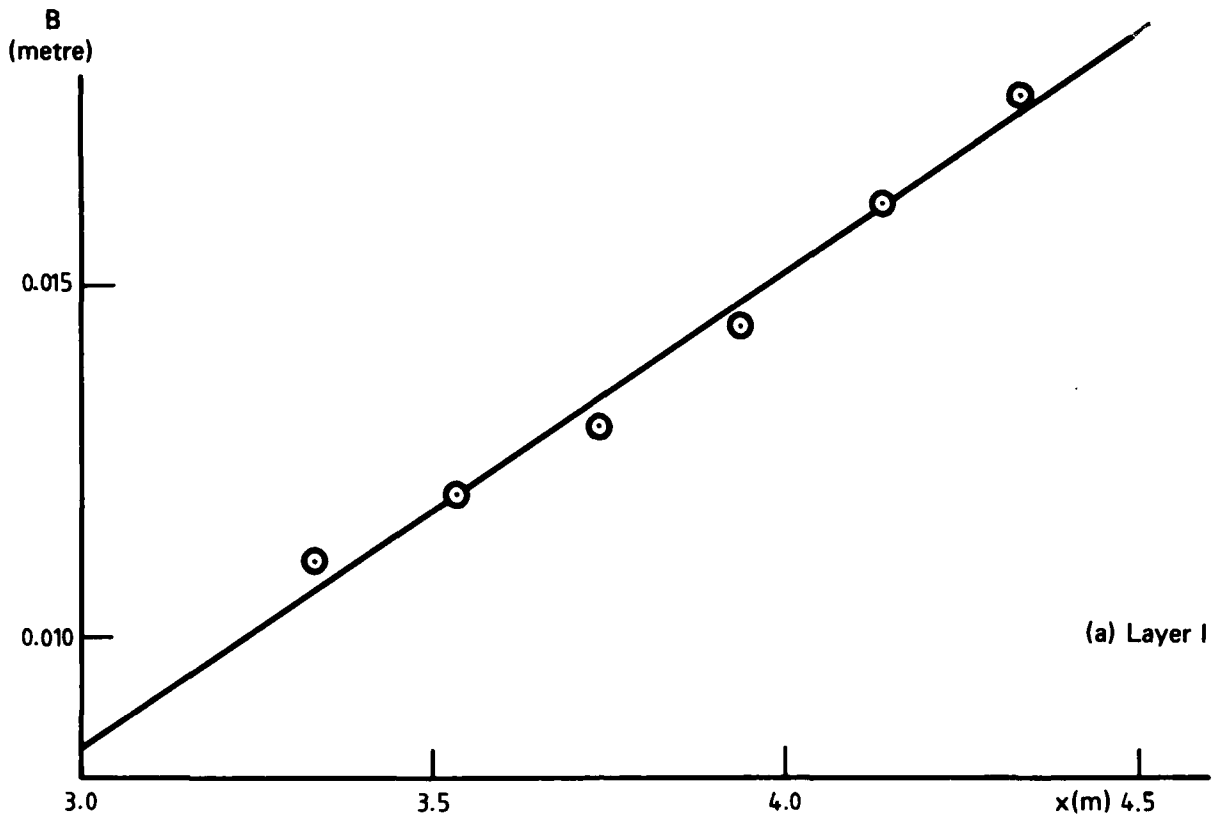

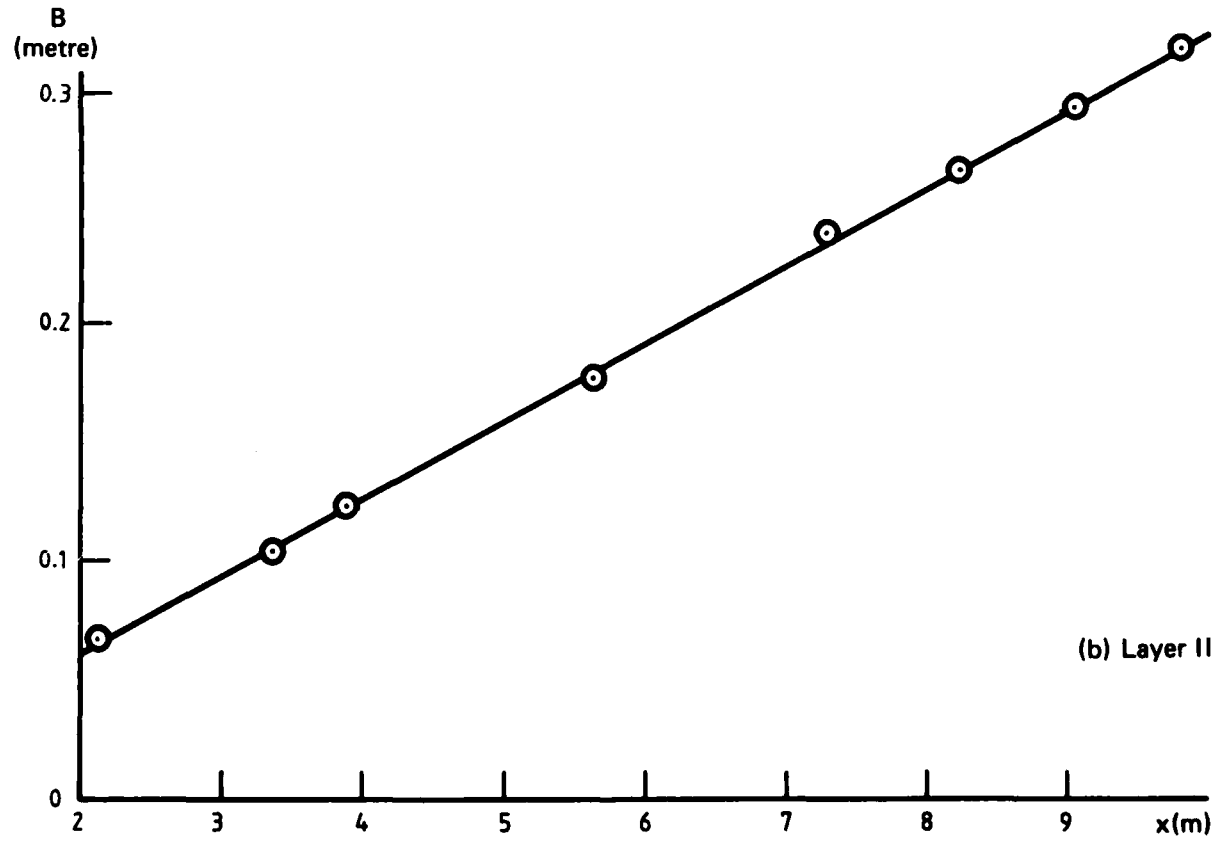

, line of best fit.

FIG. 9 GROWTH OF LAYER THICKNESS
Layer numbers as given in Fig. 5.

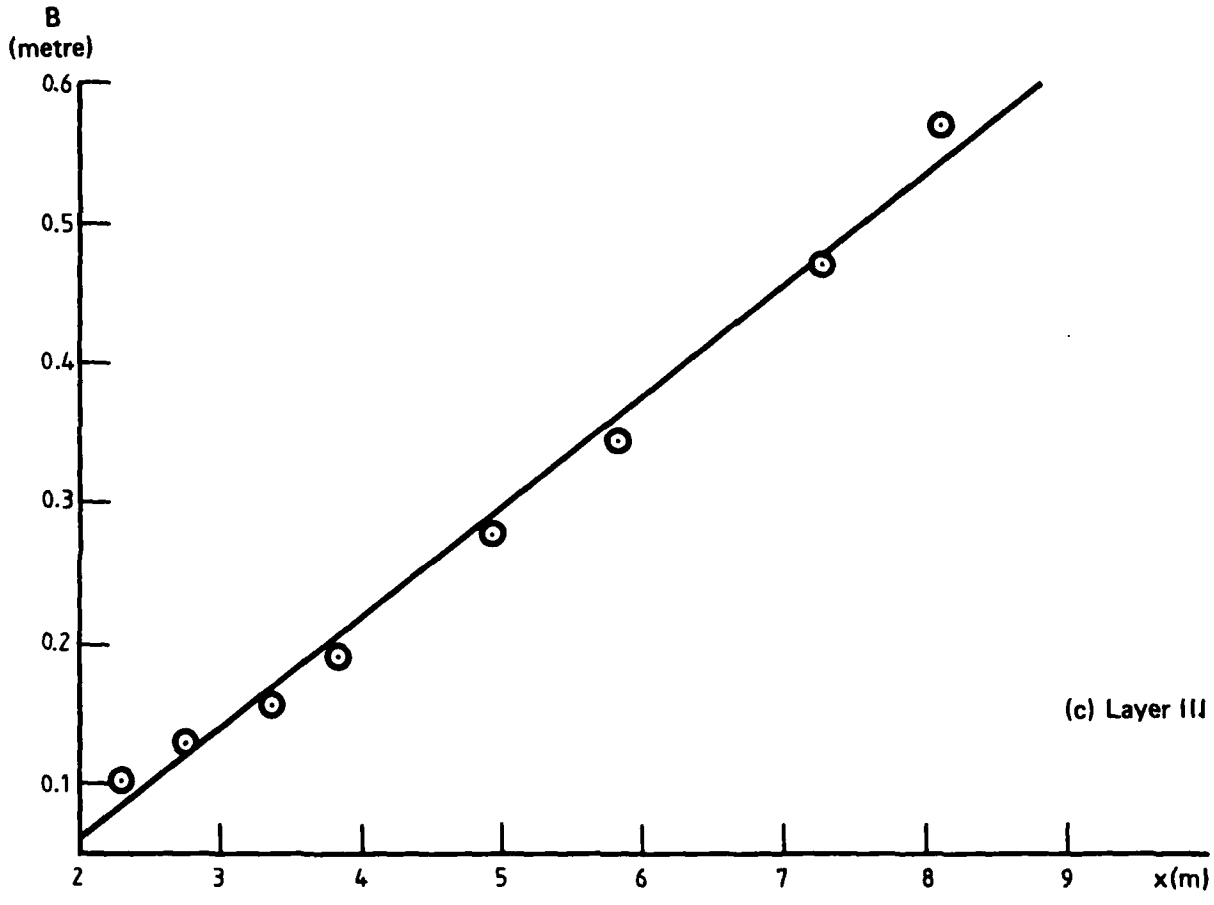

(c) Layer III

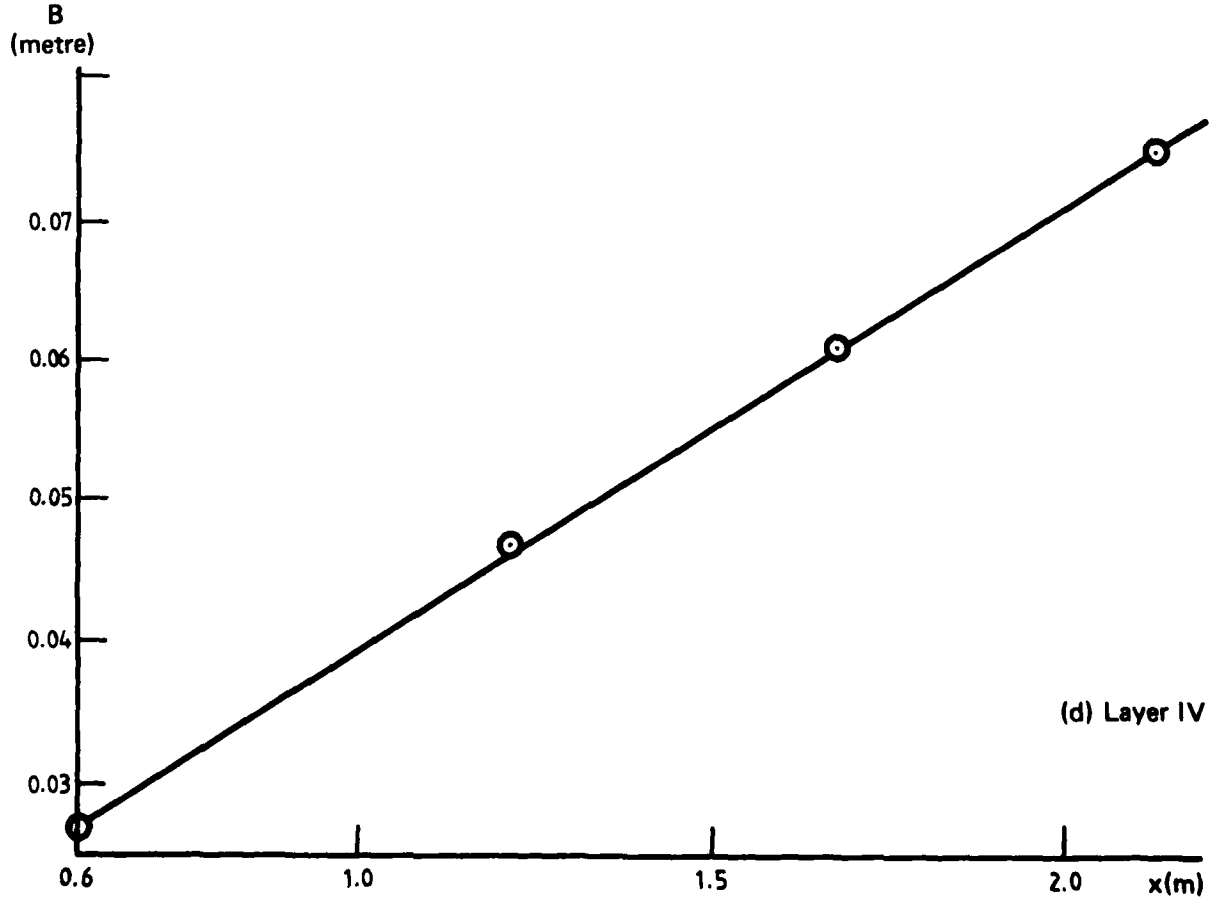

(d) Layer IV

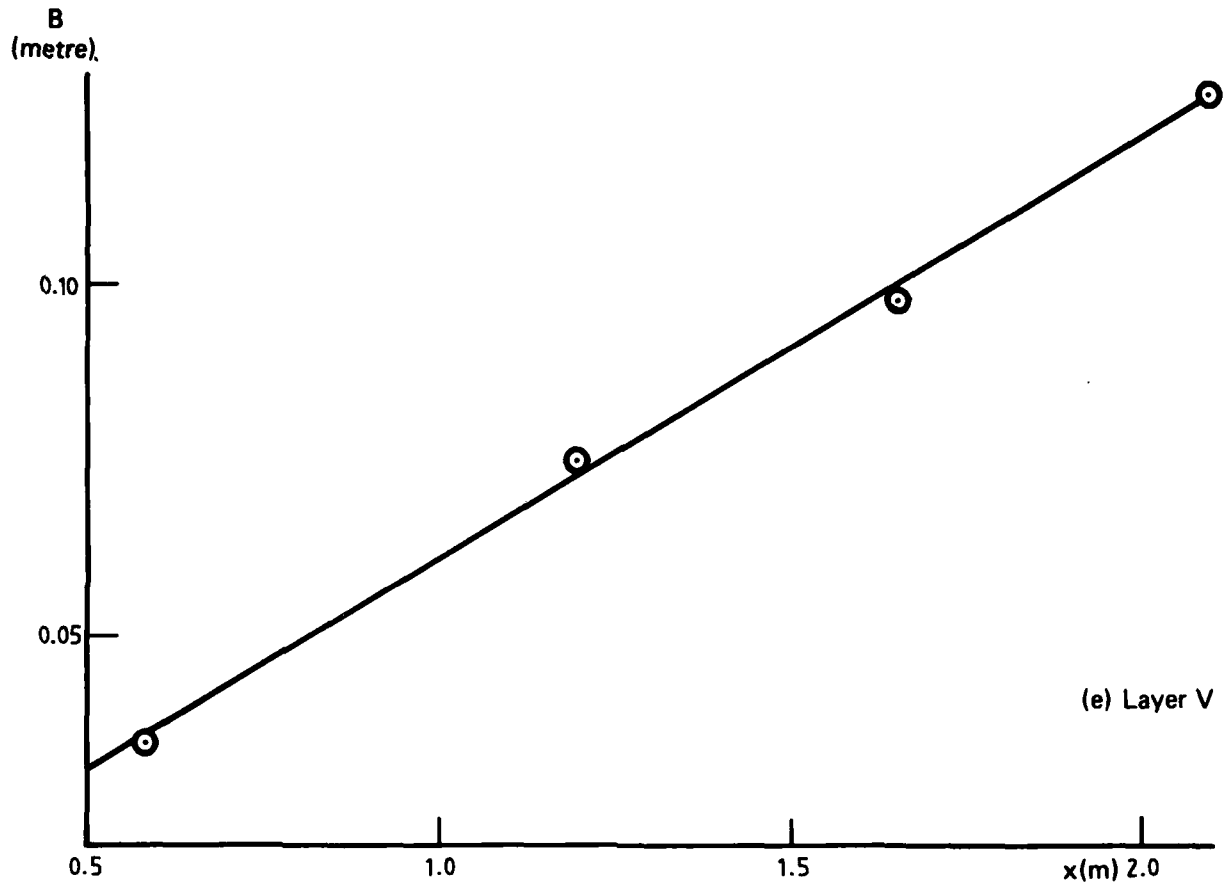

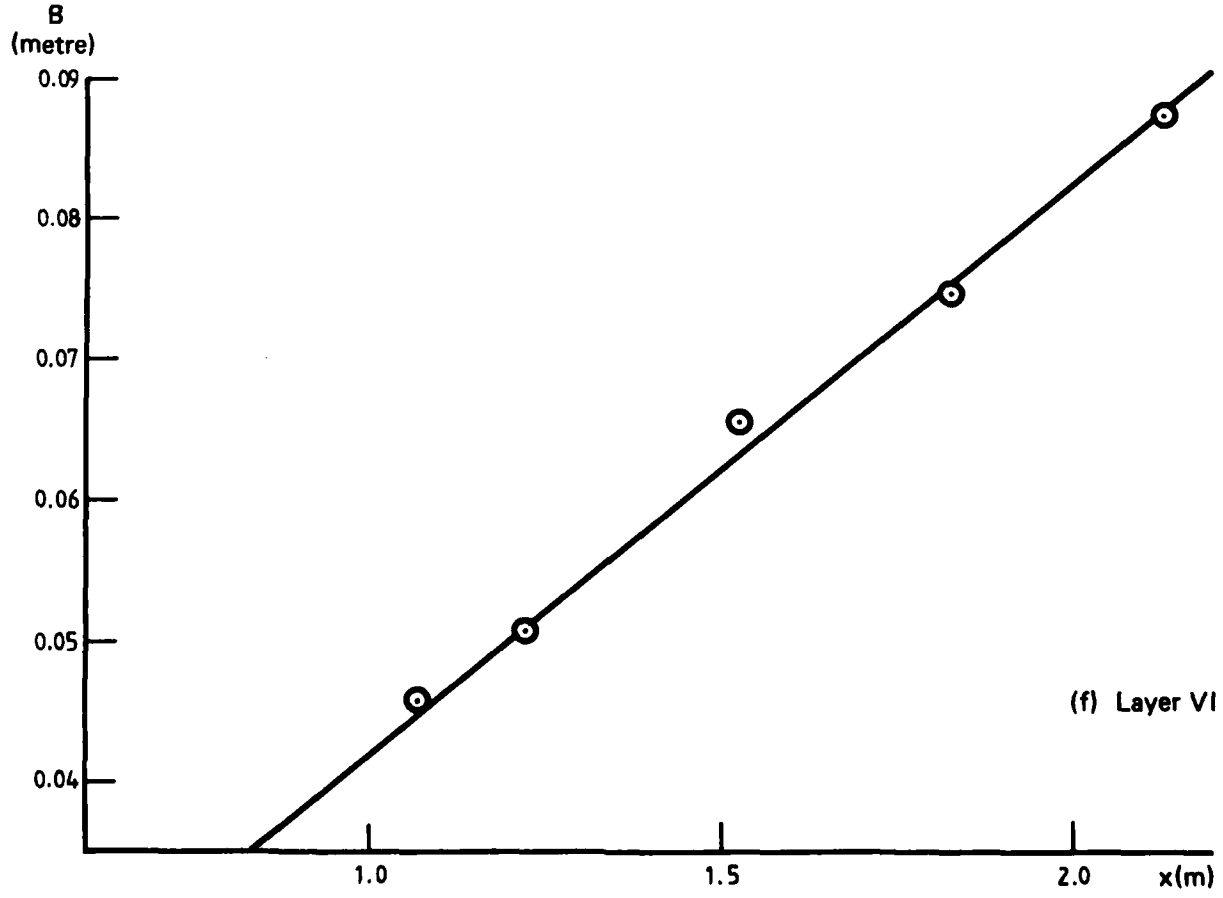

FIG. 9 Continued.

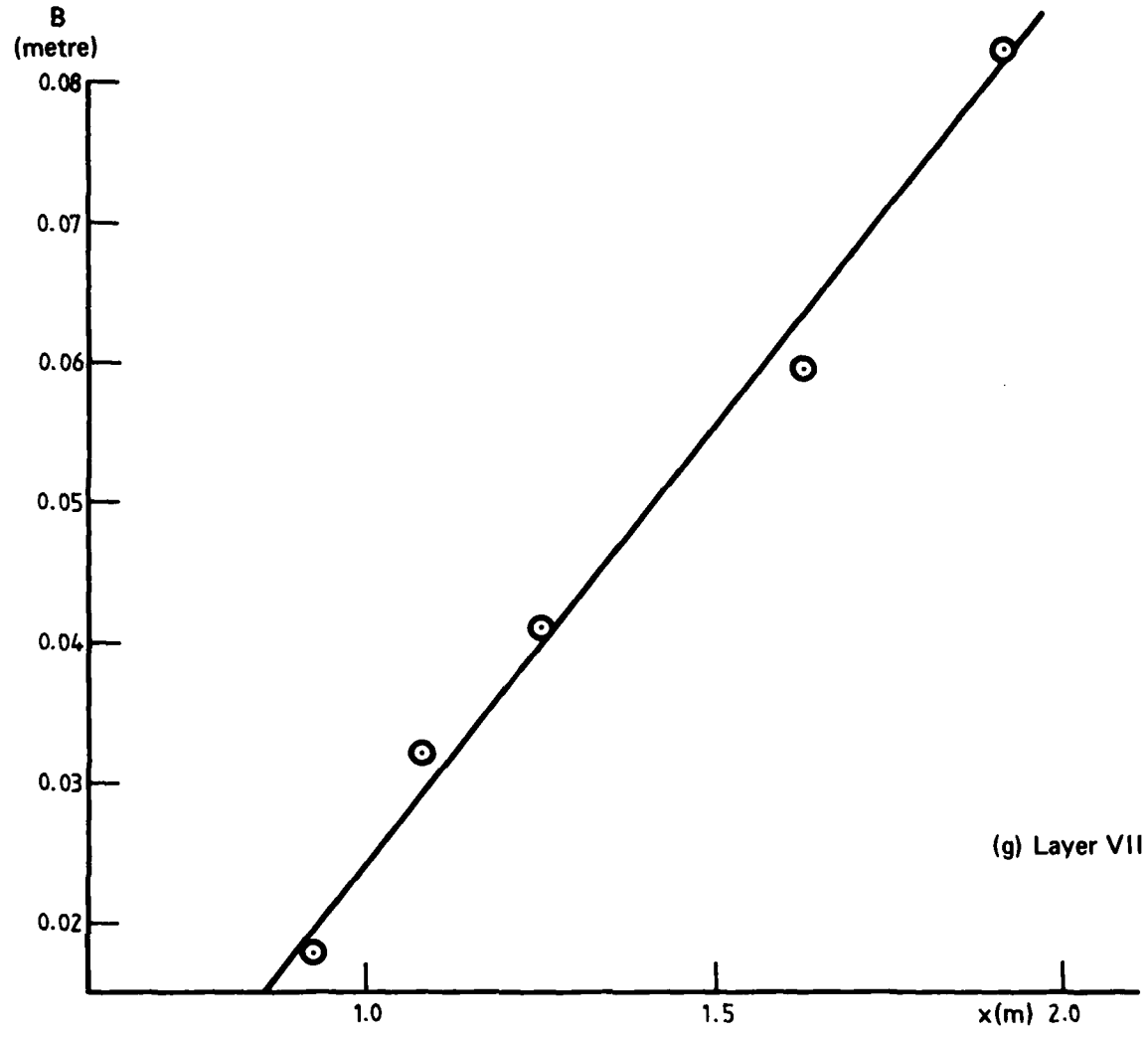

(g) Layer VII

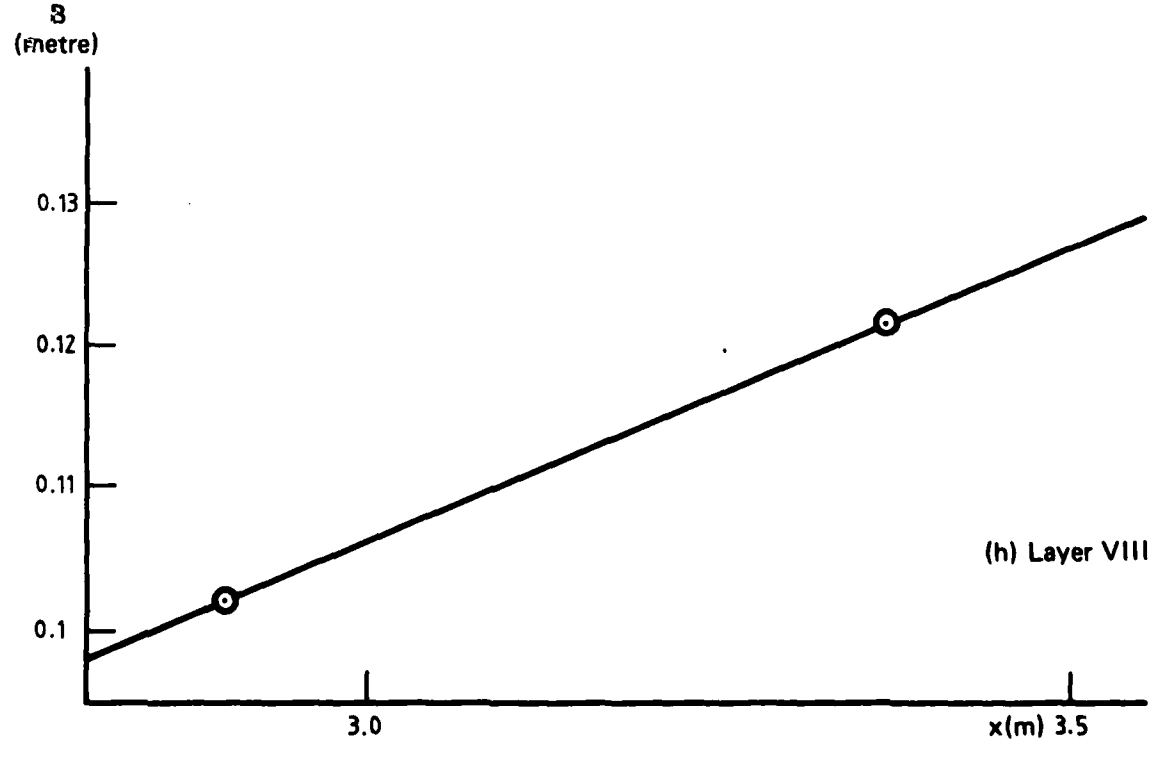

(h) Layer VIII

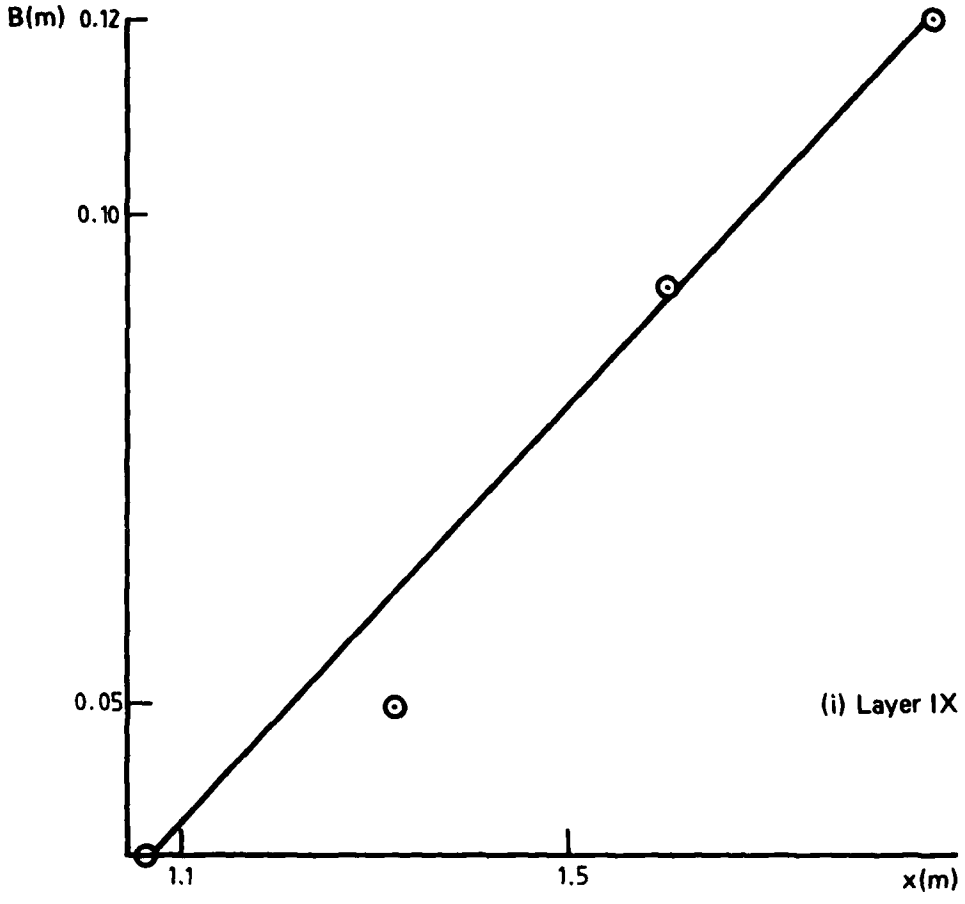

FIG. 9 Continued.

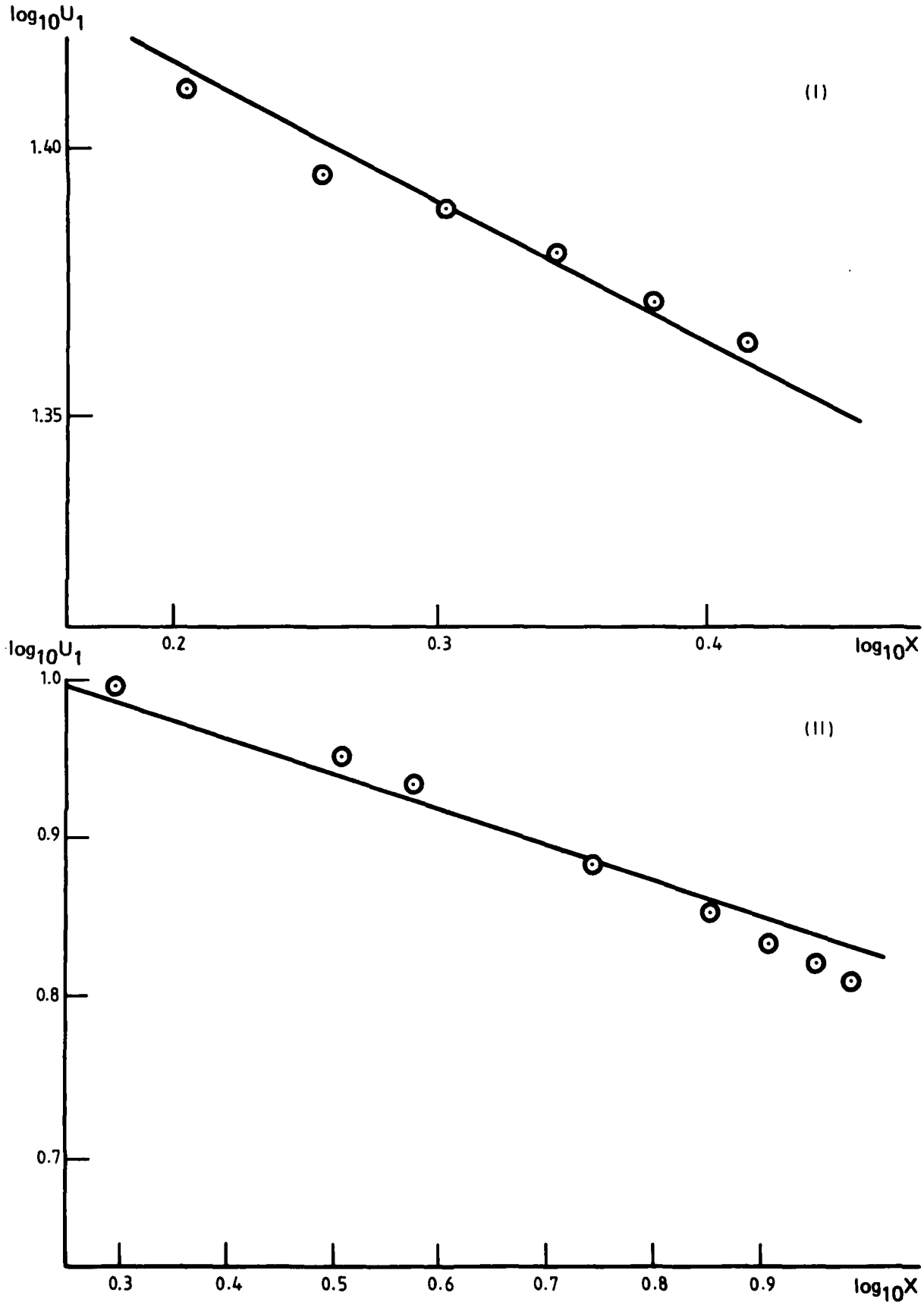

Equation (30).

FIG. 10 FREE STREAM VELOCITY VARIATIONS OF EQUILIBRIUM LAYERS.
I. Ludwieg & Tillmann (1949) mild adverse pressure gradient flow.

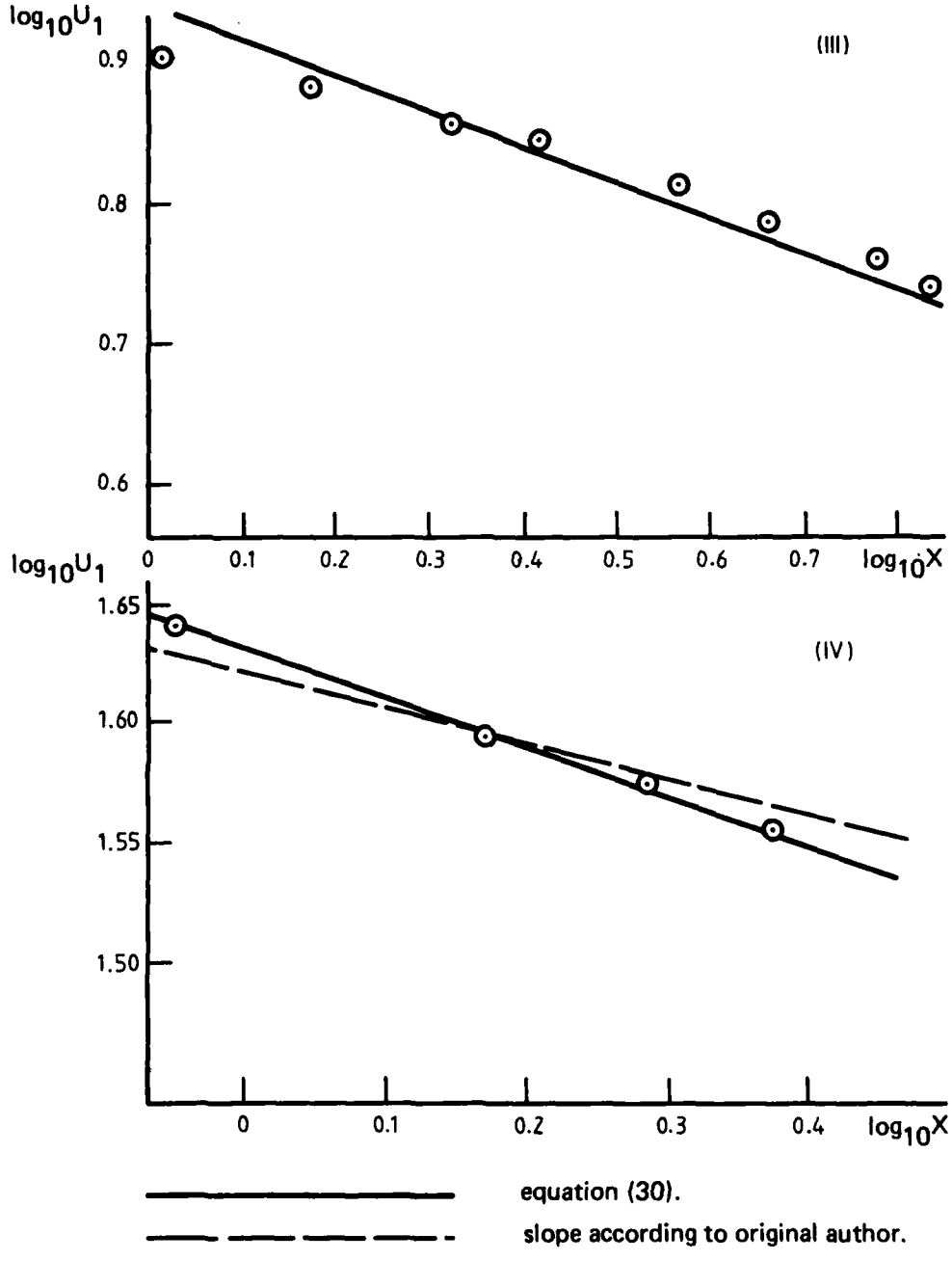

FIG. 10 Continued.
III. Clauser (1954) Flow 2

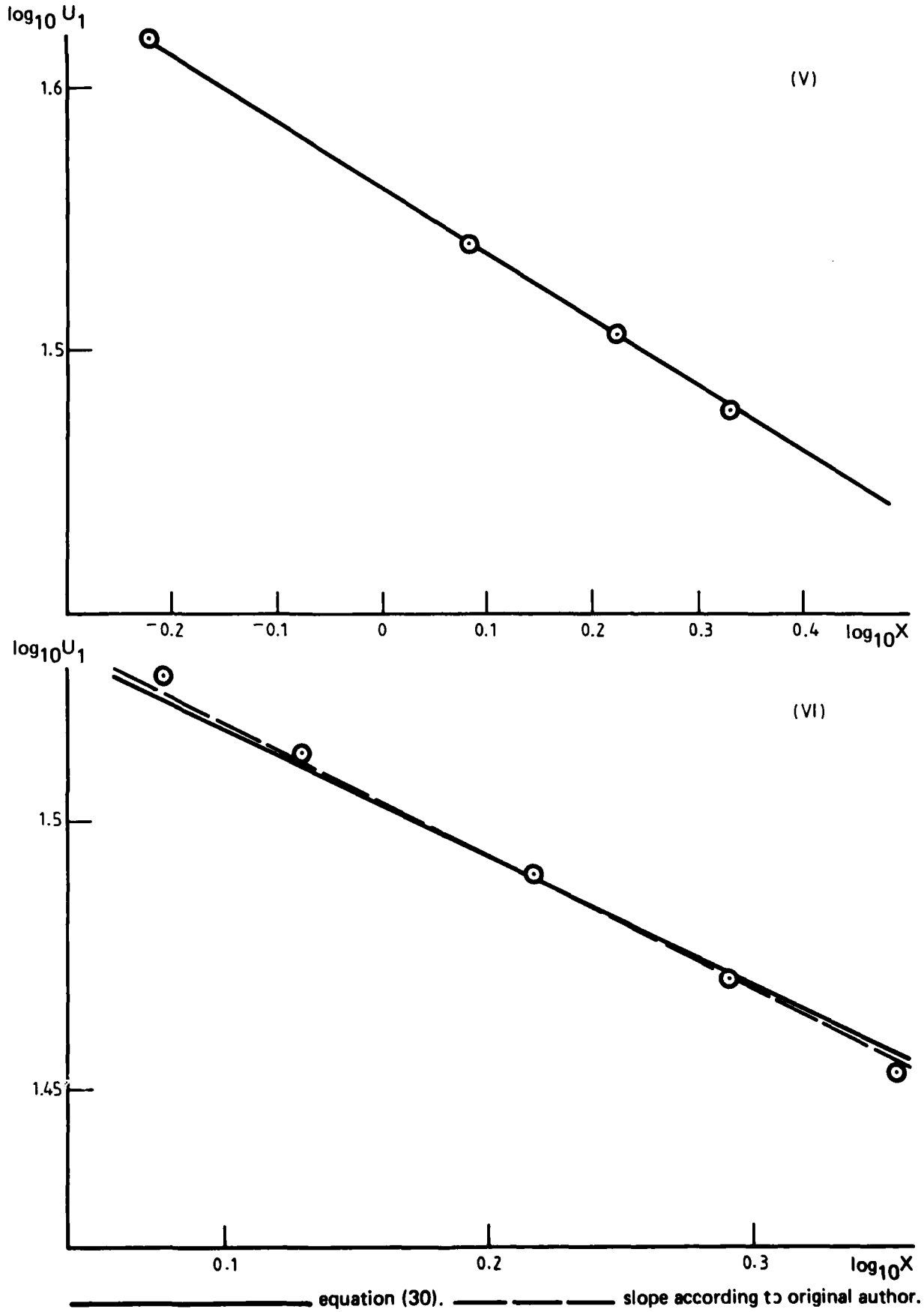

FIG. 10 Continued.

V. Bradshaw & Ferriss (1965) a = −0.255. Predicted slope and slope given by author agree within ¼%.

VI. Bradshaw (1967) a = 0—−0.255.

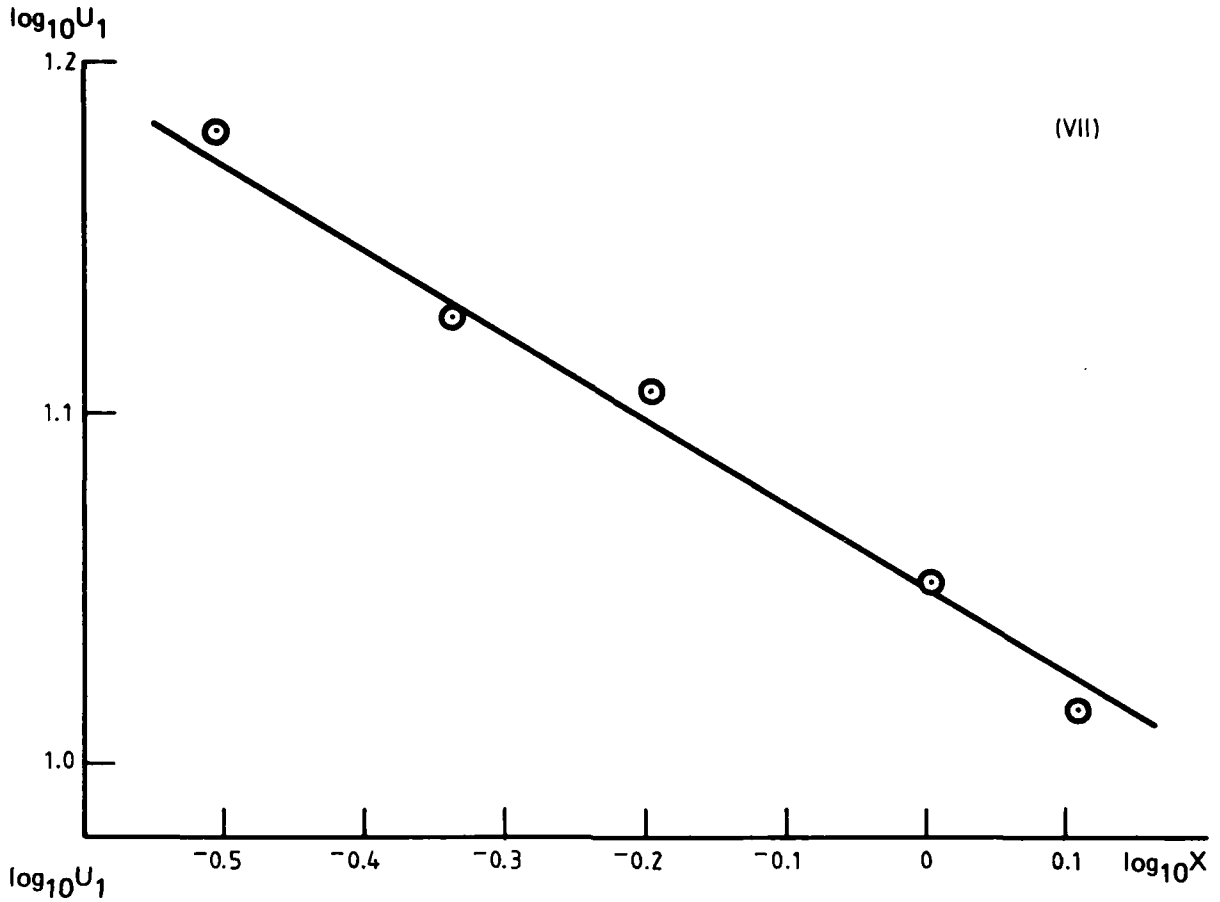

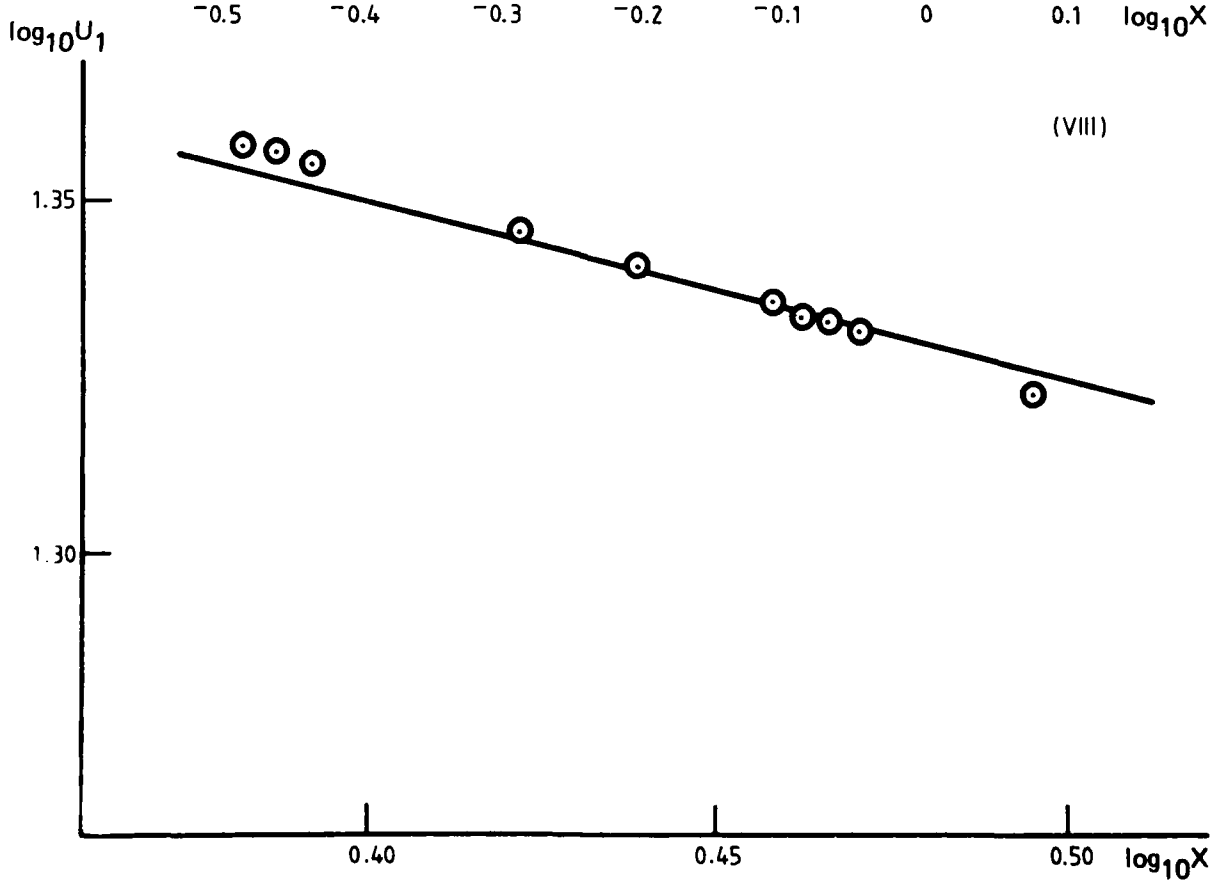

, equation (30).

FIG. 10 Continued.
VII. Stratford (1959) Flow 5.
VIII. Samuel (1973).

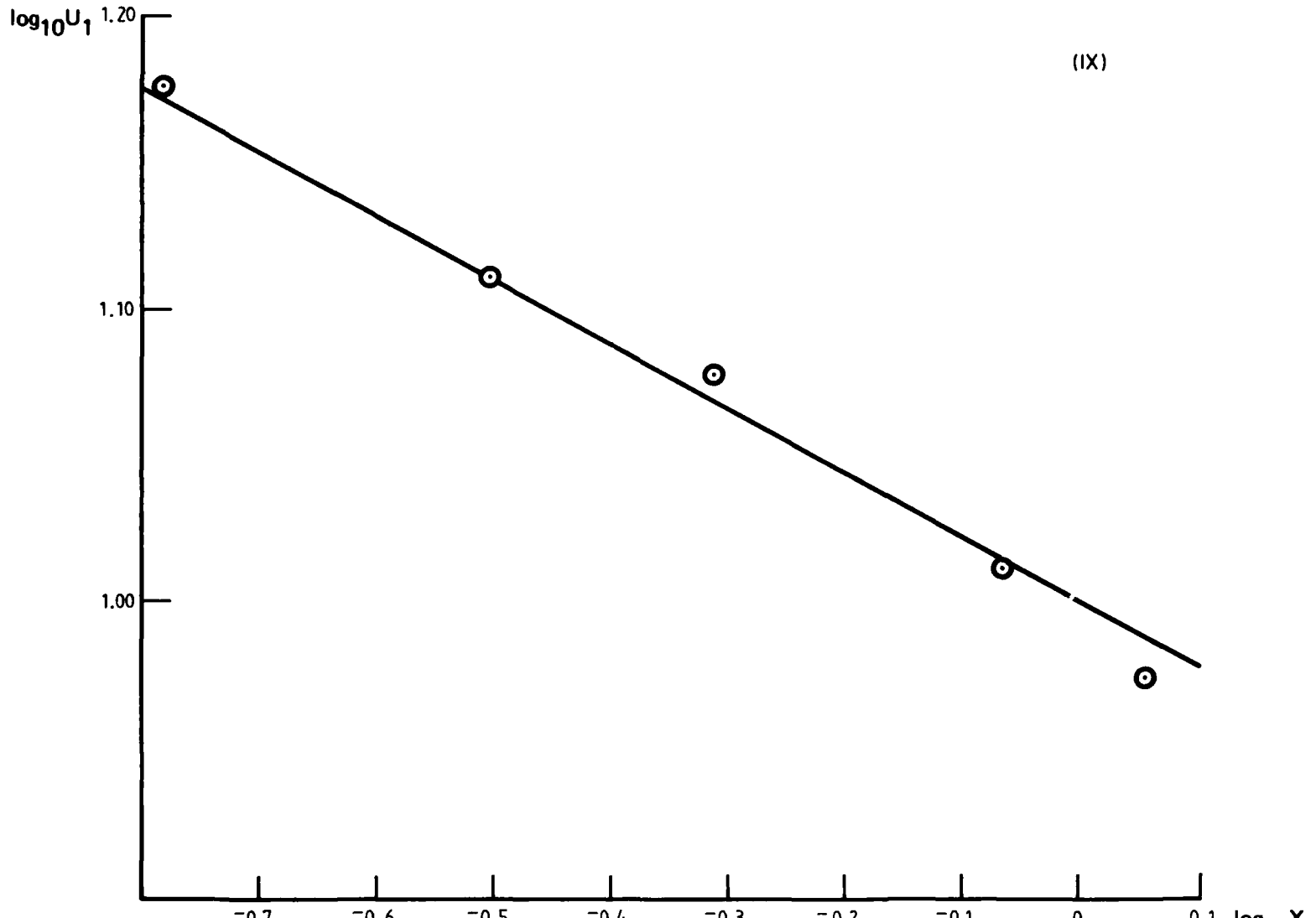

, equation 30.

FIG. 10 Continued.

IX. Stratford (1959) Flow 6

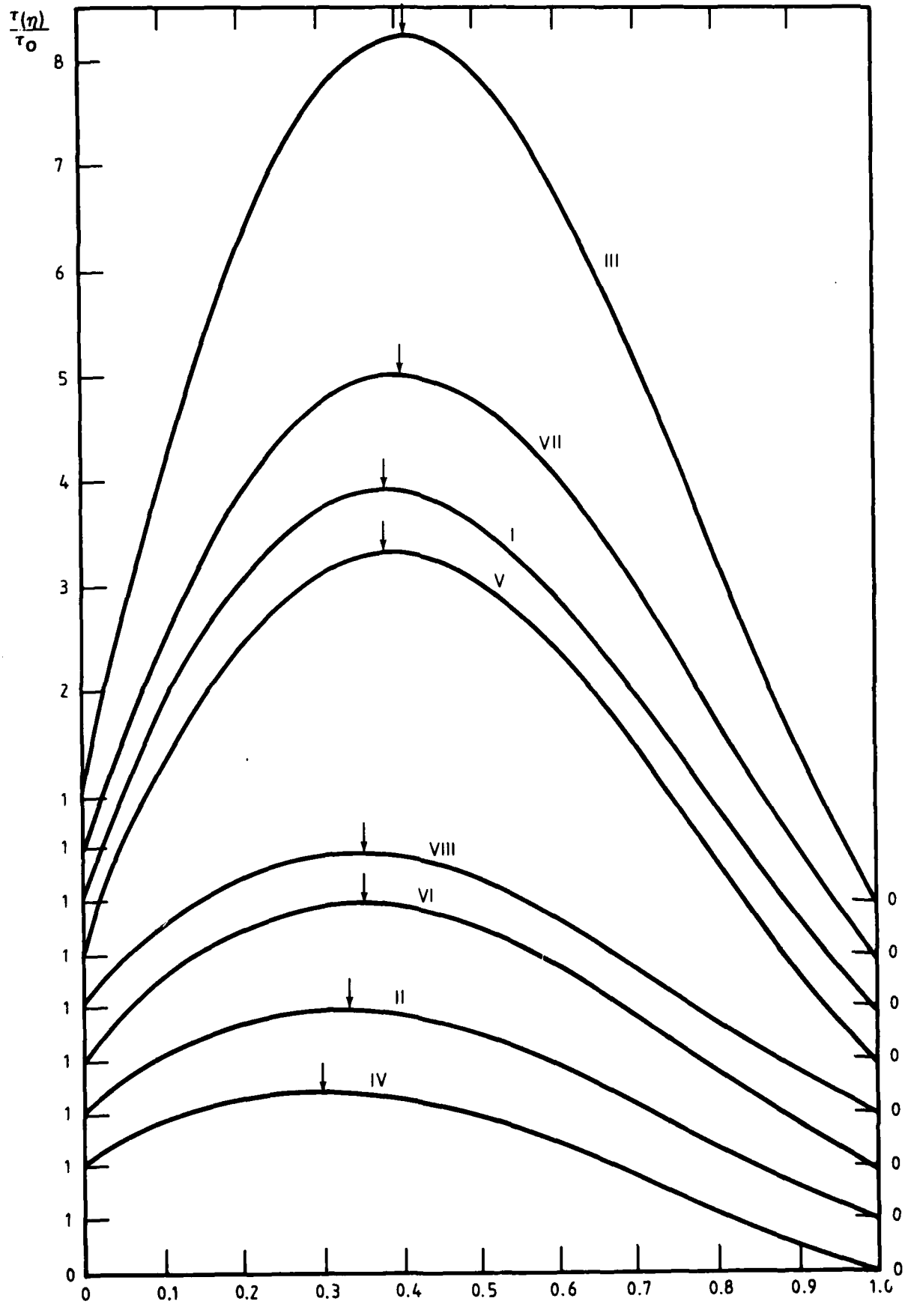

↓ Position of τ max. Profile numbers correspond to those given in Appendix III.

FIG. 11 EQUILIBRIUM SHEAR STRESS PROFILES.

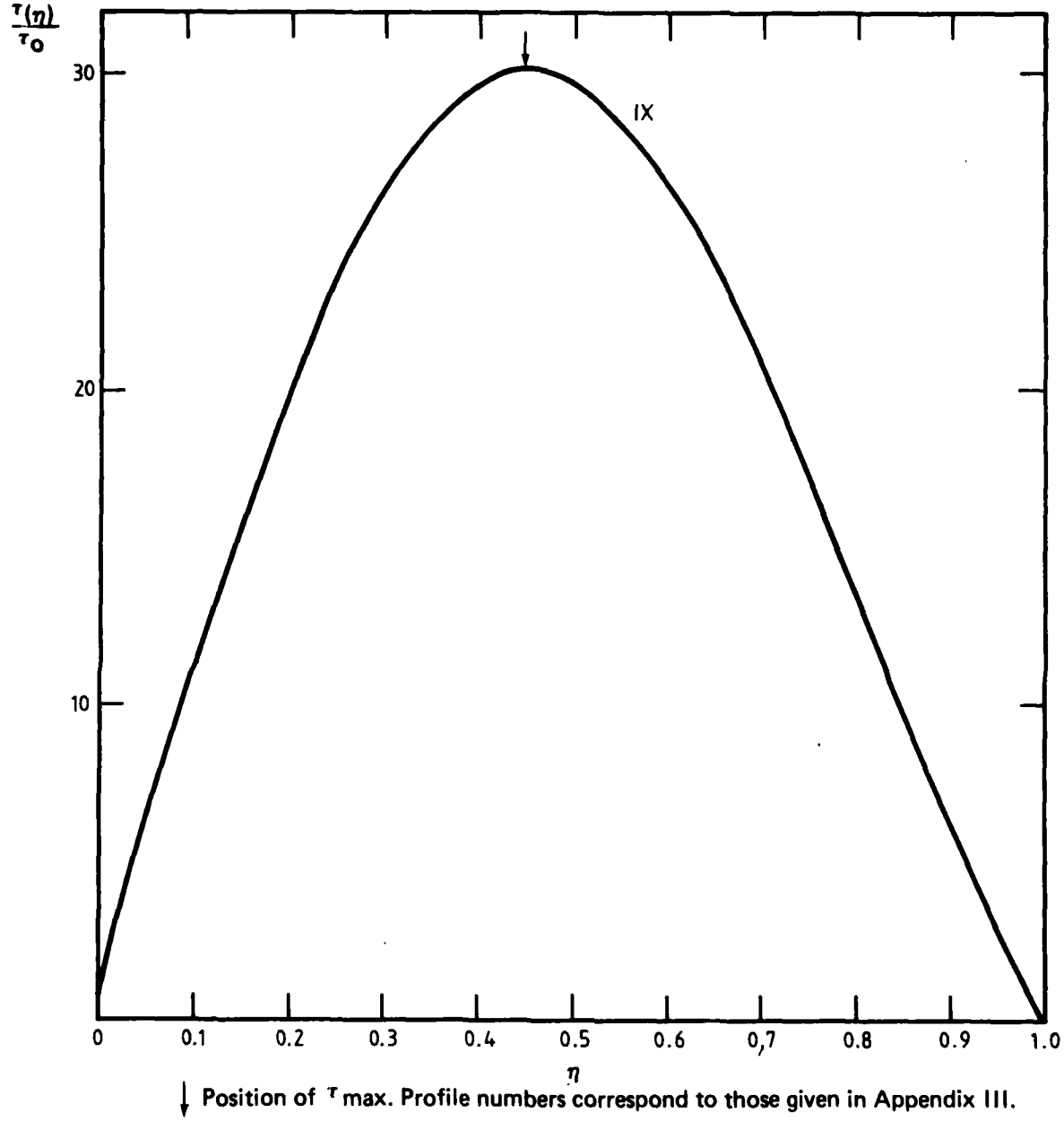

↓ Position of τ max. Profile numbers correspond to those given in Appendix III.

FIG. 11 Continued.

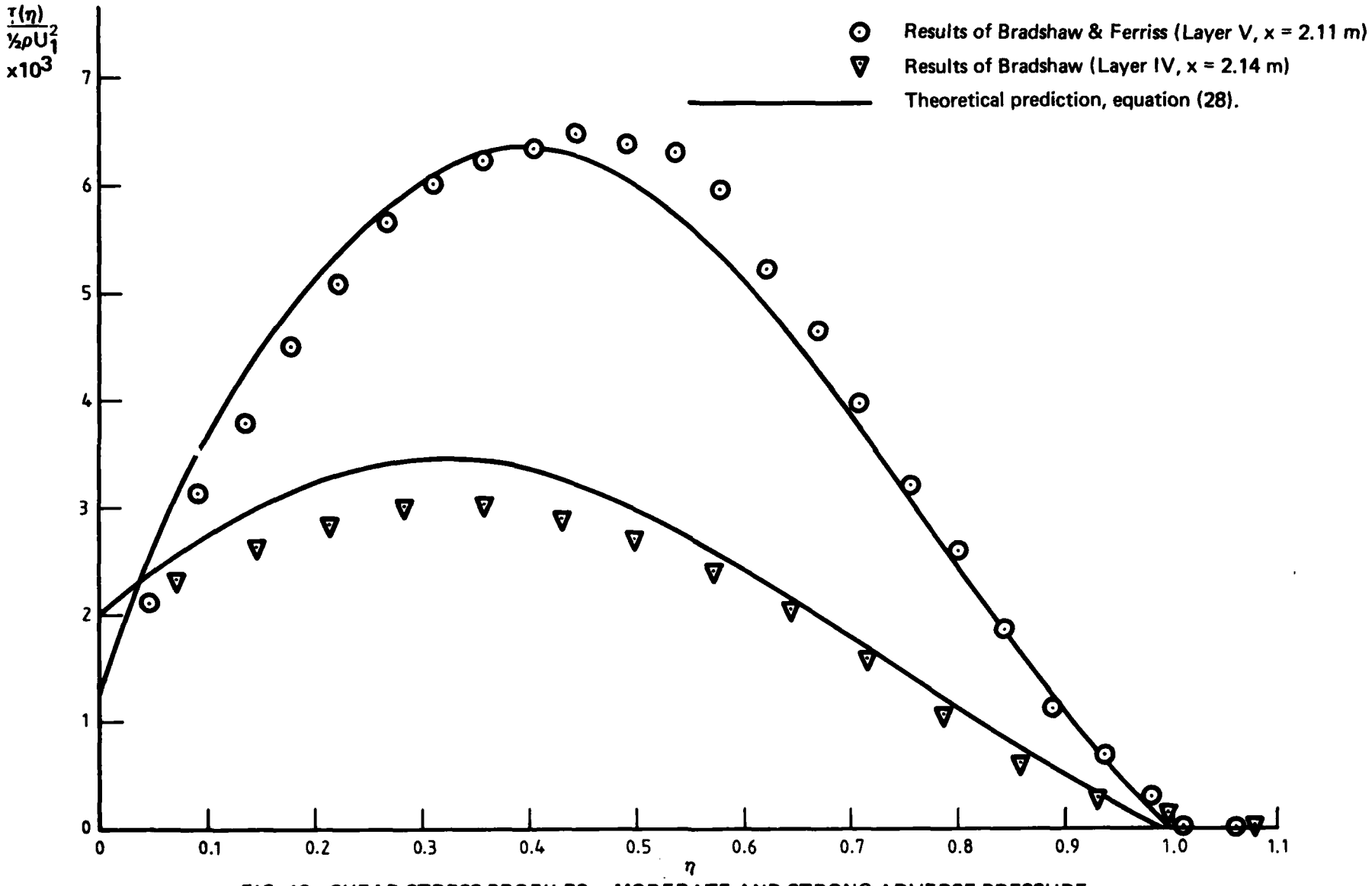

FIG. 12 SHEAR STRESS PROFILES – MODERATE AND STRONG ADVERSE PRESSURE GRADIENT LAYERS.

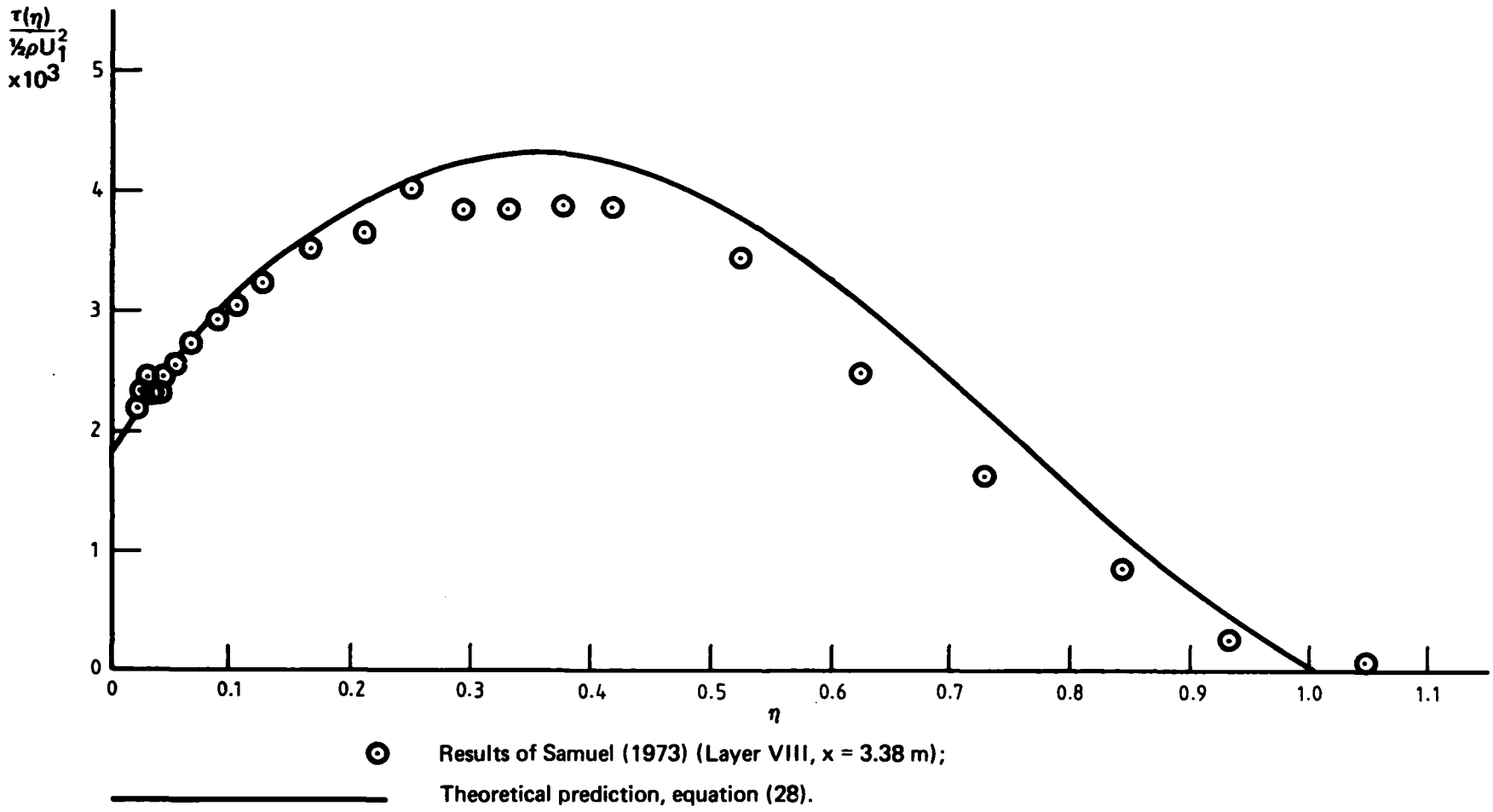

FIG. 12 CONCLUDED – MEDIUM ADVERSE PRESSURE GRADIENT LAYER

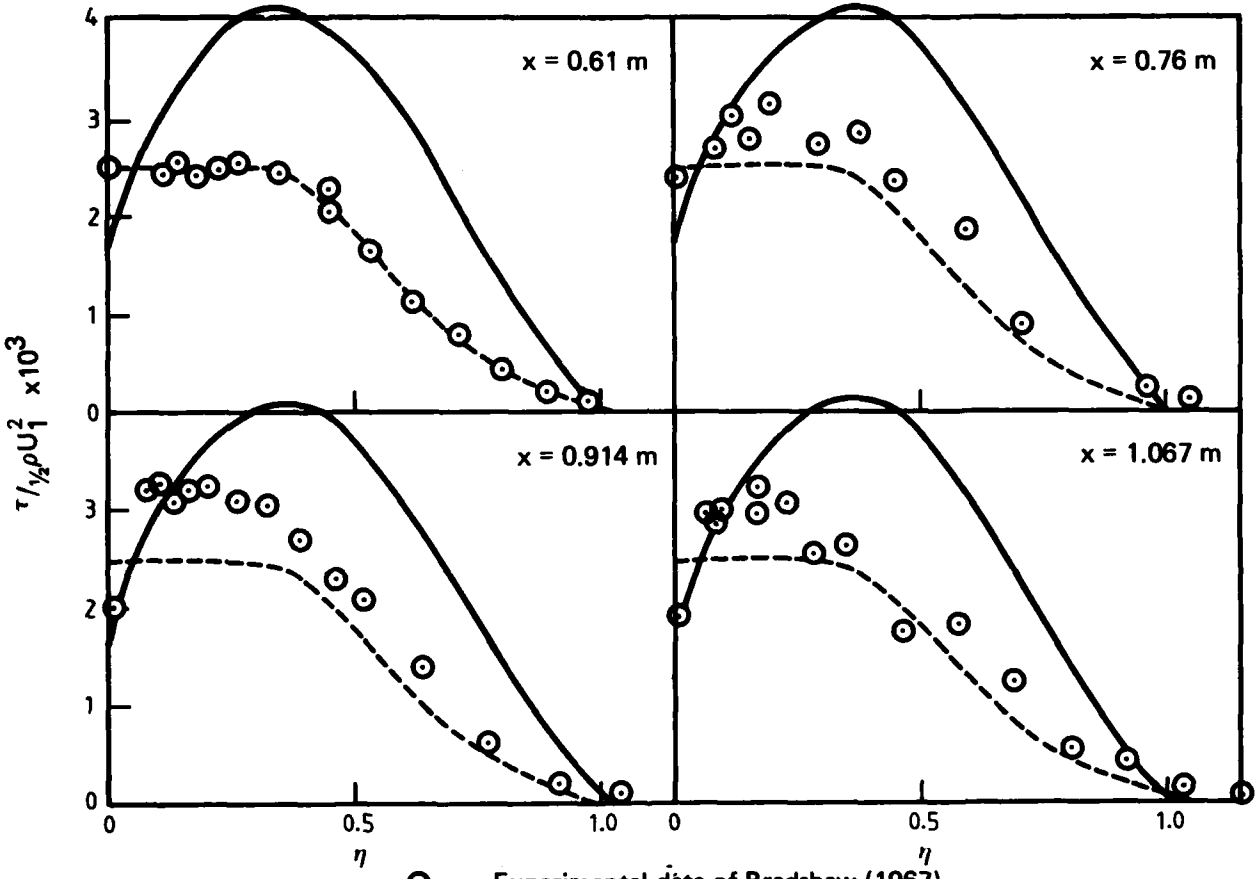

FIG. 13 SHEAR STRESS PROFILES OF A LAYER MOVING FROM A ZERO PRESSURE GRADIENT TO AN EQUILIBRIUM ADVERSE PRESSURE GRADIENT

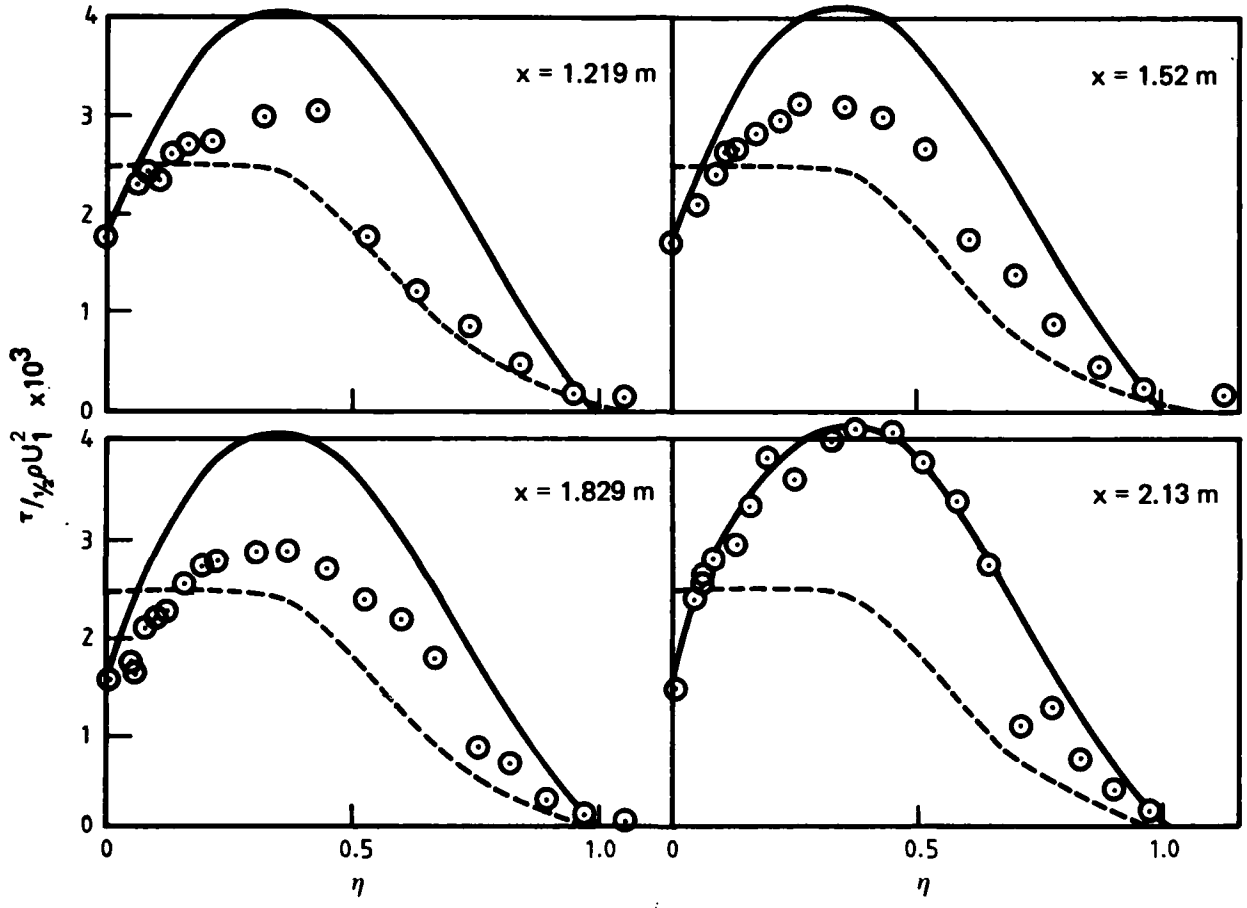

FIG. 13 CONCLUDED.

DISTRIBUTION

	Copy No.
AUSTRALIA	
Department of Defence	
Central Office	
Chief Defence Scientist	1
Deputy Chief Defence Scientist	2
Superintendent, Science and Technology Programs	3
Australian Defence Scientific and Technical Representative, UK	—
Counsellor, Defence Science, USA	—
Joint Intelligence Organisation	4
Defence Library	5
Document Exchange Centre, DISB	6–23
Aeronautical Research Laboratories	
Chief Superintendent	24
Library	25
Superintendent—Mechanical Engineering Division	26
Divisional File—Mechanical Engineering	27
Author: W. H. Schofield	28–32
D, A. Frith	33
Materials Research Laboratories	
Library	34
Defence Research Centre, Salisbury	
Library	35
Engineering Development Establishment	
Library	36
RAN Research Laboratory	
Library	37
Navy Office	
Naval Scientific Adviser	38
Army Office	
Army Scientific Adviser	39
Royal Military College Library	40
US Army Standardisation Group	41
Air Force Office	
Aircraft Research and Development Unit, Scientific Flight Group	42
Air Force Scientific Adviser	43
HQ Support Command (SENGSO)	44
Department of Productivity	
Government Aircraft Factories	
Manager	45
Library	46

Statutory, State Authorities and Industry

Australian Atomic Energy Commission, Director		47
CSIRO, Mechanical Engineering Division, Chief		48
Commonwealth Aircraft Corporation, Manager		49
Hawker de Havilland Pty. Ltd., Manager, Lidcombe		50

Universities and Colleges

Adelaide	Dr C. Abel	51
	Barr Smith Library	52
	Professor R. E. Luxton	53
Flinders	Library	54
James Cook	Library	55
LaTrobe	Library	56
Melbourne	Professor P. N. Joubert	57
	Engineering Library	58
	Dr. A. E. Perry	59
Monash	Library	60
	Professor W. Melbourne	61
	Professor I. J. Polmear	62
	Professor J. Crisp	63
Newcastle	Library	64
	Professor R. A. Antonia	65
New England	Library	66
Sydney	Engineering Library	67
	Professor G. A. Bird	68
	Professor R. I. Tanner	69
	Professor R. Bilger	70
New South Wales	Professor R. A. A. Bryant	71
Queensland	Library	72
	Professor K. Bullock	73
	Dr. K. Bremhorst	74
Tasmania	Engineering Library	75
	Professor A. R. Oliver	76
	Dr. G. Walker	77
Western Australia	Library	78
RMIT	Library	79

CANADA

NRC, National Aeronautical Establishment, Library		80
NRC, Division of Mechanical Engineering, Director		81
Gas Dynamics Laboratory, Mr. R. A. Tyler		82

Universities and Colleges

McGill	Library	83
Toronto	Institute for Aerospace Studies	84

FRANCE

AGARD, Library	85
ONERA, Library	86
Service de Documentation, Technique de l'Aeronautique	87

GERMANY

ZLDI	88

INDIA

Civil Aviation Department, Director	89
Defence Ministry, Aero. Development Establishment, Library	90
Gas Turbine Research Establishment, Director	91

Iowa State	Dr. G. K. Serory, Mechanical Engineering	179
Johns Hopkins	Professor S. Corrsin	180
Princeton	Professor G. L. Mellor, Mechanics	181
Southern Methodist University (Fort Worth, Texas)	Professor R. L. Simpson	182
Stanford	Department of Aeronautics, Library	183
Polytechnic Institute of New York	Aeronautical Labs., Library	184
California Institute of Technology	Graduate Aeronautical Labs., Library	185
Massachusetts Institute of Technology	Library	186
University of Arizona (Tucson)	Professor D. McEligot	187
	Professor F. Champagne	188
US Post-Graduate School (Monterey, Calif.)	Dr. M. Platzer	189
Spares		190–199


DAT
FILM